

Double Data Piling for Heterogeneous Covariance Models

Taehyun Kim

*Department of Statistics
Columbia University
New York, NY 10027, United States*

TK3036@COLUMBIA.EDU

Jeongyoun Ahn

*Department of Industrial and Systems Engineering
KAIST
Daejeon, 34141, South Korea*

JYAHN@KAIST.AC.KR

Sungkyu Jung

*Department of Statistics
Seoul National University
Seoul, 08826, South Korea*

SUNGKYU@SNU.AC.KR

Abstract

In this work, we characterize two data piling phenomena for a high-dimensional binary classification problem with general heterogeneous covariance models, which were previously characterized only for restricted homogeneous covariances. The data piling refers to the phenomenon where projections of the training data onto a direction vector have exactly two distinct values, one for each class. This first data piling phenomenon occurs for any data when the dimension p is larger than the sample size n . We show that the second data piling phenomenon, which refers to a data piling of independent test data, can occur in an asymptotic context where p grows while n is fixed. We further show that a second maximal data piling direction, which gives an asymptotic maximal distance between the two piles of independent test data, can be obtained by projecting the first maximal data piling direction onto the nullspace of the common leading eigenspace. Based on the second data piling phenomenon, we propose various linear classification rules which ensure perfect classification of high-dimension low-sample-size data under generalized heterogeneous spiked covariance models.

Keywords: High dimension low sample size, Classification, Maximal data piling, Spiked covariance model, High-dimensional asymptotics

1. Introduction

High-Dimension Low-Sample-Size (HDLSS) data have often been found in many of scientific fields, such as bioinformatics including next-generation sequencing data analysis, chemometrics, and image processing. Such HDLSS data are often best classified by linear classifiers since the dimension of data p is much larger than the sample size n . For binary classification with $p > n$, Ahn and Marron (2010) observed the data piling phenomenon, that is, projections of training data onto a direction vector \mathbf{w} are identical for each class. Among such directions exhibiting data piling, the *maximal data piling* direction uniquely gives the largest distance between the two piles of training data. The maximal data piling

direction is defined as

$$\mathbf{w}_{\text{MDP}} = \underset{\mathbf{w}: \|\mathbf{w}\|_2=1}{\operatorname{argmax}} \mathbf{w}^\top \mathbf{S}_B \mathbf{w} \text{ subject to } \mathbf{w}^\top \mathbf{S}_W \mathbf{w} = 0, \quad (1)$$

where \mathbf{S}_W and \mathbf{S}_B are the $p \times p$ within-class and between-class scatter matrices of training dataset \mathcal{X} , respectively. Ahn and Marron (2010) observed that a classification rule using \mathbf{w}_{MDP} as the normal vector to a discriminative hyperplane achieves better classification performance than classical linear classifiers when there are significantly correlated variables in high dimensions.

However, the maximal data piling direction has not been considered as an appropriate classifier since it depends too much on training data, resulting in poor generalization performances (Marron et al., 2007; Lee et al., 2013). In general, while the training data are piled on \mathbf{w}_{MDP} , independent test data are not piled on \mathbf{w}_{MDP} . Recently, Chang et al. (2021) revealed the existence of the *second data piling* direction, which gives a data piling of independent test data, under the HDLSS asymptotic regime of Hall et al. (2005) where the dimension of data p tends to grow while the sample size n is fixed. In addition, they showed that a negatively ridged linear discriminant vector, projected onto a low-dimensional subspace, can be a *second maximal data piling* direction, which yields a maximal asymptotic distance between two piles of independent test data.

A second data piling direction is defined asymptotically as $p \rightarrow \infty$, unlike the first data piling of training dataset \mathcal{X} for any fixed $p > n$. For a sequence of directions $\{\mathbf{w}\} = (\mathbf{w}^{(1)}, \dots, \mathbf{w}^{(p-1)}, \mathbf{w}^{(p)}, \mathbf{w}^{(p+1)}, \dots)$, in which $\mathbf{w}^{(q)} \in \mathbb{R}^q$ for $q \in \mathbb{N}$, we write $\mathbf{w} \in \mathbb{R}^p$ for the p th element of $\{\mathbf{w}\}$. Let Y, Y' be independent random vectors from the same population of \mathcal{X} , and write $\pi(Y) = k$ if Y belongs to class k . Chang et al. (2021) defined the collection of all sequences of second data piling directions as

$$\mathcal{A} = \left\{ \{\mathbf{w}\} \in \mathfrak{W}_X : \text{for any } Y, Y' \text{ with } \pi(Y) = \pi(Y'), p^{-1/2} \mathbf{w}^\top (Y - Y') \xrightarrow{P} 0 \text{ as } p \rightarrow \infty \right\}$$

where $\mathfrak{W}_X = \{\{\mathbf{w}\} : \mathbf{w} \in \mathcal{S}_X, \|\mathbf{w}\|_2 = 1 \text{ for all } p\}$, and $\mathcal{S}_X = \operatorname{span}(\mathbf{S}_W) \cup \operatorname{span}(\mathbf{S}_B)$ is the sample space. Furthermore, among the sequences of second data piling directions in \mathcal{A} , if $\{\mathbf{v}\} \in \mathcal{A}$ satisfies

$$\{\mathbf{v}\} \in \underset{\{\mathbf{w}\} \in \mathcal{A}}{\operatorname{argmax}} D(\mathbf{w}),$$

where $D(\mathbf{w})$ is the probability limit of $p^{-1/2} |\mathbf{w}^\top (Y_1 - Y_2)|$ for $\pi(Y_k) = k$ ($k = 1, 2$), then we call \mathbf{v} a *second maximal data piling* direction.

Chang et al. (2021) showed that the second maximal data piling direction exists and by using such a direction, asymptotic perfect classification of independent test data is possible. They assumed that the population mean difference is as large as $\|\boldsymbol{\mu}_{(1)} - \boldsymbol{\mu}_{(2)}\|_2 = O(p^{1/2})$ where $\boldsymbol{\mu}_{(k)} \in \mathbb{R}^p$ ($k = 1, 2$) is the population mean vector of the k th class and both populations share a common, or *homogeneous*, spiked covariance matrix. The spiked covariance model, first introduced by Johnstone (2001), refers to high-dimensional population covariance matrix structures in which a few eigenvalues of the matrix are much larger than the other nearly constant eigenvalues (Ahn et al., 2007; Jung and Marron, 2009; Shen et al., 2016). More precisely, Chang et al. (2021) assumed the common covariance matrix $\boldsymbol{\Sigma}$ has

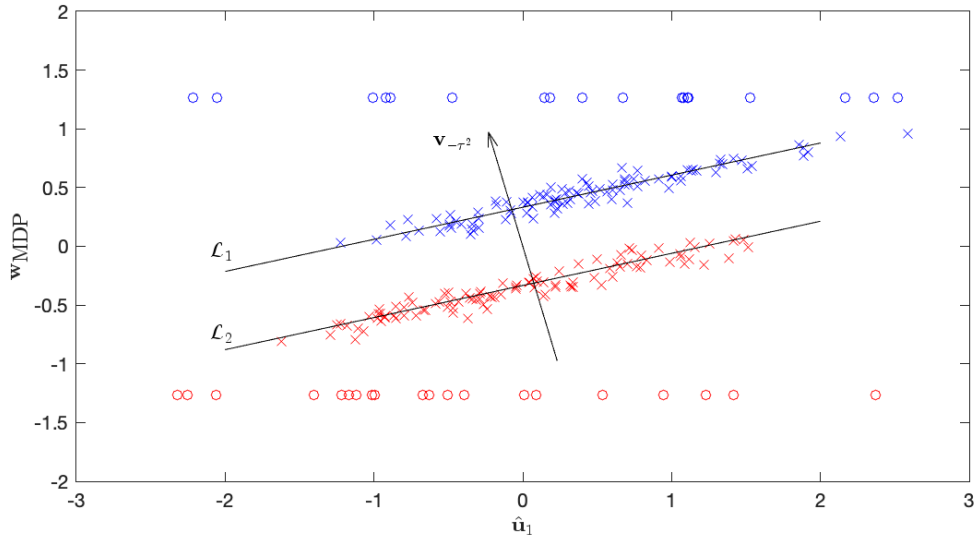


Figure 1: Double data piling phenomenon for homogeneous covariance model with one strong spike ($m = 1$). Training data (class 1: blue circles, class 2: red circles) are piled on two distinct points on \mathbf{w}_{MDP} , while The projections of independent test data (class 1: blue crosses, class 2: red crosses) are distributed along parallel lines \mathcal{L}_1 and \mathcal{L}_2 , respectively, when projected to $\mathcal{S} = \text{span}(\hat{\mathbf{u}}_1, \mathbf{w}_{\text{MDP}})$. Both \mathcal{L}_1 and \mathcal{L}_2 are nearly orthogonal to $\mathbf{v}_{-\tau^2}$.

m spikes, that is, m eigenvalues increase at the order of p^β as $p \rightarrow \infty$ with some $\beta \in [0, 1]$, while the other eigenvalues are nearly constant, averaging to $\tau^2 > 0$.

With such assumptions, Chang et al. (2021) showed that if Σ has weak spikes (that is, $0 \leq \beta < 1$), then projections of independent test data are asymptotically piled on two distinct points on \mathbf{w}_{MDP} as $p \rightarrow \infty$, similar to the projections of the training data. However, if Σ has strong spikes (that is, $\beta = 1$), then projections of independent test data tend to be respectively distributed along two parallel affine subspaces in a low-dimensional subspace $\mathcal{S} = \text{span}(\hat{\mathbf{u}}_1, \dots, \hat{\mathbf{u}}_m, \mathbf{w}_{\text{MDP}}) \subset \mathcal{S}_{\mathcal{X}}$, where $\hat{\mathbf{u}}_i$ is the i th eigenvector of \mathbf{S}_W . See Figure 1 for an illustration. Furthermore, $\mathbf{v}_{-\tau^2}$, a ridged linear discrimination vector with the choice of the negative ridge parameter $-\tau^2$, projected onto \mathcal{S} , is asymptotically orthogonal to these affine subspaces. As can be inspected from Figure 1, independent test data are asymptotically piled onto $\mathbf{v}_{-\tau^2}$, which is a second maximal data piling direction.

In this work, we show that, under generalized *heterogeneous* spiked covariance models, the second data piling phenomenon occurs when the dimension of data p grows while the sample size n is fixed, and a second maximal data piling direction can be also obtained purely from the training data. The spiked covariance models We assume that for $k = 1, 2$, the k th class has the covariance matrix $\Sigma_{(k)}$, which has m_k spikes such that m_k eigenvalues increase at the order of p^{β_k} as $p \rightarrow \infty$ while the other eigenvalues are nearly constant, averaging to

$\tau_k^2 > 0$. We say that $\Sigma_{(k)}$ has strong spikes if $\beta_k = 1$, or weak spikes if $0 \leq \beta_k < 1$. Also, we say that two covariance matrices have equal tail eigenvalues if $\tau_1^2 = \tau_2^2$, or unequal tail eigenvalues if $\tau_1^2 \neq \tau_2^2$.

Main Contributions We provide a complete characterization of the second data piling phenomenon under generalized heterogeneous spiked covariance models, which includes a wide range of scenarios where both covariance matrices have either strong spikes ($\beta_k = 1$) or weak spikes ($\beta_k < 1$), and have either equal tail eigenvalues ($\tau_1^2 = \tau_2^2$) or unequal tail eigenvalues ($\tau_1^2 \neq \tau_2^2$). We show that projections of independent test data tend to be respectively distributed along two affine subspaces, denoted \mathcal{L}_1 and \mathcal{L}_2 , in a low-dimensional subspace $\mathcal{S} \subset \mathcal{S}_{\mathcal{X}}$. The ‘signal’ subspace \mathcal{S} , spanned by some sample eigenvectors of \mathbf{S}_W and \mathbf{w}_{MDP} , is obtained by removing the noisy directions from $\mathcal{S}_{\mathcal{X}}$, and is also characterized for each of the scenarios. Unlike the homogeneous case, the affine subspaces \mathcal{L}_1 and \mathcal{L}_2 need not be parallel to each other. However, we reveal that there are two parallel affine subspaces of greater dimension, containing each of these affine subspaces, in \mathcal{S} . Also, under heterogeneous covariance assumptions, we find a somewhat counter-intuitive phenomenon that the eigenvectors of \mathbf{S}_W corresponding to the largest eigenvalues do not always contribute to \mathcal{S} , but some other seemingly unimportant eigenvectors capture important variability. Nonetheless, we show that second data piling occurs for any direction which is asymptotically perpendicular to the parallel affine subspaces. Moreover, we provide a unified view on the second *maximal* data piling direction: The second maximal data piling direction can be obtained by projecting \mathbf{w}_{MDP} onto the nullspace of the common leading eigenspace.

Based on the characterization of the second data piling phenomenon, we propose various linear classification rules that achieve perfect classification under heterogeneous covariance models. Firstly, for the case of weak spikes ($\beta_1, \beta_2 < 1$), we show that \mathbf{w}_{MDP} , which is a *ridgeless* estimator in the context of linear regression setting, also yields second data piling. We further show that a bias-corrected version of the original maximal data piling classification rule of Ahn and Marron (2010) achieves asymptotic perfect classification for this case. However, for the case of strong spikes ($\beta_1 = \beta_2 = 1$), linear classification rules based on \mathbf{w}_{MDP} do not provide the asymptotic perfect classification. For the case where $\beta_1 = \beta_2 = 1$ with equal tail eigenvalues ($\tau_1^2 = \tau_2^2$), we show that the *negatively* ridged linear discriminant vector, projected onto \mathcal{S} , can be a second maximal data piling direction even under heterogeneous covariance models. We further show that the original projected ridge classification rule of Chang et al. (2021) achieves perfect classification in more general settings. However, for the case of strong spikes and unequal tail eigenvalues ($\beta_1 = \beta_2 = 1$ and $\tau_1^2 \neq \tau_2^2$), the projected ridged linear discriminant vector may not be a second maximal data piling direction, or may not even yield second data piling for any ridge parameter. For all cases mentioned above, we propose Second Maximal Data Piling (SMDP) algorithms, which estimate a second maximal data piling direction by projecting \mathbf{w}_{MDP} onto the nullspace of the common leading eigenspace, based on a data-splitting approach, and compute discrimination rules based on the estimated directions. The resulting classifiers achieve asymptotic perfect classification for generalized heterogeneous spiked covariance models. Table 1 provides a summary of the classification rules discussed in this paper.

Our main contributions are summarized in the following:

1. A complete characterization of the second data piling phenomenon.

Setting	$0 \leq \beta_1, \beta_2 < 1$		$\beta_1 = \beta_2 = 1$		$0 \leq \beta_2 < \beta_1 = 1$	
	$\tau_1^2 = \tau_2^2$	$\tau_1^2 \neq \tau_2^2$	$\tau_1^2 = \tau_2^2$	$\tau_1^2 \neq \tau_2^2$	$\tau_1^2 = \tau_2^2$	$\tau_1^2 \neq \tau_2^2$
ϕ_{MDP}	✓*					
$\phi_{\text{b-MDP}}$	✓	✓				
$\phi_{\text{PRD},\alpha}$	✓*		✓*		✓	
$\phi_{\text{b-PRD},\alpha}$	✓	✓	✓	△	✓	✓
$\phi_{\text{SMDP-I}}$	✓	✓	✓	✓	✓	✓
$\phi_{\text{SMDP-II}}$	✓	✓	✓	✓	✓	✓

Table 1: Summary of the linear classification rules with respect to double data piling phenomenon discussed in this paper. See (7) for ϕ_{MDP} , (8) for $\phi_{\text{b-MDP}}$, (15) for $\phi_{\text{PRD},\alpha}$, (28) for $\phi_{\text{b-PRD},\alpha}$ and (19) and (20) for $\phi_{\text{SMDP-I}}$ and $\phi_{\text{SMDP-II}}$, respectively. Classification rules that can achieve asymptotic perfect classification under the corresponding setting are marked by ✓. Classification rules that can achieve asymptotic perfect classification under the corresponding setting only with further specific conditions are marked by △. Classification rules previously shown by Chang et al. (2021) to achieve asymptotic perfect classification under the homogeneous covariance model are additionally marked with *.

- a) We categorize the second data piling phenomenon by the magnitude of spikes with equal or unequal tail eigenvalues; see Section 3 and Appendix D.
 - b) We provide a unified view on the second maximal data piling direction for heterogeneous covariance models: The second maximal data piling direction can be obtained by projecting \mathbf{w}_{MDP} onto the nullspace of the common leading eigenspace; see Section 4.4.
2. Perfect classification based on the second data piling phenomenon.
- a) We show that the second data piling direction asymptotically interpolates independent test data, and thus can yield perfect classification.
 - b) We reveal exact conditions for which the projected ridged linear discriminant vector with a negative ridge parameter yields perfect classification, under the HDLSS asymptotics; see Sections 4.2–4.3 and Appendix C.
 - c) We develop Second Maximal Data Piling (SMDP) algorithms which ensure perfect classification for generalized heterogeneous spiked covariance models; see Section 4.5.

Related Works There has been relatively scarce work on binary classification problems with strongly-spiked heterogeneous covariances, which reflects much more realistic and interesting situations for HDLSS data. Aoshima and Yata (2019) proposed a distance-based classifier, while Ishii et al. (2022) proposed geometrical quadratic discriminant analysis for this problem. Both assume not only the dimension of data p but also training sample sizes of each class n_1 and n_2 tend to infinity to achieve perfect classification. Ishii (2020) proposed another distance-based classifier which achieves perfect classification even when n_1 and n_2

are fixed, but limited to the one-component covariance model (with $m_1 = m_2 = 1$). All of these works are based on a data transformation technique, which essentially projecting the independent test data onto the nullspace of the leading eigenspace. Our results are also based on a similar idea of removing the leading eigenspace, but we further suggest the concept of double data piling phenomenon and reveal the relationship between the maximal data piling direction of training data and the second maximal data piling direction of independent test data under generalized heterogeneous spiked covariance models.

It has been frequently observed that extremely complicated models which interpolate training data can also achieve nearly zero generalization error, which contradicts an important concept of the classical statistical learning framework in which a careful regularization is inevitable to achieve small generalization error (Zhang et al., 2017; Belkin et al., 2019). Recently, this phenomenon has been confirmed both empirically and theoretically in the context of linear regression (Bartlett et al., 2020; Holzmüller, 2020; Hastie et al., 2022), and it turned out that a (nearly) zero ridge parameter can be optimal in the overparameterized regime of $p > n$ (called *benign overfitting*). Kobak et al. (2020) showed that the optimal ridge parameter can be negative using one-component covariance model in the overparameterized regime, and Tsigler and Bartlett (2020) further showed that negative regularization can achieve small generalization error than nearly zero regularization under specific spiked covariance models. Wu and Xu (2020) also provided general conditions for which the optimal ridge parameter is negative in the overparameterized regime. Our findings are consistent with the above results concerning linear regression, and provide conditions when negative regularization is needed in the context of linear classification. Note that \mathbf{w}_{MDP} , which is a ridgeless estimator in the classification setting, successfully interpolates independent test data when the variables are weakly correlated. The projected ridged linear discriminant vector with a negative ridge parameter interpolates independent test data when the variables are strongly correlated and both classes have equal tail eigenvalues. In the linear classification setting, the generalization error of maximum margin classifiers is also examined in the overparameterized regime (Montanari et al., 2019; Chatterji and Long, 2021).

Organization The rest of this paper is organized as follows. In Section 2, we specifically define the generalized heterogeneous spiked covariance models. In Section 3, we characterize the second data piling phenomenon under the heterogeneous covariance models for $\beta_1 = \beta_2 = 1$ (Discussions for $\beta_1 < 1$ or $\beta_2 < 1$ are given in Appendix D). In Section 4, we study the case for which the projected ridged linear discriminant vector with a negative ridge parameter is a second maximal data piling direction. Also, we show that, in general, a second maximal data piling direction can be obtained by projecting \mathbf{w}_{MDP} onto the common leading eigenspace. By noting this fact, we propose Second Maximal Data Piling (SMDP) algorithms to estimate a second maximal data piling direction. In Section 5, we numerically confirm the performance of classification rules based on the projected ridged linear discriminant vector and SMDP algorithms through simulation studies and a real data example. Additional technical assumptions are given in Appendix A. We provide asymptotic properties of high-dimensional sample within-scatter matrix \mathbf{S}_W in Appendix B. The bias-corrected projected ridge classification rule is given in Appendix C. The proofs of main lemmas and theorems are contained in Appendix E.

2. Heterogeneous Covariance Models

We assume that for $k = 1, 2$, $X|\pi(X) = k$ follows an absolutely continuous distribution on \mathbb{R}^p with mean $\boldsymbol{\mu}_{(k)}$ and covariance matrix $\boldsymbol{\Sigma}_{(k)}$. Also, we assume $\mathbb{P}(\pi(X) = k) = \pi_k$, where $\pi_k > 0$ and $\pi_1 + \pi_2 = 1$. Write the eigen-decomposition of $\boldsymbol{\Sigma}_{(k)}$ by $\boldsymbol{\Sigma}_{(k)} = \mathbf{U}_{(k)}\boldsymbol{\Lambda}_{(k)}\mathbf{U}_{(k)}^\top$, where $\boldsymbol{\Lambda}_{(k)} = \text{Diag}(\lambda_{(k),1}, \dots, \lambda_{(k),p})$ in which the eigenvalues are arranged in descending order, and $\mathbf{U}_{(k)} = [\mathbf{u}_{(k),1}, \dots, \mathbf{u}_{(k),p}]$ for $k = 1, 2$. We make the following assumptions for generalized heterogeneous spiked covariance models.

Assumption 1 For the population mean difference vector $\boldsymbol{\mu} = \boldsymbol{\mu}_{(1)} - \boldsymbol{\mu}_{(2)}$, there exists $\delta > 0$ such that $p^{-1/2} \|\boldsymbol{\mu}\|_2 \rightarrow \delta$ as $p \rightarrow \infty$.

Assumption 2 For a fixed integer $m_k \geq 0$, $\sigma_{k,i}^2, \tau_{k,i}^2 > 0$ and $\beta_k \in [0, 1]$ ($k = 1, 2$), eigenvalues $\lambda_{(k),i} = \sigma_{k,i}^2 p^{\beta_k} + \tau_{k,i}^2$ for $1 \leq i \leq m_k$ and $\lambda_{(k),i} = \tau_{k,i}^2$ for $m_k + 1 \leq i \leq p$. Also, $\{\tau_{k,i}^2 : k = 1, 2, i = 1, 2, \dots\}$ is uniformly bounded and $p^{-1} \sum_{i=1}^p \tau_{k,i}^2 \rightarrow \tau_k^2$ as $p \rightarrow \infty$ for some $\tau_k^2 > 0$.

Assumption 1 ensures that nearly all variables are meaningfully contributing to discrimination (Hall et al., 2005; Qiao et al., 2010; Jung, 2018). Assumption 2 allows heterogeneous covariance matrices for different classes, including the homogeneous case, that is, $\boldsymbol{\Sigma}_{(1)} = \boldsymbol{\Sigma}_{(2)}$. We assume for $k = 1, 2$, $\boldsymbol{\Sigma}_{(k)}$ has m_k spikes, that is, m_k eigenvalues increase at the order of p^{β_k} as $p \rightarrow \infty$ while the other eigenvalues are nearly constant as τ_k^2 . We call the first m_k eigenvalues and their corresponding eigenvectors leading eigenvalues and eigenvectors of the k th class for $k = 1, 2$. Note that if $\beta_k > 1$, then $\boldsymbol{\Sigma}_{(k)}$ has extremely strong signals within the leading eigenspace, and thus the classification problem becomes trivial (Jung and Marron, 2009). Hence, we pay an attention to the cases of $\beta_1, \beta_2 \in [0, 1]$. In particular, we assume $\beta_1 = \beta_2 = 1$ throughout the main article, which is the most interesting and challenging setting, while the other cases where $\beta_1 < 1$ or $\beta_2 < 1$ are addressed in Appendix D. Also, we assume, without loss of generality, that $\tau_1^2 \geq \tau_2^2$ throughout the paper.

Remark 1 Assumption 2 may be relaxed so that the first m_k eigenvalues have different orders of magnitude, for example, for some $N_k > 0$, we may assume $\lambda_{(k),i} = \sigma_{k,i}^2 p^{\beta_{k,i}} + \tau_{k,i}^2$ for $1 \geq \beta_{k,1} \geq \dots \geq \beta_{k,N_k} \geq 0$. However, asymptotic results under this relaxed model are equivalent with the results under Assumption 2 with some m_k under the HDLSS asymptotic regime (see also Chang et al., 2021, Remark 2.1).

We write a $p \times m_k$ orthogonal matrix of leading eigenvectors of each class as $\mathbf{U}_{(k),1} = [\mathbf{u}_{(k),1}, \dots, \mathbf{u}_{(k),m_k}]$ for $k = 1, 2$. We call $\mathcal{U}_{(k)} = \text{span}(\mathbf{U}_{(k),1})$ the leading eigenspace of the k th class. Furthermore, let \mathcal{U} be the subspace spanned by the leading eigenvectors from both classes, that is,

$$\mathcal{U} = \text{span}([\mathbf{U}_{(1),1}, \mathbf{U}_{(2),1}]). \quad (2)$$

We call \mathcal{U} the common leading eigenspace of both classes. We assume that the dimension of \mathcal{U} ,

$$m = \dim(\mathcal{U}),$$

is a fixed constant for all p . We write an orthogonal basis of \mathcal{U} as $\mathbf{U}_1 = [\mathbf{u}_1, \dots, \mathbf{u}_m]$. Note that $\max(m_1, m_2) \leq m \leq m_1 + m_2$. In particular, if $m_1 = m_2 = 0$, then $\mathcal{U} = \mathbf{0}_p$ and $m = 0$. As indicated in Remark 1, asymptotic results with $m_k = 0$ ($k = 1, 2$) are equivalent to those under the weak spikes model ($\beta_k < 1$).

We assume that training dataset \mathcal{X} consists of X_{k1}, \dots, X_{kn_k} , which are independent and identically distributed random variables where $\pi(X_{kj}) = k$ for any $k = 1, 2$ and $1 \leq j \leq n_k$. Let $\mathbf{X}_k = [X_{k1}, \dots, X_{kn_k}]$ for $k = 1, 2$. We assume n_1 and n_2 are fixed and denote $\eta_k = n_k/n$ for $k = 1, 2$ where $n = n_1 + n_2$. We write class-wise sample mean vectors $\bar{X}_k = n_k^{-1} \sum_{j=1}^{n_k} X_{kj}$ and the total sample mean vector $\bar{X} = \eta_1 \bar{X}_1 + \eta_2 \bar{X}_2$. Also, we write $\mathbf{S}_k = (\mathbf{X}_k - \bar{\mathbf{X}}_k)(\mathbf{X}_k - \bar{\mathbf{X}}_k)^\top$ for $k = 1, 2$ where $\bar{\mathbf{X}}_k = \bar{X}_k \mathbf{1}_{n_k}^\top$ and the within-class scatter matrix $\mathbf{S}_W = \mathbf{S}_1 + \mathbf{S}_2$. We write an eigen-decomposition of \mathbf{S}_W by $\mathbf{S}_W = \hat{\mathbf{U}} \hat{\mathbf{\Lambda}} \hat{\mathbf{U}}^\top$, where $\hat{\mathbf{\Lambda}} = \text{Diag}(\hat{\lambda}_1, \dots, \hat{\lambda}_p)$ in which the eigenvalues are arranged in descending order, and $\hat{\mathbf{U}} = [\hat{\mathbf{u}}_1, \dots, \hat{\mathbf{u}}_p]$. Since $\hat{\lambda}_1 \geq \dots \geq \hat{\lambda}_{n-2} \geq \hat{\lambda}_{n-1} = \dots = \hat{\lambda}_p = 0$ with probability 1, we can write $\mathbf{S}_W = \hat{\mathbf{U}}_1 \hat{\mathbf{\Lambda}}_1 \hat{\mathbf{U}}_1^\top$ where $\hat{\mathbf{U}}_1 = [\hat{\mathbf{u}}_1, \dots, \hat{\mathbf{u}}_{n-2}]$ and $\hat{\mathbf{\Lambda}}_1 = \text{Diag}(\hat{\lambda}_1, \dots, \hat{\lambda}_{n-2})$. Also, we write $\hat{\mathbf{U}}_2 = [\hat{\mathbf{u}}_{n-1}, \dots, \hat{\mathbf{u}}_p]$. We denote the sample space as $\mathcal{S}_\mathcal{X}$, which is the $(n-1)$ -dimensional subspace spanned by $X_{kj} - \bar{X}$ for $k = 1, 2$ and $1 \leq j \leq n_k$. Note that the sample space $\mathcal{S}_\mathcal{X}$ can be equivalently expressed as $\text{span}(\hat{\mathbf{u}}_1, \dots, \hat{\mathbf{u}}_{n-2}, \mathbf{w}_{\text{MDP}})$ (Ahn and Marron, 2010; Chang et al., 2021). We denote the sample mean difference vector as $\mathbf{d} = \bar{X}_1 - \bar{X}_2$. Note that the sphered data matrix of \mathbf{X}_k is $\mathbf{Z}_k = \mathbf{\Lambda}_{(k)}^{-1/2} \mathbf{U}_{(k)}^\top (\mathbf{X}_k - \boldsymbol{\mu}_{(k)} \mathbf{1}_{n_k}^\top) = [\mathbf{z}_{k,1}, \dots, \mathbf{z}_{k,p}]^\top \in \mathbb{R}^{p \times n_k}$ for $k = 1, 2$. Then the elements of \mathbf{Z}_k are uncorrelated with each other, and have mean zero and unit variance.

We regulate the dependency of the true principal components $\mathbf{z}_{kj} = \mathbf{\Lambda}_{(k)}^{-1/2} \mathbf{U}_{(k)}^\top (X_{kj} - \boldsymbol{\mu}_{(k)}) \in \mathbb{R}^p$ ($k = 1, 2, 1 \leq j \leq n_k$) by introducing the concept of ρ -mixing condition. This allows us to make use of the law of large numbers applied to $p \rightarrow \infty$ introduced in Hall et al. (2005) and Jung and Marron (2009). We refer the reader to Kolmogorov and Rozanov (1960) and Bradley (2005) for a detailed explanation of ρ -mixing condition.

Assumption 3 *The elements of the p -vector \mathbf{z}_{kj} have uniformly bounded fourth moments, and for each p , \mathbf{z}_{kj} consists of the first p elements of an infinite random sequence*

$$(z_{k,1}, z_{k,2}, \dots)_j,$$

which is ρ -mixing under some permutation.

We define $\text{Angle}(\mathbf{w}_1, \mathbf{w}_2) := \arccos\{\mathbf{w}_1^\top \mathbf{w}_2 / (\|\mathbf{w}_1\|_2 \|\mathbf{w}_2\|_2)\}$ for $\mathbf{w}_1, \mathbf{w}_2 \in \mathbb{R}^p \setminus \{\mathbf{0}_p\}$. For $\mathbf{w} \in \mathbb{R}^p \setminus \{\mathbf{0}_p\}$ and a subspace \mathcal{V} of \mathbb{R}^p , let $P_\mathcal{V} \mathbf{w}$ be the orthogonal projection of \mathbf{w} onto \mathcal{V} and define $\text{Angle}(\mathbf{w}, \mathcal{V}) := \arccos\{\mathbf{w}^\top P_\mathcal{V} \mathbf{w} / (\|\mathbf{w}\|_2 \|P_\mathcal{V} \mathbf{w}\|_2)\}$. We also assume that limiting angles between leading eigenvectors and the population mean difference vector $\boldsymbol{\mu}$ exist as $p \rightarrow \infty$. Related technical assumptions are deferred to Appendix A (see Assumptions 4 and 5 therein). Let $\varphi \in (0, \pi/2]$ denote the limiting angle between $\boldsymbol{\mu}$ and \mathcal{U} . Throughout, we assume that $\varphi \neq 0$, that is, we do not consider the case where $\boldsymbol{\mu}$ lies within the common leading eigenspace \mathcal{U} . Lastly, we use the convention that if the dimension $m = 0$, then $\varphi = \pi/2$.

3. Data Piling of Independent Test Data

The *first data piling* refers to the phenomenon where projections of training data onto a direction vector $\mathbf{w} \in \mathbb{R}^p$ are piled on two distinct points in binary classification (Ahn and Marron, 2010). This first data piling phenomenon occurs whenever $p > n - 2$. Ahn and Marron (2010) revealed the existence of the *first maximal data piling* direction, \mathbf{w}_{MDP} in (1), which uniquely maximizes the distance between two piles of training data among directions exhibiting first data piling. While \mathbf{w}_{MDP} yields the first data piling, it does not generally yield the *second data piling* of independent test data (see Figure 1).

In this section, we show that independent test data, projected onto a low-dimensional signal subspace \mathcal{S} of the sample space $\mathcal{S}_{\mathcal{X}}$, tend to be respectively distributed along two affine subspaces as p increases. It should be emphasized that the second data piling phenomenon occurs asymptotically as $p \rightarrow \infty$, while the first data piling phenomenon occurs for any fixed $p > n - 2$. Chang et al. (2021) showed that there are two affine subspaces, each with dimension $m = m_1 = m_2$, such that they are parallel to each other if each class has common covariance matrix, that is, $\Sigma_{(1)} = \Sigma_{(2)}$. We show that if $\Sigma_{(1)} \neq \Sigma_{(2)}$, these affine subspaces may not be parallel to each other, but there exist *parallel* affine subspaces, of greater dimension, containing each of these affine subspaces.

In Section 3.1, we illustrate this phenomenon under various conditions on covariance matrices. In Section 3.2, we formally characterize the signal subspace \mathcal{S} , which captures important variability of independent test data, for each scenario of covariance matrices. In Section 3.3, we provide the main theorem (Theorem 3) that generalizes propositions in Section 3.1. Throughout, let \mathcal{Y}_k be an independent test data of the k th class whose element $Y \in \mathcal{Y}_k$ satisfies $\pi(Y) = k$ for $k = 1, 2$ and is independent to training data \mathcal{X} . Write $\mathcal{Y} = \mathcal{Y}_1 \cup \mathcal{Y}_2$.

3.1 Illustration of Second Data Piling

In this subsection, we investigate the phenomenon of data pile of independent test data in four scenarios. We consider various settings where the two covariance matrices $\Sigma_{(1)}$ and $\Sigma_{(2)}$ have either weak spikes or strong spikes, have either a common leading eigenvector or different leading eigenvectors, and have either equal tail eigenvalues or unequal tail eigenvalues.

Example 1 ($m = 0$) Consider the scaled identity covariance model, $\Sigma_{(1)} = \tau_1^2 \mathbf{I}_p$ and $\Sigma_{(2)} = \tau_2^2 \mathbf{I}_p$, which corresponds to the case of $m = 0$ and $\mathcal{U} = \mathbf{0}_p$. Figure 2 indicates that projections of \mathcal{Y}_1 and \mathcal{Y}_2 onto \mathbf{w}_{MDP} are piled on two distinct points, respectively, as well as projections of training data \mathcal{X} . Note that the piling locations of \mathcal{Y}_1 and \mathcal{Y}_2 do not coincide with each other, nor with those of \mathcal{X} . In this case, \mathbf{w}_{MDP} yields the second data piling for both cases of equal and unequal tail eigenvalues ($\tau_1^2 = \tau_2^2$ and $\tau_1^2 \neq \tau_2^2$). In fact, Hall et al. (2005) also observed that second data piling occurs with support vector machine (SVM) or distance-weighted discrimination (DWD) under proper conditions.

Next, we assume the one-component covariance model as follows:

$$\begin{aligned} \Sigma_{(1)} &= \sigma_{1,1}^2 p \mathbf{u}_{(1),1} \mathbf{u}_{(1),1}^\top + \tau_1^2 \mathbf{I}_p; \\ \Sigma_{(2)} &= \sigma_{2,1}^2 p \mathbf{u}_{(2),1} \mathbf{u}_{(2),1}^\top + \tau_2^2 \mathbf{I}_p. \end{aligned} \tag{3}$$

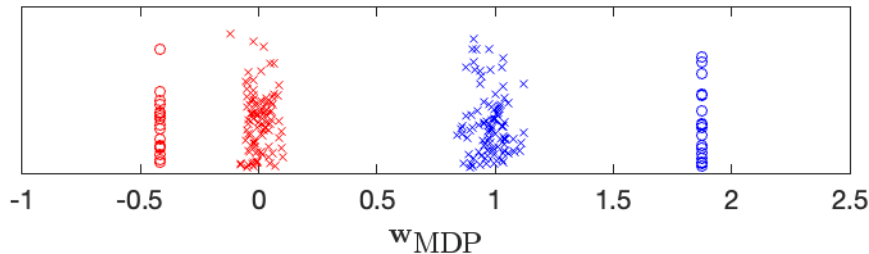


Figure 2: Projections of training data \mathcal{X} and independent test data \mathcal{Y} onto \mathbf{w}_{MDP} under the model in Example 1. The first and second data piling occur on \mathbf{w}_{MDP} . Note that this is a jitter plot with respect to the vertical axis.

Note that this model assumes that both classes have strongly correlated variables. First, we assume that two covariance matrices have equal tail eigenvalues, that is, $\tau_1^2 = \tau_2^2$. For the sake of simplicity, denote $\tau^2 := \tau_1^2 = \tau_2^2$.

Example 2 ($\mathbf{u}_{(1),1} = \mathbf{u}_{(2),1}$, $\tau_1^2 = \tau_2^2$ and $m = 1$) Consider the case where both classes have the common leading eigenvector, that is, $\mathbf{u}_{(1),1} = \mathbf{u}_{(2),1} = \mathbf{u}_1$. Note that if $\sigma_{1,1}^2 = \sigma_{2,1}^2$, then this model is equivalent to the homogeneous covariance model $\Sigma_{(1)} = \Sigma_{(2)}$, studied in Chang et al. (2021).

It turns out that the angle between $\hat{\mathbf{u}}_1$ and \mathbf{u}_1 converges to a random quantity between 0 and $\pi/2$, while $\hat{\mathbf{u}}_2, \dots, \hat{\mathbf{u}}_{n-2}$ are strongly inconsistent with \mathbf{u}_1 in the sense that $\text{Angle}(\hat{\mathbf{u}}_i, \mathbf{u}_1) \xrightarrow{P} \pi/2$ as $p \rightarrow \infty$ for $2 \leq i \leq n-2$ (Detailed explanations are given in Section 3.2 and Appendix B). We can check that even if $\sigma_{1,1}^2 \neq \sigma_{2,1}^2$, projections of independent test data \mathcal{Y} onto $\mathcal{S} = \text{span}(\hat{\mathbf{u}}_1, \mathbf{w}_{\text{MDP}})$ tend to be distributed along two parallel lines, while those of training data \mathcal{X} are piled on two distinct points along \mathbf{w}_{MDP} . This result is consistent with the findings of Chang et al. (2021) where $\Sigma_{(1)} = \Sigma_{(2)}$; see Figure 1. Also, the direction of these lines are asymptotically parallel to $P_{\mathcal{S}}\mathbf{u}_1$, which is the projection of common leading eigenvector \mathbf{u}_1 onto \mathcal{S} ; see Proposition 1.

Example 3 ($\mathbf{u}_{(1),1} \neq \mathbf{u}_{(2),1}$, $\tau_1^2 = \tau_2^2$ and $m = 2$) Two classes do not have a common leading eigenvector, that is, $\mathbf{u}_{(1),1} \neq \mathbf{u}_{(2),1}$. Under this model, the common leading eigenspace has the dimension $m = 2$ (In contrast, $m = 1$ in the model of Example 2).

In this case, the angle between $\hat{\mathbf{u}}_i$ and $\mathcal{U} = \text{span}(\mathbf{u}_{(1),1}, \mathbf{u}_{(2),1})$ converges to a random quantity between 0 and $\pi/2$ for $i = 1, 2$, while the other sample eigenvectors are strongly inconsistent with \mathcal{U} . In Figure 3, independent test data \mathcal{Y} projected onto $\mathcal{S}_1 = \text{span}(\hat{\mathbf{u}}_1, \mathbf{w}_{\text{MDP}})$ and $\mathcal{S}_2 = \text{span}(\hat{\mathbf{u}}_2, \mathbf{w}_{\text{MDP}})$ are also concentrated along lines, but in both subspaces these lines are not parallel to each other. However, within the 3-dimensional subspace $\mathcal{S} = \text{span}(\hat{\mathbf{u}}_1, \hat{\mathbf{u}}_2, \mathbf{w}_{\text{MDP}})$, there are two parallel 2-dimensional planes ($\mathcal{L}_1, \mathcal{L}_2$) that include these lines, one for each line. See Figure 3. In fact, \mathcal{Y}_1 is distributed along the direction $P_{\mathcal{S}}\mathbf{u}_{(1),1}$, while \mathcal{Y}_2 is distributed along the direction $P_{\mathcal{S}}\mathbf{u}_{(2),1}$. Thus, these lines are asymptotically contained in 2-dimensional affine subspaces, that are parallel to $P_{\mathcal{S}}\mathcal{U} := \text{span}(P_{\mathcal{S}}\mathbf{u}_{(1),1}, P_{\mathcal{S}}\mathbf{u}_{(2),1})$.

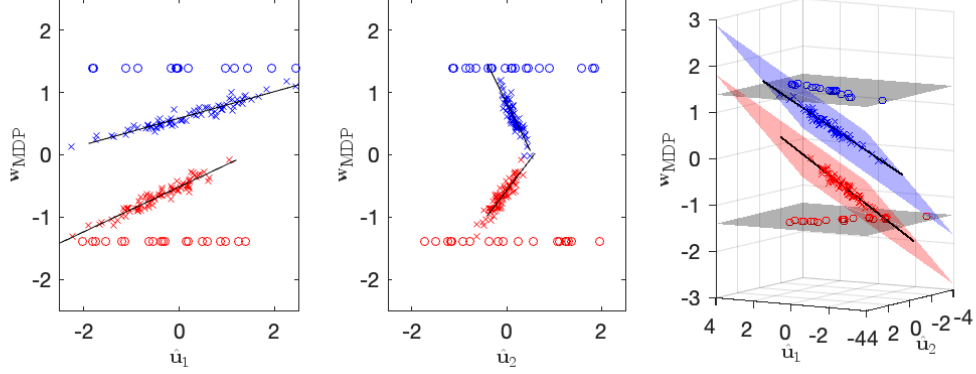


Figure 3: Projections of \mathcal{X} and \mathcal{Y} under the model in Example 3, onto $\mathcal{S}_1 = \text{span}(\hat{\mathbf{u}}_1, \mathbf{w}_{\text{MDP}})$, $\mathcal{S}_2 = \text{span}(\hat{\mathbf{u}}_2, \mathbf{w}_{\text{MDP}})$ and $\mathcal{S} = \text{span}(\hat{\mathbf{u}}_1, \hat{\mathbf{u}}_2, \mathbf{w}_{\text{MDP}})$. Second data piling occurs along the direction orthogonal to \mathcal{L}_1 and \mathcal{L}_2 (blue and red planes).

We formally state the above results. Write the scaled training data piling distance as

$$\kappa_{\text{MDP}} = p^{-1/2} \|\mathbf{w}_{\text{MDP}}^\top (\bar{X}_1 - \bar{X}_2)\|_2. \quad (4)$$

For $Y \in \mathcal{Y}$ and a subspace \mathcal{S} of \mathbb{R}^p , let $Y_{\mathcal{S}} = p^{-1/2} P_{\mathcal{S}} Y$, which is a scaled projection of Y onto \mathcal{S} . Similarly, write $\bar{X}_{\mathcal{S}} = p^{-1/2} P_{\mathcal{S}} \bar{X}$. Recall that $\mathbf{u}_1, \dots, \mathbf{u}_m$ are orthogonal basis of the common leading eigenspace $\mathcal{U} = \text{span}(\mathbf{u}_1, \dots, \mathbf{u}_m)$. Let projections of \mathbf{u}_i onto \mathcal{S} as $\mathbf{u}_{i,\mathcal{S}} = P_{\mathcal{S}} \mathbf{u}_i$ and write $\mathbf{U}_{1,\mathcal{S}} = [\mathbf{u}_{1,\mathcal{S}}, \dots, \mathbf{u}_{m,\mathcal{S}}]$. The following proposition states that for $m = 1, 2$, projections of \mathcal{Y} onto the $(m+1)$ -dimensional subspace $\mathcal{S} = \text{span}(\hat{\mathbf{u}}_1, \dots, \hat{\mathbf{u}}_m, \mathbf{w}_{\text{MDP}})$ are distributed along two m -dimensional affine subspaces, which become parallel to each other, and also to $P_{\mathcal{S}} \mathcal{U} := \text{span}(\mathbf{u}_{1,\mathcal{S}}, \dots, \mathbf{u}_{m,\mathcal{S}})$, as p increases.

Proposition 1 (One-spike, equal tail) *Suppose Assumptions 1–5 hold and assume $\beta_1 = \beta_2 = 1$, $\tau_1^2 = \tau_2^2$ and $m_1 = m_2 = 1$. Also,*

(i) *if $m = 1$ (Example 2), let $\mathcal{S} = \text{span}(\hat{\mathbf{u}}_1, \mathbf{w}_{\text{MDP}})$ and $\mathcal{L}_k = \{\mathbf{u}_{1,\mathcal{S}} t + \nu_k \mathbf{w}_{\text{MDP}} + \bar{X}_{\mathcal{S}} : t \in \mathbb{R}\}$,*

(ii) *if $m = 2$ (Example 3), let $\mathcal{S} = \text{span}(\hat{\mathbf{u}}_1, \hat{\mathbf{u}}_2, \mathbf{w}_{\text{MDP}})$ and $\mathcal{L}_k = \{\mathbf{U}_{1,\mathcal{S}} \mathbf{t} + \nu_k \mathbf{w}_{\text{MDP}} + \bar{X}_{\mathcal{S}} : \mathbf{t} \in \mathbb{R}^2\}$*

for $k = 1, 2$ where $\nu_1 = \kappa_{\text{MDP}}^{-1} (\eta_2 (1 - \cos^2 \varphi) \delta^2)$ and $\nu_2 = \kappa_{\text{MDP}}^{-1} (-\eta_1 (1 - \cos^2 \varphi) \delta^2)$. Then for any independent observation $Y \in \mathcal{Y}$ and for any $\epsilon > 0$,

$$\lim_{p \rightarrow \infty} \mathbb{P} \left(\inf_{a \in \mathcal{L}_k} \|Y_{\mathcal{S}} - a\| > \epsilon |\pi(Y) = k\right) = 0$$

for $k = 1, 2$.

Note that if $m = 1$, then \mathcal{Y}_k is concentrated along the line \mathcal{L}_k in $\mathcal{S} = \text{span}(\hat{\mathbf{u}}_1, \mathbf{w}_{\text{MDP}})$, for $k = 1, 2$. If $m = 2$, then \mathcal{Y}_k is concentrated along a line \mathcal{L}'_k , which is parallel to $P_{\mathcal{S}}\mathbf{u}_{(k),1}$ in $\mathcal{S} = \text{span}(\hat{\mathbf{u}}_1, \hat{\mathbf{u}}_2, \mathbf{w}_{\text{MDP}})$, for $k = 1, 2$. Then each of the 2-dimensional subspaces \mathcal{L}_1 and \mathcal{L}_2 contains \mathcal{L}'_1 and \mathcal{L}'_2 respectively, and these subspaces are parallel to each other.

We now investigate the case where two covariance matrices have unequal tail eigenvalues, that is, $\tau_1^2 \neq \tau_2^2$. Without loss of generality, assume $\tau_1^2 > \tau_2^2$. In the next example, we observe that asymptotic properties of eigenvectors of \mathbf{S}_W are different from the case of $\tau_1^2 = \tau_2^2$, and that unequal tail eigenvalues affects the behavior of data piling of independent test data.

Example 4 ($\mathbf{u}_{(1),1} \neq \mathbf{u}_{(2),1}$, $\tau_1^2 \neq \tau_2^2$ and $m = 2$) *Two classes do not have a common leading eigenvector, that is, $\mathbf{u}_{(1),1} \neq \mathbf{u}_{(2),1}$. Also, we assume $\tau_1^2 > \tau_2^2$ instead of $\tau_1^2 = \tau_2^2$ in Example 3. Note that in this case $m = 2$.*

Similarly to Example 3, $\hat{\mathbf{u}}_1$ captures the largest variation within the common leading eigenspace \mathcal{U} from the data. For the equal tail case (Example 3), $\hat{\mathbf{u}}_2$ always captures the remaining variation in \mathcal{U} . On the other hand, for the unequal tail case, the eigenvector that captures the remaining variation could be $\hat{\mathbf{u}}_{n_1}$ instead of $\hat{\mathbf{u}}_2$. This situation— $\text{span}(\hat{\mathbf{u}}_1, \hat{\mathbf{u}}_{n_1}, \mathbf{w}_{\text{MDP}})$ (rather than $\text{span}(\hat{\mathbf{u}}_1, \hat{\mathbf{u}}_2, \mathbf{w}_{\text{MDP}})$) captures the significant variations of independent test data \mathcal{Y} —is displayed in Figure 4.

Perhaps surprisingly, which eigenvector, $\hat{\mathbf{u}}_2$ or $\hat{\mathbf{u}}_{n_1}$, captures the variation is decided at random. To understand this phenomenon, recall the geometric representation of HDLSS data: Jung et al. (2012) showed that HDLSS data from a strongly spiked covariance model (that is, $\beta_k = 1$) can asymptotically be decomposed into random and deterministic parts; the random variation remains in $\text{span}(\mathbf{u}_{(k),1})$, while the deterministic simplex structure with edge length $\tau_k\sqrt{p}$ remains in the orthogonal complement of $\text{span}(\mathbf{u}_{(k),1})$. For sufficiently large p , $\hat{\mathbf{u}}_1$ explains the most important variation within $\mathcal{U} = \text{span}(\mathbf{u}_{(1),1}, \mathbf{u}_{(2),1})$ in the data from both classes. If the remaining variation within \mathcal{U} in the data from both classes is larger than $\tau_1^2 p$, then this variation is captured by $\hat{\mathbf{u}}_2$, while $\hat{\mathbf{u}}_3, \dots, \hat{\mathbf{u}}_{n_1}$ (and $\hat{\mathbf{u}}_{n_1+1}, \dots, \hat{\mathbf{u}}_{n-2}$) explain the deterministic simplex of data with edge length $\tau_1\sqrt{p}$ (and $\tau_2\sqrt{p}$) from the first (and second) class, respectively. In contrast, if the remaining variation is smaller than $\tau_1^2 p$, then the roles of $\hat{\mathbf{u}}_2$ and $\hat{\mathbf{u}}_{n_1}$ are reversed and $\hat{\mathbf{u}}_{n_1}$ explains the remaining variation. In Section 3.2 and Appendix B, we will see that this variation may be either larger or smaller than $\tau_1^2 p$ depending on the true leading principal components scores of training data \mathcal{X} .

The following proposition states that even if $\tau_1^2 \neq \tau_2^2$, projections of \mathcal{Y} onto a carefully chosen signal space \mathcal{S} are asymptotically contained in parallel affine subspaces. However, in this case, \mathcal{S} may not be the subspace spanned by the first m eigenvectors of \mathbf{S}_W and \mathbf{w}_{MDP} .

Proposition 2 (One-spike, unequal tail) *Suppose Assumptions 1–5 hold. Also, assume $\beta_1 = \beta_2 = 1$, $\tau_1^2 > \tau_2^2$ and $m_1 = m_2 = 1$.*

(i) *If $m = 1$, let $\mathcal{S} = \text{span}(\hat{\mathbf{u}}_1, \hat{\mathbf{u}}_{n_1}, \mathbf{w}_{\text{MDP}})$ and $\mathcal{L}_k = \{\mathbf{u}_{1,S}t + \nu_k \mathbf{w}_{\text{MDP}} + \bar{X}_S : t \in \mathbb{R}\}$*

(ii) *(Example 4) If $m = 2$, let*

$$\mathcal{S} = \begin{cases} \text{span}(\hat{\mathbf{u}}_1, \hat{\mathbf{u}}_{n_1}, \mathbf{w}_{\text{MDP}}) & \text{if } k_0 = 1, \\ \text{span}(\hat{\mathbf{u}}_1, \hat{\mathbf{u}}_2, \mathbf{w}_{\text{MDP}}) & \text{if } k_0 = 2, \end{cases}$$

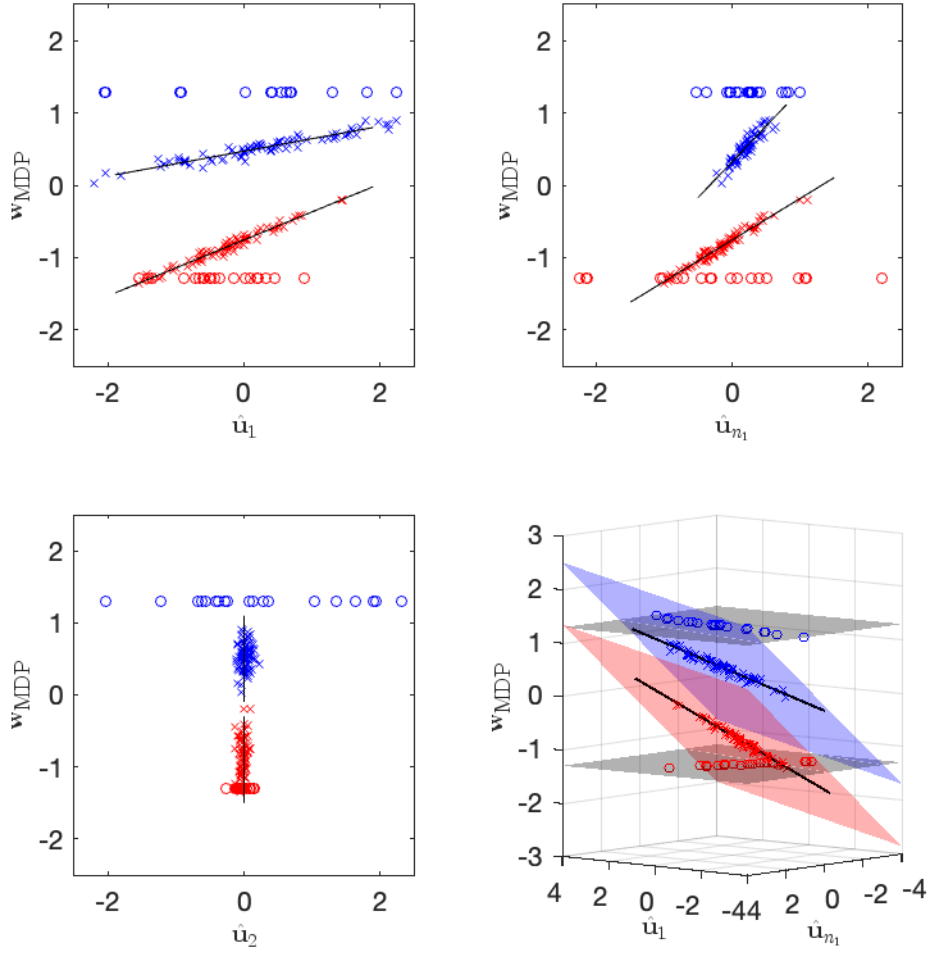


Figure 4: Projections of \mathcal{X} and \mathcal{Y} under the model in Example 4, onto $\mathcal{S}_1 = \text{span}(\hat{\mathbf{u}}_1, \mathbf{w}_{\text{MDP}})$, $\mathcal{S}_2 = \text{span}(\hat{\mathbf{u}}_2, \mathbf{w}_{\text{MDP}})$, $\mathcal{S}_{n_1} = \text{span}(\hat{\mathbf{u}}_{n_1}, \mathbf{w}_{\text{MDP}})$ and $\mathcal{S}_{1,n_1} = \text{span}(\hat{\mathbf{u}}_1, \hat{\mathbf{u}}_{n_1}, \mathbf{w}_{\text{MDP}})$. Second data piling occurs along the direction orthogonal to \mathcal{L}_1 and \mathcal{L}_2 (blue and red planes) in \mathcal{S}_{1,n_1} .

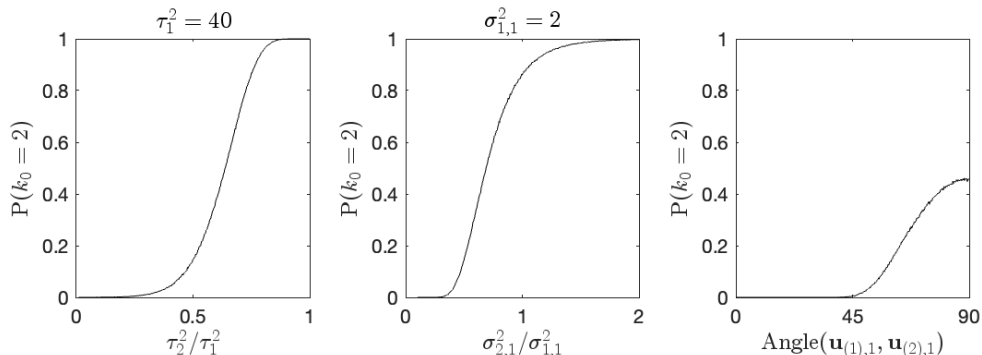


Figure 5: Average estimates of $\mathbb{P}(k_0 = 2)$, the probability that $\hat{\mathbf{u}}_2$ captures variability within \mathcal{U} instead of $\hat{\mathbf{u}}_{n_1}$ under the one-component model in Example 4 and Figure 4. $\mathbb{P}(k_0 = 2)$ is empirically estimated under the Gaussian assumption with $(\sigma_{1,1}^2, \sigma_{2,1}^2) = (2, 1)$, $(\tau_1^2, \tau_2^2) = (40, 20)$, $\text{Angle}(\mathbf{u}_{(1),1}, \mathbf{u}_{(2),1}) = \pi/4$ and $(n_1, n_2) = (20, 20)$. The panels show the average estimates with different τ_2^2 (left), $\sigma_{2,1}^2$ (middle), $\text{Angle}(\mathbf{u}_{(1),1}, \mathbf{u}_{(2),1})$ (right) while the other parameters are fixed, respectively.

where k_0 is a random variable depending on the true principal component scores of the training data \mathcal{X} (formally defined in Lemma 17 in Appendix B) and $\mathcal{L}_k = \{\mathbf{U}_{1,S}\mathbf{t} + \nu_k \mathbf{w}_{\text{MDP}} + \bar{X}_S : \mathbf{t} \in \mathbb{R}^2\}$

for $k = 1, 2$ where $\nu_1 = \kappa_{\text{MDP}}^{-1}(\eta_2(1 - \cos^2 \varphi)\delta^2 - (\tau_1^2 - \tau_2^2)/n)$ and $\nu_2 = \kappa_{\text{MDP}}^{-1}(-\eta_1(1 - \cos^2 \varphi)\delta^2 - (\tau_1^2 - \tau_2^2)/n)$. Then, for any independent observation $Y \in \mathcal{Y}$ and for any $\epsilon > 0$,

$$\lim_{p \rightarrow \infty} \mathbb{P} \left(\inf_{a \in \mathcal{L}_k} \|Y_S - a\| > \epsilon | \pi(Y) = k \right) = 0$$

for $k = 1, 2$.

Under the model in Example 4, $\mathbb{P}(k_0 = i)$ ($i = 1, 2$) depends on the magnitude of signals $\sigma_{1,1}^2$ and $\sigma_{2,1}^2$, the tail eigenvalues τ_1^2 and τ_2^2 , and the angle between $\mathbf{u}_{(1),1}$ and $\mathbf{u}_{(2),1}$. See Figure 5 for an illustration of $\mathbb{P}(k_0 = 2) = \mathbb{P}(\mathcal{S} = \text{span}(\hat{\mathbf{u}}_1, \hat{\mathbf{u}}_2, \mathbf{w}_{\text{MDP}}))$.

Remark 2 In Proposition 2 (i) where $m_1 = m_2 = m = 1$ and $\tau_1^2 > \tau_2^2$, $\hat{\mathbf{u}}_{n_1}$ always explains the variation of data along the common leading eigenvector $\mathbf{u}_1 = \mathbf{u}_{(1),1} = \mathbf{u}_{(2),1}$ while $\hat{\mathbf{u}}_2$ does not. In this case, projections of independent test data \mathcal{Y} onto the 3-dimensional subspace $\mathcal{S} = \text{span}(\hat{\mathbf{u}}_1, \hat{\mathbf{u}}_{n_1}, \mathbf{w}_{\text{MDP}})$ are concentrated along parallel lines.

3.2 Characterization of the Signal Subspace \mathcal{S}

In Section 3.1, we have observed that there exists a low-dimensional ‘signal’ subspace \mathcal{S} such that projections of independent test data \mathcal{Y} onto \mathcal{S} tend to lie on parallel affine subspaces,

τ_1^2, τ_2^2	\mathcal{D}	$ \mathcal{D} $
$\tau_1^2 = \tau_2^2$	$\{1, \dots, m\}$	m
$\tau_1^2 > \tau_2^2$	$\{1, \dots, k_0, k_0 + (n_1 - m_1), \dots, n_1 + m_2 - 1\}$	$m_1 + m_2$

Table 2: The index set \mathcal{D} for the strong spike case ($\beta_1 = \beta_2 = 1$). See Table 6 in Appendix D for cases with weak spikes. k_0 is a random number depending on the true principal component scores of training data \mathcal{X} defined in Lemma 17 in Appendix B.

one for each class. The subspace \mathcal{S} depends on the situations, and was $\text{span}(\mathbf{w}_{\text{MDP}})$, $\text{span}(\hat{\mathbf{u}}_1, \mathbf{w}_{\text{MDP}})$, $\text{span}(\hat{\mathbf{u}}_1, \hat{\mathbf{u}}_2, \mathbf{w}_{\text{MDP}})$ or $\text{span}(\hat{\mathbf{u}}_1, \hat{\mathbf{u}}_{n_1}, \mathbf{w}_{\text{MDP}})$ in Examples 1–4.

We now formally characterize the signal subspace \mathcal{S} for general cases. For this, we will utilize the index set $\mathcal{D} \subset \{1, \dots, n - 2\}$ collecting the indices of the sample eigenvectors of \mathbf{S}_W that are capable of explaining variations contained in the common leading eigenspace \mathcal{U} . In the examples of the previous subsection, $\mathcal{D} = \emptyset, \{1\}, \{1, 2\}$, and $\{1, n_1\}$, respectively.

As demonstrated in Section 3.1 for single-spike scenarios, the asymptotic behavior of the sample eigenvectors of \mathbf{S}_W varies significantly depending on whether the tail eigenvalues are equal or differ. In the more general case with m_1 and m_2 spikes, these differences in asymptotic behavior lead to distinct characterizations of \mathcal{D} , which are summarized in Table 2. Detailed derivations of this result are given in Appendix B. Here, we provide a summary of some important observations for strong spike models.

- If $\tau_1^2 = \tau_2^2$, then only the first m leading eigenvectors of \mathbf{S}_W can explain the variation within the common leading eigenspace \mathcal{U} (see Proposition 1 for the special single spike case).
- If $\tau_1^2 > \tau_2^2$, then there always exist $m_1 + m_2$ sample eigenvectors of \mathbf{S}_W explaining the variation within the common leading eigenspace \mathcal{U} , regardless of m . While the first m_1 sample eigenvectors are always capable of explaining this variation, some non-leading eigenvectors (after n_1 th) may capture variability within \mathcal{U} that could otherwise be explained by other leading eigenvectors beyond m_1 th. In particular, if $m = m_1$, then k_0 in Table 2 is m_1 with probability 1, that is, \mathcal{D} always consist of the first m_1 leading eigenvectors and m_2 non-leading eigenvectors (see Proposition 2 (i)). In general, k_0 is a random number depending on true leading principal component scores of \mathcal{X} , which is difficult to estimate in practice (see Proposition 2 (ii)).

In general, we define the signal subspace \mathcal{S} as

$$\mathcal{S} = \text{span}(\{\hat{\mathbf{u}}_i\}_{i \in \mathcal{D}}, \mathbf{w}_{\text{MDP}}), \quad (5)$$

where \mathcal{D} is given in Table 2. The signal subspace \mathcal{S} is a low-dimensional subspace of the sample space $\mathcal{S}_{\mathcal{X}}$, and is obtained by removing noisy directions in $\mathcal{S}_{\mathcal{X}}$. In case of $m = 0$, we use the convention of $\mathcal{D} = \emptyset$, that is, $\mathcal{S} = \text{span}(\mathbf{w}_{\text{MDP}})$.

3.3 Main Theorem

Propositions 1 and 2 are extended to general heterogeneous covariance models. Specifically, we establish that projections of \mathcal{Y} onto the signal subspace \mathcal{S} , defined in (5), are distributed

along parallel affine subspaces, one for each class, and that these affine subspaces do not overlap. Recall that κ_{MDP} , defined in (4), represents the training data piling distance.

Theorem 3 *Suppose Assumptions 1–5 hold. Let $\mathcal{S} = \text{span}(\{\hat{\mathbf{u}}_i\}_{i \in \mathcal{D}}, \mathbf{w}_{\text{MDP}})$, where \mathcal{D} is defined in Table 2 for each case. Let*

$$\mathcal{L}_k = \{\mathbf{U}_{1,\mathcal{S}}\mathbf{t} + \nu_k \mathbf{w}_{\text{MDP}} + \bar{X}_{\mathcal{S}} : \mathbf{t} \in \mathbb{R}^m\}$$

for $k = 1, 2$ where $\nu_1 = \kappa_{\text{MDP}}^{-1}(\eta_2(1 - \cos^2 \varphi)\delta^2 - (\tau_1^2 - \tau_2^2)/n)$ and $\nu_2 = \kappa_{\text{MDP}}^{-1}(-\eta_1(1 - \cos^2 \varphi)\delta^2 - (\tau_1^2 - \tau_2^2)/n)$. Then for any independent observation $Y \in \mathcal{Y}$ and for any $\epsilon > 0$,

$$\lim_{p \rightarrow \infty} \mathbb{P} \left(\inf_{a \in \mathcal{L}_k} \|Y_{\mathcal{S}} - a\| > \epsilon | \pi(Y) = k \right) = 0$$

for $k = 1, 2$.

If $m = 0$, projections of \mathcal{Y}_1 and \mathcal{Y}_2 are asymptotically piled on two distinct points on \mathbf{w}_{MDP} , one for each class (as seen in Example 1). For this special case, Theorem 3 remain valid with $\mathcal{L}_k = \{\nu_k \mathbf{w}_{\text{MDP}} + \bar{X}_{\mathcal{S}}\}$ for $k = 1, 2$ and $\cos^2 \varphi = 0$.

We remark that, in general, the test data from class 1, \mathcal{Y}_1 projected onto \mathcal{S} , are distributed along an m_1 -dimensional affine subspace \mathcal{L}'_1 . Similarly, projections of \mathcal{Y}_2 are distributed along an m_2 -dimensional affine subspace \mathcal{L}'_2 . Write the projections of $\mathbf{u}_{(k),i}$ ($k = 1, 2$) onto a subspace \mathcal{S} of \mathbb{R}^p as $\mathbf{u}_{(k),i,\mathcal{S}} = P_{\mathcal{S}}\mathbf{u}_{(k),i}$ and $\mathbf{U}_{(k),1,\mathcal{S}} = [\mathbf{u}_{(k),1,\mathcal{S}}, \dots, \mathbf{u}_{(k),m_k,\mathcal{S}}]$ for $k = 1, 2$. For each $k = 1, 2$, \mathcal{L}'_k is parallel to $\text{span}(\mathbf{U}_{(k),1,\mathcal{S}})$. While \mathcal{L}'_1 and \mathcal{L}'_2 are not necessarily parallel to each other, each of them are contained in the m -dimensional affine subspace \mathcal{L}_k (appeared in Theorem 3), respectively.

Theorem 3 tells that independent test data are asymptotically distributed along parallel m -dimensional affine subspaces \mathcal{L}_1 and \mathcal{L}_2 in \mathcal{S} . It implies that if we find a direction $\mathbf{w} \in \mathcal{S}$ such that \mathbf{w} is asymptotically orthogonal to \mathcal{L}_1 and \mathcal{L}_2 , then $P_{\mathbf{w}}\mathcal{Y}$ yields second data piling and in turn achieves perfect classification of independent test data. Since $\dim \mathcal{S} - m \geq 1$ for all cases, there always exists a direction $\mathbf{w} \in \mathcal{S}$ which yields second data piling. Meanwhile, any direction $\mathbf{w} \in \mathcal{S}_{\mathcal{X}} \setminus \mathcal{S}$ also yields second data piling since \mathbf{w} is asymptotically orthogonal to the common leading eigenspace \mathcal{U} , resulting in projections of \mathcal{Y}_1 and \mathcal{Y}_2 converge to a same location. Among the many second data piling directions, we will find a second maximal data piling direction, which provides asymptotic maximal distance between the two piles of independent test data.

4. Estimation of Second Maximal Data Piling Direction

In this section, we show that a *second maximal data piling* direction can be estimated from training data, and can provide classification rules which guarantee asymptotic perfect classification based on such direction.

We begin our development by investigating the special case of no spike ($m = 0$), for which \mathbf{w}_{MDP} is indeed a second data piling direction. We then show that some negatively ridged classification directions yield second data piling for some cases, but not for all cases. We then establish that a second maximal data piling direction is obtained by projecting \mathbf{w}_{MDP} onto the orthogonal complement of $\text{span}(\mathbf{U}_{1,\mathcal{S}})$, which is the nullspace of the common leading eigenspace \mathcal{U} . This insight is then used in estimating the second data piling direction.

4.1 The Case of No Spike

Recall that in Example 1 where there is no spike, projections of test data \mathcal{Y}_1 and \mathcal{Y}_2 onto \mathbf{w}_{MDP} are asymptotically piled on two distinct points, respectively. To be specific, Theorem 3 tells that for any independent observation $Y \in \mathcal{Y}$,

$$\frac{1}{\sqrt{p}} \mathbf{w}_{\text{MDP}}^\top (Y - \bar{X}) \xrightarrow{P} \begin{cases} \kappa^{-1}(\eta_2 \delta^2 - (\tau_1^2 - \tau_2^2)/n), & \pi(Y) = 1, \\ \kappa^{-1}(-\eta_1 \delta^2 - (\tau_1^2 - \tau_2^2)/n), & \pi(Y) = 2 \end{cases} \quad (6)$$

as $p \rightarrow \infty$ where κ is the probability limit of κ_{MDP} defined in (4), which implies that \mathbf{w}_{MDP} also yields second data piling of independent test data. In fact, it can be shown that \mathbf{w}_{MDP} is a second *maximal* data piling direction (when $m = 0$). In this non-spike case, the signal subspace \mathcal{S} is $\text{span}(\mathbf{w}_{\text{MDP}})$, and any direction $\mathbf{w} \in \mathcal{S}_X \setminus \mathcal{S} = \text{span}(\{\hat{\mathbf{u}}_i\}_{i=1}^{n-2})$ yields asymptotically zero piling distance of independent test data. Hence, \mathbf{w}_{MDP} gives an asymptotic maximal distance between two piles of independent test data among second data piling directions.

From (6), we can also check that the original maximal data piling classification rule (Ahn and Marron, 2010),

$$\phi_{\text{MDP}}(Y; \mathcal{X}) = \begin{cases} 1, & \mathbf{w}_{\text{MDP}}^\top (Y - \bar{X}) \geq 0, \\ 2, & \mathbf{w}_{\text{MDP}}^\top (Y - \bar{X}) < 0, \end{cases} \quad (7)$$

achieves perfect classification if $\tau_1^2 = \tau_2^2$. However, if $\tau_1^2 \neq \tau_2^2$, then ϕ_{MDP} may fail to achieve perfect classification, since the total mean threshold in ϕ_{MDP} should be adjusted by the bias term in (6). In the following, we provide a bias-corrected classification rule using \mathbf{w}_{MDP} to achieve asymptotic perfect classification even if $\tau_1^2 \neq \tau_2^2$.

Bias-corrected maximal data piling classification rule We define the bias-corrected maximal data piling classification rule as

$$\phi_{\text{b-MDP}}(Y; \mathcal{X}) = \begin{cases} 1, & p^{-1/2} \mathbf{w}_{\text{MDP}}^\top (Y - \bar{X}) - (\hat{\alpha}_1 - \hat{\alpha}_2)/(n\kappa_{\text{MDP}}) \geq 0, \\ 2, & p^{-1/2} \mathbf{w}_{\text{MDP}}^\top (Y - \bar{X}) - (\hat{\alpha}_1 - \hat{\alpha}_2)/(n\kappa_{\text{MDP}}) < 0, \end{cases} \quad (8)$$

where $\hat{\alpha}_k$ is an HDLSS-consistent estimator of $-\tau_k^2$ for $k = 1, 2$.

Note that $\hat{\lambda}_{(k),i}/p \xrightarrow{P} \tau_k^2$ as $p \rightarrow \infty$ for $m_k + 1 \leq i \leq n_k - 1$ (Jung et al., 2012), where $\hat{\lambda}_{(k),i}$ is i th largest eigenvalue of \mathbf{S}_k . Based on this fact, from now on, we fix

$$\hat{\alpha}_k = -\frac{1}{n_k - m_k - 1} \sum_{i=m_k+1}^{n_k-1} \frac{\hat{\lambda}_{(k),i}}{p} \quad (9)$$

for $k = 1, 2$.

4.2 Ridged Discriminant Directions and Second Maximal Data Piling

In this section, we reveal the relationship between ridged linear discriminant vectors and the second data piling phenomenon under various heterogeneous and spiked covariance

assumptions. The ridged linear discriminant (direction) vector \mathbf{w}_α is

$$\mathbf{w}_\alpha \propto \alpha_p (\mathbf{S}_W + \alpha_p \mathbf{I}_p)^{-1} \mathbf{d} = \sum_{i=1}^{n-2} \frac{\alpha_p}{\hat{\lambda}_i + \alpha_p} \hat{\mathbf{u}}_i \hat{\mathbf{u}}_i^\top \mathbf{d} + \hat{\mathbf{U}}_2 \hat{\mathbf{U}}_2^\top \mathbf{d}, \quad (10)$$

satisfying $\|\mathbf{w}_\alpha\|_2 = 1$, where $\alpha_p = \alpha p$ for a ridge parameter $\alpha \in \mathbb{R}$. Note that \mathbf{w}_{MDP} is a special case of \mathbf{w}_α since $\lim_{\alpha \rightarrow 0} \mathbf{w}_\alpha = \mathbf{w}_{\text{MDP}}$, that is, \mathbf{w}_{MDP} is a *ridgeless* estimator in the context of linear classification. In the next theorem, we observe that the ridged linear discriminant vector \mathbf{w}_α concentrates toward the signal subspace \mathcal{S} , defined in (5), in high dimensions under heterogeneous covariance assumptions.

Theorem 4 *Suppose Assumptions 1–5 hold. Let $\mathcal{S} = \text{span}(\{\hat{\mathbf{u}}_i\}_{i \in \mathcal{D}}, \mathbf{w}_{\text{MDP}})$ with \mathcal{D} be given in Table 2 for each case. For any $\alpha \in \mathbb{R} \setminus \{-\tau_1^2, -\tau_2^2\}$ for which (10) is defined, $\text{Angle}(\mathbf{w}_\alpha, \mathcal{S}) \xrightarrow{P} 0$ as $p \rightarrow \infty$.*

Based on this, we consider removing noise terms in \mathbf{w}_α and define a *projected* ridged linear discriminant vector \mathbf{v}_α ,

$$\mathbf{v}_\alpha \propto \sum_{i \in \mathcal{D}} \frac{\alpha_p}{\hat{\lambda}_i + \alpha_p} \hat{\mathbf{u}}_i \hat{\mathbf{u}}_i^\top \mathbf{d} + \hat{\mathbf{U}}_2 \hat{\mathbf{U}}_2^\top \mathbf{d} \quad (11)$$

satisfying $\|\mathbf{v}_\alpha\| = 1$. Note that if $m = 0$, $\mathbf{v}_\alpha = \mathbf{w}_{\text{MDP}}$ for any $\alpha \in \mathbb{R}$. Also, if $\Sigma_{(1)} = \Sigma_{(2)}$ with m strong spikes, then $\mathcal{D} = \{1, \dots, m\}$ and

$$\mathbf{v}_\alpha \propto \sum_{i=1}^m \frac{\alpha_p}{\hat{\lambda}_i + \alpha_p} \hat{\mathbf{u}}_i \hat{\mathbf{u}}_i^\top \mathbf{d} + \hat{\mathbf{U}}_2 \hat{\mathbf{U}}_2^\top \mathbf{d}, \quad (12)$$

which was also considered by Chang et al. (2021) for homogeneous cases. They showed that if $\Sigma_{(1)} = \Sigma_{(2)}$, then \mathbf{v}_α , for $\alpha = \hat{\alpha}$, is a second maximal data piling direction. Here, $\hat{\alpha}$ is any HDLSS-consistent estimator of $-\tau^2$. We will show that the results of Chang et al. (2021) can be generalized to the case where two populations have heterogeneous strongly-spiked covariance matrices but with equal tail eigenvalues ($\tau_1^2 = \tau_2^2 =: \tau^2$).

Recall that second data piling occurs when a direction $\mathbf{w} \in \mathcal{S}$ is asymptotically orthogonal to the common leading eigenspace \mathcal{U} . Theorem 5 confirms that $\mathbf{v}_{\hat{\alpha}}$ is such a direction, even if two populations do not have a common covariance matrix but equal tail eigenvalues. Moreover, both $P_{\mathbf{v}_{\hat{\alpha}}} \mathcal{Y}_1$ and $P_{\mathbf{v}_{\hat{\alpha}}} \mathcal{Y}_2$ asymptotically pile on two distinct points, respectively.

Theorem 5 *Suppose Assumptions 1–5 hold and assume $\beta_1 = \beta_2 = 1$ and $\tau_1^2 = \tau_2^2$. Then (i) for $\hat{\alpha}$ chosen as an HDLSS-consistent estimator of $-\tau^2$, $\text{Angle}(\mathbf{v}_{\hat{\alpha}}, \mathbf{u}_{i,\mathcal{S}}) \xrightarrow{P} \pi/2$ as $p \rightarrow \infty$ for $1 \leq i \leq m$. (ii) Moreover, for any independent observation $Y \in \mathcal{Y}$,*

$$\frac{1}{\sqrt{p}} \mathbf{v}_{\hat{\alpha}}^\top (Y - \bar{X}) \xrightarrow{P} \begin{cases} \gamma(\eta_2(1 - \cos^2 \varphi)\delta^2), & \pi(Y) = 1, \\ \gamma(-\eta_1(1 - \cos^2 \varphi)\delta^2), & \pi(Y) = 2 \end{cases} \quad (13)$$

as $p \rightarrow \infty$ where γ is a strictly positive random variable depending on the true principal component scores of \mathcal{X} .

We note that $\mathbf{v}_{\hat{\alpha}}$ can be obtained purely from the training data \mathcal{X} . Also, $\hat{\alpha}$ can be estimated purely from the sample eigenvalues of the pooled within-covariance matrix \mathbf{S}_W , since $\hat{\lambda}_i/p \xrightarrow{P} \tau^2$ for $m+1 \leq i \leq n-2$ as $p \rightarrow \infty$ (see Lemma 16). Throughout, we use

$$\hat{\alpha} = -\frac{1}{n-m-2} \sum_{i=m+1}^{n-2} \frac{\hat{\lambda}_i}{p}. \quad (14)$$

Our next result shows that any second data piling direction is asymptotically close to a linear combination of $\mathbf{v}_{\hat{\alpha}}$ and $\{\hat{\mathbf{u}}_i\}_{i=m+1}^{n-2}$ (the sample eigenvectors strongly-inconsistent with \mathcal{U}). Among the sequences of the second data piling directions, $\mathbf{v}_{\hat{\alpha}}$ provides a non-trivial distance between the two piles of independent test data, while all noisy directions $\{\hat{\mathbf{u}}_i\}_{i=m+1}^{n-2}$ do not. This naturally leads to the conclusion that $\mathbf{v}_{\hat{\alpha}}$ is a second maximal data piling direction. It can also be seen that the ‘closest’ direction to \mathbf{w}_{MDP} among the second data piling directions is in fact *maximal*. In the next theorem, \mathcal{A} (or \mathfrak{W}_X) represents the collection of sequences of second data piling directions (or directions in sample space, respectively).

Theorem 6 *Suppose Assumptions 1–5 hold and assume $\beta_1 = \beta_2 = 1$ and $\tau_1^2 = \tau_2^2$.*

- (i) *For any given $\{\mathbf{w}\} \in \mathcal{A}$, there exists a sequence $\{\mathbf{v}\} \in \mathcal{B}$ such that $\|\mathbf{w} - \mathbf{v}\| \xrightarrow{P} 0$ as $p \rightarrow \infty$, where $\mathcal{B} = \left\{ \{\mathbf{v}\} \in \mathfrak{W}_X : \mathbf{v} \in \text{span}(\mathbf{v}_{\hat{\alpha}}) \oplus \text{span}(\{\hat{\mathbf{u}}_i\}_{i=m+1}^{n-2}) \right\}$.*
- (ii) *For any $\{\mathbf{w}\} \in \mathcal{A}$ such that $D(\mathbf{w})$ exists, $\{\mathbf{w}\} \in \mathcal{A}$ is a sequence of second maximal data piling directions if and only if $\|\mathbf{w} - \mathbf{v}_{\hat{\alpha}}\| \xrightarrow{P} 0$ as $p \rightarrow \infty$.*

Note that from (13), the original projected ridge classification rule $\phi_{\text{PRD},\alpha}(Y; \mathcal{X})$ for a given α (Chang et al., 2021),

$$\phi_{\text{PRD},\alpha}(Y; \mathcal{X}) = \begin{cases} 1, & \mathbf{v}_{\alpha}^{\top}(Y - \bar{X}) \geq 0, \\ 2, & \mathbf{v}_{\alpha}^{\top}(Y - \bar{X}) < 0, \end{cases} \quad (15)$$

with $\mathcal{D} = \{1, \dots, m\}$ also achieves perfect classification when $\alpha := \hat{\alpha}$, as long as the tail eigenvalues are equal. Thus, our result extends the conclusion of Chang et al. (2021) in the sense that $\phi_{\text{PRD},\alpha}$ yields perfect classification not only in case of $\Sigma_{(1)} = \Sigma_{(2)}$ but also in case of $\Sigma_{(1)} \neq \Sigma_{(2)}$ and $\tau_1^2 = \tau_2^2$.

Remark 3 *It can be shown that $\phi_{\text{PRD},\alpha}$ achieves perfect classification only at a negative ridge parameter $\alpha := -\tau^2$ when $\tau_1^2 = \tau_2^2$ with a regularizing condition on the distribution of $(\mathbf{z}_{k,1}, \dots, \mathbf{z}_{k,m_k})^{\top}$ for $k = 1, 2$ as in Theorem 3.7 of Chang et al. (2021).*

4.3 Second Maximal Data Piling under Unequal Tails

In this section, we focus on the unequal tail eigenvalues case ($\tau_1^2 > \tau_2^2$), and reveal the situations under which \mathbf{v}_{α} does not yield second maximal data piling. For clearer presentation, we investigate two cases of simple one-spike models (with $m_1 = 1$ and $m_2 = 1$).

4.3.1 ONE-SPIKE MODEL WITH COMMON LEADING EIGENSPACE

Recall from Section 3.1 that if $\mathbf{u}_{(1),1} = \mathbf{u}_{(2),1} = \mathbf{u}_1$ (i.e., $m = 1$), then \mathcal{S} is $\text{span}(\hat{\mathbf{u}}_1, \hat{\mathbf{u}}_{n_1}, \mathbf{w}_{\text{MDP}})$ and $\dim \mathcal{S} - m = 2$. It implies that there may exist two second data piling directions that are orthogonal to each other and to $\mathbf{u}_{1,\mathcal{S}}$. This is in fact true, and Proposition 7 below shows that both $\mathbf{v}_{\hat{\alpha}_1}$ and $\mathbf{v}_{\hat{\alpha}_2}$ are asymptotically orthogonal to \mathbf{u}_1 . Also, the two piles of $P_{\mathbf{v}_{\hat{\alpha}_k}} \mathcal{Y}_1$ and $P_{\mathbf{v}_{\hat{\alpha}_k}} \mathcal{Y}_2$ are apart from each other.

Proposition 7 *Suppose Assumptions 1–5 hold and assume $\beta_1 = \beta_2 = 1$, $\tau_1^2 > \tau_2^2$ and $m_1 = m_2 = m = 1$. Then (i) for $\hat{\alpha}_k$ chosen as an HDLSS-consistent estimator of $-\tau_k^2$, $\text{Angle}(\mathbf{v}_{\hat{\alpha}_k}, \mathbf{u}_{1,\mathcal{S}}) \xrightarrow{P} \pi/2$ as $p \rightarrow \infty$ for $k = 1, 2$. (ii) Also, $\text{Angle}(\mathbf{v}_\alpha, \mathbf{u}_{1,\mathcal{S}}) \xrightarrow{P} \pi/2$ as $p \rightarrow \infty$ if and only if $\alpha = -\tau_1^2$ or $\alpha = -\tau_2^2$. (iii) Moreover, for any independent observation $Y \in \mathcal{Y}$ and $k = 1, 2$,*

$$\frac{1}{\sqrt{p}} \mathbf{v}_{\hat{\alpha}_k}^\top (Y - \bar{X}) \xrightarrow{P} \begin{cases} \gamma_k(\eta_2(1 - \cos^2 \varphi)\delta^2 - (\tau_1^2 - \tau_2^2)/n), & \pi(Y) = 1, \\ \gamma_k(-\eta_1(1 - \cos^2 \varphi)\delta^2 - (\tau_1^2 - \tau_2^2)/n), & \pi(Y) = 2 \end{cases} \quad (16)$$

as $p \rightarrow \infty$ where γ_k ($k = 1, 2$) is a strictly positive random variable depending on the true principal component scores of \mathcal{X} .

Remark 4 *From (16), if $\tau_1^2 \neq \tau_2^2$, we can check that $\phi_{\text{PRD},\alpha}$ in (15) may fail to achieve perfect classification due to the bias term. However, we can still achieve perfect classification using \mathbf{v}_α with a bias-correction strategy. This bias correction is similar to (8) used for non-spike case. The bias-corrected projected ridge classification rule $\phi_{\text{b-PRD},\alpha}$ is given in Appendix C (See (28)), and ensures asymptotic perfect classification under common leading eigenspace conditions.*

In contrast to the equal-tail case discussed in Section 4.2, \mathbf{v}_α achieves perfect classification with two negative ridge parameters. This naturally raises the question of which, between $\mathbf{v}_{\hat{\alpha}_1}$ and $\mathbf{v}_{\hat{\alpha}_2}$, results in a larger asymptotic distance between the two piles of independent test data.

Writing $D(\mathbf{w})$ for the asymptotic distance between the two piles of independent test data projected on $\{\mathbf{w}\} \in \mathcal{A}$, Proposition 7 establishes that $D(\mathbf{v}_{\hat{\alpha}_k}) = \gamma_k(1 - \cos^2 \varphi)\delta^2$ (for $k = 1, 2$). Although this distance is not intuitive to interpret, our next result demonstrates that neither $\mathbf{v}_{\hat{\alpha}_1}$ nor $\mathbf{v}_{\hat{\alpha}_2}$ necessarily gives a larger asymptotic distance of the two piles than the other.

Theorem 8 *Suppose Assumptions 1–5 hold and assume $\beta_1 = \beta_2 = 1$, $\tau_1^2 > \tau_2^2$ and $m_1 = m_2 = m = 1$. Then,*

(i) $D(\mathbf{v}_{\hat{\alpha}_1}) \leq D(\mathbf{v}_{\hat{\alpha}_2}) \Leftrightarrow \tau_1^{-2} \Phi_1 \leq \tau_2^{-2} \Phi_2$ where Φ_1 (and Φ_2) are the sum of squared scores of the first principal component of the first (and second, respectively) class [see (22)].

(ii) *If the distribution of $X|\pi(X) = k$ is Gaussian, then for $F \sim F(n_1 - 1, n_2 - 1)$,*

$$\zeta = \mathbb{P}(\tau_1^{-2} \Phi_1 \leq \tau_2^{-2} \Phi_2) = \mathbb{P}\left(F \leq \frac{(n_2 - 1)\tau_2^{-2}\sigma_{2,1}^2}{(n_1 - 1)\tau_1^{-2}\sigma_{1,1}^2}\right).$$

In Theorem 8, $\tau_k^{-2}\sigma_{k,1}^2$ can be understood as a signal-to-noise ratio of the k th class.

Our next question is whether $\mathbf{v}_{\hat{\alpha}_1}$ or $\mathbf{v}_{\hat{\alpha}_2}$ can be a second maximal data piling direction or not. If not, which direction in $\mathcal{S} = \text{span}(\hat{\mathbf{u}}_1, \hat{\mathbf{u}}_{n_1}, \mathbf{w}_{\text{MDP}})$ gives an asymptotic maximal distance between the two piles of independent test data?

To answer these questions, recall that second data piling occurs when a direction $\mathbf{w} \in \mathcal{S}$ is asymptotically orthogonal to $\mathbf{u}_{1,\mathcal{S}} = (\hat{\mathbf{u}}_1^\top \mathbf{u}_1)\hat{\mathbf{u}}_1 + (\hat{\mathbf{u}}_{n_1}^\top \mathbf{u}_1)\hat{\mathbf{u}}_{n_1} + (\mathbf{w}_{\text{MDP}}^\top \mathbf{u}_1)\mathbf{w}_{\text{MDP}}$, and there are (infinitely) many sets of two linearly independent directions in \mathcal{S} , both orthogonal to $\mathbf{u}_{1,\mathcal{S}}$.

Our choices (which turns out to be optimal) of two directions are obtained as follows. Since \mathbf{w}_{MDP} plays a distinct role among the basis of \mathcal{S} , let $\mathbf{f}_1 \in \mathcal{S}$ be the vector orthogonal to both $\mathbf{u}_{1,\mathcal{S}}$ and \mathbf{w}_{MDP} . To be specific, $\mathbf{f}_1 \propto (-\hat{\mathbf{u}}_{n_1}^\top \mathbf{u}_1)\hat{\mathbf{u}}_1 + (\hat{\mathbf{u}}_1^\top \mathbf{u}_1)\hat{\mathbf{u}}_{n_1}$. The vector $\mathbf{f}_0 \in \mathcal{S}$ parallel to the nullspace of $[\mathbf{f}_1, \mathbf{u}_{1,\mathcal{S}}]$ completes the pair. It turns out that \mathbf{f}_0 is the orthogonal projection of \mathbf{w}_{MDP} onto the orthogonal complement of $\text{span}(\mathbf{u}_{1,\mathcal{S}})$ within \mathcal{S} . Projections of the test data onto \mathbf{f}_0 and \mathbf{f}_1 are discussed next.

Proposition 9 *Suppose Assumptions 1–5 hold and assume $\beta_1 = \beta_2 = 1$, $\tau_1^2 > \tau_2^2$ and $m_1 = m_2 = m = 1$. Then, for any independent observation $Y \in \mathcal{Y}$, the following holds. (i) $p^{-1/2}\mathbf{f}_1^\top(Y - \bar{X}) \xrightarrow{P} 0$ as $p \rightarrow \infty$ whenever $\pi(Y) = 1$ or $\pi(Y) = 2$. (ii)*

$$\frac{1}{\sqrt{p}}\mathbf{f}_0^\top(Y - \bar{X}) \xrightarrow{P} \begin{cases} v_0(\eta_2(1 - \cos^2 \varphi)\delta^2 - (\tau_1^2 - \tau_2^2)/n), & \pi(Y) = 1, \\ v_0(-\eta_1(1 - \cos^2 \varphi)\delta^2 - (\tau_1^2 - \tau_2^2)/n), & \pi(Y) = 2 \end{cases}$$

as $p \rightarrow \infty$ where v_0 is a strictly positive random variable depending on the true principal component scores of \mathcal{X} . (iii) $v_0 > \max\{\gamma_1, \gamma_2\}$ with probability 1, where γ_k is defined in Proposition 7.

Proposition 9 implies that \mathbf{f}_0 provides the largest asymptotic distance between the two piles of independent test data ((i) and (ii)) and in particular, the piling gap is larger than those from $\mathbf{v}_{\hat{\alpha}_1}$ and $\mathbf{v}_{\hat{\alpha}_2}$ (iii). In contrast, \mathbf{f}_1 is not a meaningful second data piling direction since both of $P_{\mathbf{f}_1}\mathcal{Y}_1$ and $P_{\mathbf{f}_1}\mathcal{Y}_2$ converge to a same location.

These findings are graphically displayed in Figure 6. The left panel displays the data on $\mathcal{T}_{1,n_1} = \text{span}(\hat{\mathbf{u}}_1, \hat{\mathbf{u}}_{n_1})$, where the ‘meaningless’ direction \mathbf{f}_1 lies. Although test data projected on \mathbf{f}_1 exhibit second data piling, the piling gap is nearly zero.

The right panel of Figure 6 shows that $\mathbf{f}_0 \in \mathcal{S}$, which is orthogonal to both of $\mathbf{u}_{1,\mathcal{S}}$ and \mathbf{f}_1 , gives a meaningful distance between the two piles of independent test data \mathcal{Y} . It naturally implies that \mathbf{f}_0 is a second maximal data piling direction. Neither $\mathbf{v}_{\hat{\alpha}_1}$ nor $\mathbf{v}_{\hat{\alpha}_2}$ is a second maximal data piling direction since these classifiers are affected by the meaningless direction \mathbf{f}_1 .

4.3.2 GENERAL ONE-SPIKE MODEL WITH HETEROGENEOUS LEADING EIGENSPACE

We now consider the general case of heterogeneous leading eigenvectors. In this case, $\mathbf{u}_{(1),1} \neq \mathbf{u}_{(2),1}$ and $m = 2$, and the signal subspace \mathcal{S} is given at random (either $\mathcal{S} = \text{span}(\hat{\mathbf{u}}_1, \hat{\mathbf{u}}_2, \mathbf{w}_{\text{MDP}})$ or $\text{span}(\hat{\mathbf{u}}_1, \hat{\mathbf{u}}_{n_1}, \mathbf{w}_{\text{MDP}})$), depending on the true leading principal component scores. Although a second data piling occurs for a direction orthogonal to the 2-dimensional common leading eigenspace $P_{\mathcal{S}}\mathcal{U} := \text{span}(\mathbf{u}_{(1),1,\mathcal{S}}, \mathbf{u}_{(2),1,\mathcal{S}})$, it is impossible to

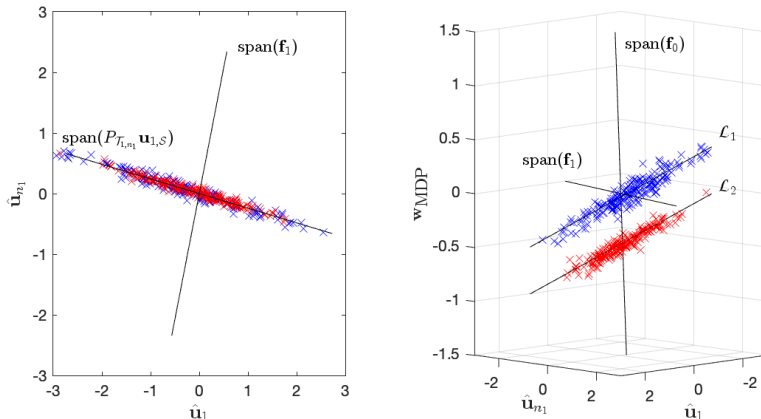


Figure 6: 2-dimensional projections onto $\mathcal{T}_{1,n_1} = \text{span}(\hat{\mathbf{u}}_1, \hat{\mathbf{u}}_{n_1})$ and 3-dimensional projections onto $\mathcal{S} = \mathcal{T}_{1,n_1} \oplus \text{span}(\mathbf{w}_{\text{MDP}})$ of independent test data \mathcal{Y} under the unequal-tail model with $m_1 = m_2 = m = 1$.

determine the random \mathcal{S} . This indeterminacy of \mathcal{S} precludes the use of \mathbf{v}_α (which is the ridge direction projected on \mathcal{S}). It turns out that even if we knew \mathcal{S} , there is no \mathbf{v}_α , for any $\alpha \in \mathbb{R}$, that yields second data piling.

Proposition 10 *Suppose Assumptions 1–5 hold and assume $\beta_1 = \beta_2 = 1$, $\tau_1^2 > \tau_2^2$, $m_1 = m_2 = 1$ and $m = 2$. For any given training data \mathcal{X} and $\hat{\alpha}_k$ chosen as an HDLSS-consistent estimator of $-\tau_k^2$, (i) $\text{Angle}(\mathbf{v}_{\hat{\alpha}_k}, \mathbf{u}_{(k),1,\mathcal{S}}) \xrightarrow{P} \pi/2$ as $p \rightarrow \infty$ for $k = 1, 2$. (ii) However, $\{\mathbf{v}_\alpha\} \notin \mathcal{A}$ for any ridge parameter $\alpha \in \mathbb{R}$.*

Proposition 10 shows that $\mathbf{v}_{\hat{\alpha}_k}$ is asymptotically orthogonal to $\mathbf{u}_{(k),1}$, which is the leading eigenvector of the k th class, but not asymptotically orthogonal to both of $\mathbf{u}_{(1),1}$ and $\mathbf{u}_{(2),1}$. Thus, the projected ridge classifier does not necessarily provides perfect classification.

We note that the conclusion of Proposition 10 remains valid for general m_k -spike cases.

Remark 5 *In the special case that the leading eigenspace of the one class includes that of the other class (that is, $\mathcal{U} = \mathcal{U}_{(k)}$), \mathbf{v}_α can yield second data piling with the negative ridge parameter $-\tau_k^2$. Moreover, in such cases, the bias-corrected projected ridge classification rule $\phi_{\text{b-PRD},\alpha}$ (defined in (28)) can achieve asymptotic perfect classification. See Appendix C for further discussion.*

4.4 Second Maximal Data Piling Direction for General Heterogeneous Spiked Covariance

So far, we have seen that \mathbf{v}_α may not be a second maximal data piling direction, and may not even yield second data piling for any ridge parameter $\alpha \in \mathbb{R}$. In this subsection, we extend discussions in Sections 4.2 and 4.3 to the general cases $m_1 \geq 1$ and $m_2 \geq 1$ and investigate a theoretical second maximal data piling direction.

Building on the discussions in Section 4.3 and Figure 6, we decompose the signal space $\mathcal{S} = \text{span}(\{\hat{\mathbf{u}}_i\}_{i \in \mathcal{D}}) \oplus \text{span}(\mathbf{w}_{\text{MDP}})$ into three orthogonal parts:

$$\mathcal{S} = \text{span}(\mathbf{U}_{1,\mathcal{S}}) \oplus \text{span}(\mathbf{U}_{1,\mathcal{S}}^\perp) = \text{span}(\mathbf{U}_{1,\mathcal{S}}) \oplus \mathcal{T}_p \oplus \text{span}(\mathbf{f}_0).$$

Here, $\text{span}(\mathbf{U}_{1,\mathcal{S}})$ is the subspace to which the second data piling directions are orthogonal. The orthogonal complement of $\text{span}(\mathbf{U}_{1,\mathcal{S}})$ within \mathcal{S} , $\text{span}(\mathbf{U}_{1,\mathcal{S}}^\perp)$ is further decomposed into ‘useless’ data piling part $\mathcal{T}_p := \text{span}(\{\hat{\mathbf{u}}_i\}_{i \in \mathcal{D}}) \cap \text{span}(\mathbf{U}_{1,\mathcal{S}}^\perp)$ and the rest. The dimension of \mathcal{T}_p is $m_1 + m_2 - m$, which is nonnegative but can be zero (depending on the model parameters). The last part, $\text{span}(\mathbf{f}_0)$, is $\text{span}(\mathbf{U}_{1,\mathcal{S}}^\perp) \setminus \mathcal{T}_p$, for which \mathbf{f}_0 is the orthogonal projection of \mathbf{w}_{MDP} onto $\text{span}(\mathbf{U}_{1,\mathcal{S}}^\perp)$.

Next result confirms that \mathcal{T} is indeed not useful, and also characterized the piling distance on \mathbf{f}_0 .

Theorem 11 *Suppose Assumptions 1–5 hold and assume $\beta_1 = \beta_2 = 1$, $\tau_1^2 > \tau_2^2$. Then,*

(i) *For any $\{\mathbf{w}\} \in \mathcal{T} = \{\{\mathbf{w}\} \in \mathfrak{W}_X : \mathbf{w} \in \mathcal{T}_p \text{ for all } p\}$ and any independent observation $Y \in \mathcal{Y}$, $p^{-1/2} \mathbf{w}^\top (Y - \bar{X}) \xrightarrow{P} 0$ as $p \rightarrow \infty$ whenever $\pi(Y) = 1$ or $\pi(Y) = 2$.*

(ii) *For any independent observation $Y \in \mathcal{Y}$,*

$$\frac{1}{\sqrt{p}} \mathbf{f}_0^\top (Y - \bar{X}) \xrightarrow{P} \begin{cases} v_0(\eta_2(1 - \cos^2 \varphi)\delta^2 - (\tau_1^2 - \tau_2^2)/n), & \pi(Y) = 1, \\ v_0(-\eta_1(1 - \cos^2 \varphi)\delta^2 - (\tau_1^2 - \tau_2^2)/n), & \pi(Y) = 2 \end{cases}$$

as $p \rightarrow \infty$ with a strictly positive random variable v_0 .

The above result naturally implies that \mathbf{f}_0 is a second maximal data piling direction, as we state next.

Theorem 12 *Suppose Assumptions 1–5 hold and assume $\beta_1 = \beta_2 = 1$, $\tau_1^2 > \tau_2^2$. Then,*

(i) *For any given $\{\mathbf{w}\} \in \mathcal{A}$, there exists a sequence $\{\mathbf{v}\} \in \mathcal{B}$ such that $\|\mathbf{w} - \mathbf{v}\| \xrightarrow{P} 0$ as $p \rightarrow \infty$, where $\mathcal{B} = \left\{ \{\mathbf{v}\} \in \mathfrak{W}_X : \mathbf{v} \in \text{span}(\mathbf{f}_0) \oplus \mathcal{T}_p \oplus \text{span}(\{\hat{\mathbf{u}}_i\}_{i \in \{1, \dots, n-2\} \setminus \mathcal{D}})\right\}$.*

(ii) *For any $\{\mathbf{w}\} \in \mathcal{A}$ such that $D(\mathbf{w})$ exists, $\{\mathbf{w}\}$ is a sequence of second maximal data piling directions if and only if $\|\mathbf{w} - \mathbf{f}_0\| \xrightarrow{P} 0$ as $p \rightarrow \infty$.*

It is important to note that a second maximal data piling direction is a direction $\mathbf{w} \in \mathcal{S}$ which is asymptotically orthogonal to both of $\text{span}(\mathbf{U}_{1,\mathcal{S}})$ and \mathcal{T}_p . A second maximal data piling direction lies in $\text{span}(\mathbf{U}_{1,\mathcal{S}}^\perp)$, but is also orthogonal to \mathcal{T}_p that is orthogonal to \mathbf{w}_{MDP} . This observation gives a unified view on the theoretical second maximal data piling direction and the estimates of such directions (\mathbf{w}_{MDP} and $\mathbf{v}_{\hat{\alpha}}$ in Section 4.2):

“Second maximal data piling directions are the projection of \mathbf{w}_{MDP} onto the orthogonal complement of $\text{span}(\mathbf{U}_{1,\mathcal{S}})$ (or its estimate).”

In the next section, the above intuition is utilized in developing an estimation strategy for second maximal data piling direction.

4.5 Data-splitting Approach for Second Maximal Data Piling Direction

We propose a data-splitting approach to estimate a second maximal data piling direction, that can be applied to all cases we have discussed. Suppose for now that an independent test dataset \mathcal{Y} is available to us. (Later, we will split the original training data into training and test data sets.) The idea we use is to estimate $\text{span}(\mathbf{U}_{1,S})$ using \mathcal{Y} , and to project \mathbf{w}_{MDP} (obtained from \mathcal{X}) onto the orthogonal complement of the estimate of $\text{span}(\mathbf{U}_{1,S})$. In the following, we verify that such a data-splitting approach is theoretically sound, and outline algorithmic procedures.

Denote the horizontally concatenated data matrix of the given independent test dataset \mathcal{Y} by $\mathbf{Y} = [Y_{11}, \dots, Y_{1n_1^*}, Y_{21}, \dots, Y_{2n_2^*}]$. The $p \times n^*$ data matrix \mathbf{Y} consists of the $n^* := n_1^* + n_2^*$ observations independent to \mathcal{X} and arranged so that $\pi(Y_{kj}) = k$ for any k, j . We assume that n_k^* is fixed and $n_k^* > m_k$ for $k = 1, 2$. Write class-wise sample mean vectors $\bar{Y}_k = n_k^{*-1} \sum_{j=1}^{n_k^*} Y_{kj}$. We define the within-scatter matrix of \mathcal{Y} as $\mathbf{S}_W^* = (\mathbf{Y} - \bar{\mathbf{Y}})(\mathbf{Y} - \bar{\mathbf{Y}})^\top$, where $\bar{\mathbf{Y}}_k = \bar{Y}_k \mathbf{1}_{n_k^*}^\top$ for $k = 1, 2$ and $\bar{\mathbf{Y}} = [\bar{\mathbf{Y}}_1, \bar{\mathbf{Y}}_2]$. Let $\mathbf{V} = [\hat{\mathbf{u}}_1, \dots, \hat{\mathbf{u}}_{n-2}, \mathbf{w}_{\text{MDP}}]$, which collects an orthonormal basis of the sample space \mathcal{S}_X (from the training dataset \mathcal{X}).

We are interested in characterizing the second data piling directions $\mathbf{w} \in \mathcal{S}_X$ (or the sequence $\{\mathbf{w}\} \in \mathfrak{W}_X$). Observe that \mathbf{w} is a second data piling direction if the (scaled) within-class scatter $p^{-1} \mathbf{w}^\top \mathbf{S}_W^* \mathbf{w}$ becomes negligible. Thus, we write the collection of sequences of second data piling directions (for the case where both \mathcal{X} and \mathcal{Y} are available) as

$$\bar{\mathcal{A}} = \left\{ \{\mathbf{w}\} \in \mathfrak{W}_X : \frac{1}{p} \mathbf{w}^\top \mathbf{S}_W^* \mathbf{w} \xrightarrow{P} 0 \text{ as } p \rightarrow \infty \right\}.$$

For any $\{\mathbf{w}\} \in \mathfrak{W}_X$, we can write $\mathbf{w} = \mathbf{V}\mathbf{a}$ for some $\mathbf{a} = (a_1, \dots, a_{n-2}, a_{\text{MDP}})^\top \in \mathbb{R}^{n-1}$. Without loss of generality, we assume $a_{\text{MDP}} \geq 0$ for all p . For $\{\mathbf{w}\} \in \bar{\mathcal{A}}$, we can write

$$\frac{1}{p} \mathbf{w}^\top \mathbf{S}_W^* \mathbf{w} = \frac{1}{p} \mathbf{a}^\top \mathbf{V}^\top \mathbf{S}_W^* \mathbf{V} \mathbf{a} = \mathbf{a}^\top \left(\frac{1}{p} \mathbf{V}^\top \mathbf{S}_W^* \mathbf{V} \right) \mathbf{a}. \quad (17)$$

Note that the $(n-1) \times (n-1)$ matrix $p^{-1} \mathbf{V}^\top \mathbf{S}_W^* \mathbf{V}$ can be understood as the scatter of the independent test data \mathcal{Y} projected onto the sample space \mathcal{S}_X . Theorem 13 shows that independent test data \mathcal{Y} are asymptotically supported on a m -dimensional subspace in \mathcal{S}_X .

Theorem 13 $p^{-1} \mathbf{V}^\top \mathbf{S}_W^* \mathbf{V}$ converges to a rank- m matrix in probability as $p \rightarrow \infty$.

Write the eigen-decomposition of the scatter matrix as follows:

$$p^{-1} \mathbf{V}^\top \mathbf{S}_W^* \mathbf{V} = \hat{\mathbf{Q}} \mathbf{H} \hat{\mathbf{Q}}^\top,$$

where $\mathbf{H} = \text{Diag}(h_1, \dots, h_{n-1})$ arranged in descending order, and $\hat{\mathbf{Q}} = [\hat{\mathbf{Q}}_1, \hat{\mathbf{Q}}_2]$ with $\hat{\mathbf{Q}}_1 = [\hat{\mathbf{q}}_1, \dots, \hat{\mathbf{q}}_m]$ and $\hat{\mathbf{Q}}_2 = [\hat{\mathbf{q}}_{m+1}, \dots, \hat{\mathbf{q}}_{n-1}]$. Accordingly, the coefficients \mathbf{a} can be expressed as $\mathbf{a} = \hat{\mathbf{Q}} \boldsymbol{\iota} = \sum_{i=1}^{n-1} \iota_i \hat{\mathbf{q}}_i$ by $\boldsymbol{\iota} = (\iota_1, \dots, \iota_{n-1})^\top$. Since

$$\frac{1}{p} \mathbf{w}^\top \mathbf{S}_W^* \mathbf{w} = \mathbf{a}^\top \left(\frac{1}{p} \mathbf{V}^\top \mathbf{S}_W^* \mathbf{V} \right) \mathbf{a} = \sum_{i=1}^{n-1} h_i \iota_i^2 = \sum_{i=1}^m h_i \iota_i^2 + o_p(1) \quad (18)$$

by Theorem 13 and (17), $\{\mathbf{w}\} \in \bar{\mathcal{A}}$ if and only if $\iota_1, \dots, \iota_m \xrightarrow{P} 0$ as $p \rightarrow \infty$. In other words, any second data piling direction $\mathbf{w} \in \bar{\mathcal{A}}$ satisfies $\mathbf{w} \in \text{span}(\mathbf{V}\hat{\mathbf{Q}}_2)$ (asymptotically). This fact plays a crucial role in our next observation: $\{\mathbf{w}\} \in \bar{\mathcal{A}}$ is indeed asymptotically orthogonal to the common leading eigenspace \mathcal{U} .

Theorem 14 *Suppose Assumptions 1–5 hold. Then for any given $\{\mathbf{w}\} \in \bar{\mathcal{A}}$, (i) $\mathbf{w}^\top \mathbf{u}_j \xrightarrow{P} 0$ for $1 \leq j \leq m$. (ii) Write*

$$\mathbf{w} = \mathbf{V}\mathbf{a} = \sum_{k=1}^{n-2} a_k \hat{\mathbf{u}}_k + a_{\text{MDP}} \mathbf{w}_{\text{MDP}}$$

with $\mathbf{a} = (a_1, \dots, a_{n-2}, a_{\text{MDP}})^\top$ and assume $a_{\text{MDP}} \xrightarrow{P} \psi_{\text{MDP}}$ as $p \rightarrow \infty$. Then for any independent observation Y , which is independent to both of \mathcal{X} and \mathcal{Y} ,

$$\frac{1}{\sqrt{p}} \mathbf{w}^\top (Y - \bar{X}) \xrightarrow{P} \begin{cases} \frac{\psi_{\text{MDP}}}{\kappa} (\eta_2 (1 - \cos^2 \varphi) \delta^2 - (\tau_1^2 - \tau_2^2)/n), & \pi(Y) = 1, \\ \frac{\psi_{\text{MDP}}}{\kappa} (-\eta_1 (1 - \cos^2 \varphi) \delta^2 - (\tau_1^2 - \tau_2^2)/n), & \pi(Y) = 2, \end{cases}$$

as $p \rightarrow \infty$, where κ is the probability limit of κ_{MDP} defined in (4).

The above theorem also implies that for a carefully chosen \mathbf{a} , the direction \mathbf{w} can be used to yield perfect classification of new independent observation Y , which is independent to both of \mathcal{X} and \mathcal{Y} . Requirements for such an \mathbf{a} are $\{\mathbf{w}\} \in \bar{\mathcal{A}}$ (where $\mathbf{w} = \mathbf{V}\mathbf{a}$) and $\lim_{p \rightarrow \infty} a_{\text{MDP}} > 0$.

Theorem 14 also implies that the piling gap is maximized when the limiting value ψ_{MDP} of a_{MDP} is largest. Combining this observation with (18), it is natural to project \mathbf{w}_{MDP} onto $\text{span}(\mathbf{V}\hat{\mathbf{Q}}_2)$: \mathbf{w}_{MDP} is used to maximize ψ_{MDP} , and $\text{span}(\mathbf{V}\hat{\mathbf{Q}}_2)$ is used to ensure second data piling. Next result confirms that such an estimate is indeed maximal.

Theorem 15 *Suppose Assumptions 1–5 hold. Write $\mathbf{e}_{\text{MDP}} = (\mathbf{0}_{n-2}^\top, 1)^\top$ so that $\mathbf{w}_{\text{MDP}} = \mathbf{V}\mathbf{e}_{\text{MDP}}$. Also, let $\{\mathbf{w}_{\text{SMDP}}\}$ be a sequence of directions such that $\mathbf{w}_{\text{SMDP}} = \mathbf{V}\mathbf{a}_{\text{SMDP}}$ where*

$$\mathbf{a}_{\text{SMDP}} = \frac{P_{\text{span}(\hat{\mathbf{Q}}_2)} \mathbf{e}_{\text{MDP}}}{\|P_{\text{span}(\hat{\mathbf{Q}}_2)} \mathbf{e}_{\text{MDP}}\|} = \frac{\hat{\mathbf{Q}}_2 \hat{\mathbf{Q}}_2^\top \mathbf{e}_{\text{MDP}}}{\|\hat{\mathbf{Q}}_2 \hat{\mathbf{Q}}_2^\top \mathbf{e}_{\text{MDP}}\|} \in \mathbb{R}^{n-1}.$$

Then $\{\mathbf{w}\} \in \bar{\mathcal{A}}$ is a sequence of second maximal data piling directions if and only if $\|\mathbf{w} - \mathbf{w}_{\text{SMDP}}\| \xrightarrow{P} 0$ as $p \rightarrow \infty$.

We have shown that a second maximal data piling direction in the sample space $\mathcal{S}_{\mathcal{X}}$ can be obtained with a help of independent test data. In practice, we randomly split \mathcal{X}_k , which is the original training dataset of the k th class, into training dataset $\mathcal{X}_{k,tr}$ and test dataset $\mathcal{X}_{k,te}$ so that the sample size of test data of k th class $n_{k,te}$ is larger than m_k for $k = 1, 2$. Then, the estimate \mathbf{w}_{SMDP} is computed using both $\mathcal{X}_{tr} = \mathcal{X}_{1,tr} \cup \mathcal{X}_{2,tr}$ and $\mathcal{X}_{te} = \mathcal{X}_{1,te} \cup \mathcal{X}_{2,te}$.

The small sample size characteristic of HDLSS data suggests that classification based on a single data split may be unreliable in practice (albeit theoretically valid). In order to resolve this concern, we repeat the above procedure several times and set a final estimate of

a second maximal data piling direction as the average of estimates of a second maximal data piling direction obtained from each repetition. A detailed algorithm is given in Algorithm 1.

In Algorithm 1, one needs to specify m_1 , m_2 and m , the true numbers of leading eigenvalues of $\Sigma_{(1)}$, $\Sigma_{(2)}$ and $\Sigma_{(0)} = \pi_1 \Sigma_{(1)} + \pi_2 \Sigma_{(2)}$. We do not address estimation of these numbers, but refer the readers to the relevant literature: See, e.g., Kritchman and Nadler (2008); Leek (2010); Passemier and Yao (2014); Jung et al. (2018).

The classification rule $\phi_{\text{SMDP-I}}$ of Algorithm 1 ensures perfect classification of independent test data under the HDLSS asymptotic regime (by Theorem 14). In Algorithm 1, we also estimate a bias term as $g_{j,\text{SMDP}}$ for each repetition. In fact, we do not need to estimate this term since projections of \mathcal{X}_{te} onto \mathbf{w}_{SMDP} tend to converge two distinct points, one for each class. Hence, we propose another classification rule $\phi_{\text{SMDP-II}}$, which is almost same as $\phi_{\text{SMDP-I}}$ except that $\phi_{\text{SMDP-II}}$ computes the classification threshold by utilizing the simple LDA rule. Taking this approach eliminates the need to estimate m_1 and m_2 . A detailed algorithm is given in Algorithm 2.

5. Numerical Studies

In Section 5.1, we numerically demonstrate that our proposed classification rules can achieve asymptotic perfect classification under various heterogeneous covariance models via a simulation study. We also show that these methods achieve competitive classification performance in classifying Olivetti faces data in Section 5.2.

5.1 Simulation Study

We investigate classification performances of the MDP classification rules (ϕ_{MDP} , $\phi_{\text{b-MDP}}$), the PRD classification rules ($\phi_{\text{PRD},\alpha}$, $\phi_{\text{b-PRD},\alpha}$) and the SMDP algorithms ($\phi_{\text{SMDP-I}}$, $\phi_{\text{SMDP-II}}$) through a simulation study. For comparison, we consider Distance-Based Discriminant Analysis (DBDA) by Aoshima and Yata (2013), Transformed Distance-Based Discriminant Analysis (T-DBDA) by Aoshima and Yata (2019) and the distance-based linear classifier using the data transformation procedure (DT) by Ishii (2020), all of which were developed for the classification of HDLSS data with a spiked covariance model. In particular, T-DBDA and DT were proposed for strongly spiked eigenvalue models where $\beta_k \geq 1/2$ ($k = 1, 2$), which are based on the idea of removing the leading eigenspace (but DT only considers the case of $m_1 = m_2 = 1$). We also compare our methods with Distance Weighted Discrimination (DWD) by Marron et al. (2007) and Support Vector Machine (SVM) by Vapnik (1995), which are well-known to achieve successful classification performances in high-dimensional classification (see Qiao et al. (2010) and Huang (2017)). We do not consider classifiers that require a sparse estimation of the discriminant direction vector, as they are known to perform poorly under a spiked covariance model. We also do not consider nonparametric classification methods, such as nearest neighbors or decision tree-based classifiers, because the sample size is quite small, while the dimension is sufficiently high in the HDLSS classification problem, and tuning becomes practically meaningless.

We generate training data of size $n_1 = n_2 = 20$ from multivariate normal distribution with mean $\boldsymbol{\mu}_{(k)}$ and covariance matrix $\Sigma_{(k)}$ with $p = 10,000$. We assume $\boldsymbol{\mu}_{(1)} =$

Algorithm 1 Second Maximal Data Piling (SMDP) algorithm (Type I)

Require: Original training data matrix of the k th class \mathbf{X}_k for $k = 1, 2$.

Require: The number of repetitions K , estimated m_1 , m_2 and m

- 1: **for** $j = 1, \dots, K$ **do**
- 2: Randomly split \mathbf{X}_k into $\begin{cases} \mathbf{X}_{k,tr} = [X_{k1}, \dots, X_{kn_{k,tr}}] \\ \mathbf{X}_{k,te} = [X_{k1}^*, \dots, X_{kn_{k,te}}^*] \end{cases}$ so that $n_{k,te} > m_k$ ($k = 1, 2$)
- 3: Set $n_{tr} = n_{1,tr} + n_{2,tr}$, $\bar{X}_{k,tr} = n_{k,tr}^{-1} \mathbf{X}_{k,tr} \mathbf{1}_{n_{k,tr}}$ and $\bar{\mathbf{X}}_{k,tr} = \bar{X}_{k,tr} \mathbf{1}_{n_{k,tr}}^\top$ ($k = 1, 2$)
- 4: Set $\mathbf{S}_{tr} = \sum_{k=1}^2 (\mathbf{X}_{k,tr} - \bar{\mathbf{X}}_{k,tr})(\mathbf{X}_{k,tr} - \bar{\mathbf{X}}_{k,tr})^\top$ and $\mathbf{d}_{tr} = \bar{X}_{1,tr} - \bar{X}_{2,tr}$
- 5: Write an eigen-decomposition of \mathbf{S}_{tr} by $\mathbf{S}_{tr} = \hat{\mathbf{U}} \hat{\mathbf{\Lambda}} \hat{\mathbf{U}}^\top = \hat{\mathbf{U}}_1 \hat{\mathbf{\Lambda}}_1 \hat{\mathbf{U}}_1^\top$ where $\hat{\mathbf{\Lambda}} = \text{Diag}(\hat{\lambda}_1, \dots, \hat{\lambda}_{n_{tr}-2}, 0, \dots, 0)$ arranged in descending order, and $\hat{\mathbf{U}} = [\hat{\mathbf{U}}_1, \hat{\mathbf{U}}_2]$ with $\hat{\mathbf{U}}_1 = [\hat{\mathbf{u}}_1, \dots, \hat{\mathbf{u}}_{n_{tr}-2}]$, $\hat{\mathbf{U}}_2 = [\hat{\mathbf{u}}_{n_{tr}-1}, \dots, \hat{\mathbf{u}}_p]$
- 6: Set $\mathbf{w}_{\text{MDP}} = \|\hat{\mathbf{U}}_2 \hat{\mathbf{U}}_2^\top \mathbf{d}_{tr}\|^{-1} \hat{\mathbf{U}}_2 \hat{\mathbf{U}}_2^\top \mathbf{d}_{tr}$ and $\kappa_{\text{MDP}} = p^{-1/2} \|\hat{\mathbf{U}}_2 \hat{\mathbf{U}}_2^\top \mathbf{d}_{tr}\|$
- 7: Set $\mathbf{V} = [\hat{\mathbf{u}}_1, \dots, \hat{\mathbf{u}}_{n_{tr}-2}, \mathbf{w}_{\text{MDP}}]$
- 8: Set $\bar{X}_{k,te} = n_{k,te}^{-1} \mathbf{X}_{k,te} \mathbf{1}_{n_{k,te}}$ and $\bar{\mathbf{X}}_{k,te} = \bar{X}_{k,te} \mathbf{1}_{n_{k,te}}^\top$ ($k = 1, 2$)
- 9: Set $\mathbf{S}_{te} = \sum_{k=1}^2 (\mathbf{X}_{k,te} - \bar{\mathbf{X}}_{k,te})(\mathbf{X}_{k,te} - \bar{\mathbf{X}}_{k,te})^\top$
- 10: Write an eigen-decomposition of $p^{-1} \mathbf{V}^\top \mathbf{S}_{te} \mathbf{V}$ by $p^{-1} \mathbf{V}^\top \mathbf{S}_{te} \mathbf{V} = \hat{\mathbf{Q}} \mathbf{H} \hat{\mathbf{Q}}^\top$ where $\mathbf{H} = \text{Diag}(h_1, \dots, h_{n_{tr}-1})$ arranged in descending order, and $\hat{\mathbf{Q}} = [\hat{\mathbf{Q}}_1, \hat{\mathbf{Q}}_2]$ with $\hat{\mathbf{Q}}_1 = [\hat{\mathbf{q}}_1, \dots, \hat{\mathbf{q}}_m]$ and $\hat{\mathbf{Q}}_2 = [\hat{\mathbf{q}}_{m+1}, \dots, \hat{\mathbf{q}}_{n_{tr}-1}]$
- 11: Set $\mathbf{a}_{j,\text{SMDP}} = \|\hat{\mathbf{Q}}_2 \hat{\mathbf{Q}}_2^\top \mathbf{e}_{\text{MDP}}\|^{-1} \hat{\mathbf{Q}}_2 \hat{\mathbf{Q}}_2^\top \mathbf{e}_{\text{MDP}}$ where $\mathbf{e}_{\text{MDP}} = (\mathbf{0}_{n-2}^\top, 1)^\top$
- 12: Set $\mathbf{w}_{j,\text{SMDP}} = \mathbf{V} \mathbf{a}_{j,\text{SMDP}}$
- 13: Set $\bar{X}_{j,\text{SMDP}} = n_{tr}^{-1} (n_{1,tr} \bar{X}_{1,tr} + n_{2,tr} \bar{X}_{2,tr})$
- 14: Set $\hat{\alpha}_k = -p^{-1} \sum_{i=m_k+1}^{n_{k,tr}-1} \hat{\lambda}_{(k),i}$ where $\hat{\lambda}_{(k),i}$ is the i th largest eigenvalue of

$$\mathbf{S}_{k,tr} = (\mathbf{X}_{k,tr} - \bar{\mathbf{X}}_{k,tr})(\mathbf{X}_{k,tr} - \bar{\mathbf{X}}_{k,tr})^\top$$

- 15: Set $g_{j,\text{SMDP}} = (n_{tr} \kappa_{\text{MDP}})^{-1} (\mathbf{e}_{\text{MDP}}^\top \mathbf{a}_{j,\text{SMDP}}) (\hat{\alpha}_1 - \hat{\alpha}_2)$

16: **end for**

- 17: Set $\mathbf{w}_{\text{SMDP}} = K^{-1} \sum_{j=1}^K \mathbf{w}_{j,\text{SMDP}}$
- 18: Set $\bar{X}_{\text{SMDP}} = K^{-1} \sum_{j=1}^K \mathbf{w}_{j,\text{SMDP}}^\top \bar{X}_{j,\text{SMDP}}$
- 19: Set $g_{\text{SMDP}} = K^{-1} \sum_{j=1}^K g_{j,\text{SMDP}}$
- 20: Use the following classification rule:

$$\phi_{\text{SMDP-I}}(Y; \mathcal{X}) = \begin{cases} 1, & p^{-1/2} (\mathbf{w}_{\text{SMDP}}^\top Y - \bar{X}_{\text{SMDP}}) - g_{\text{SMDP}} \geq 0, \\ 2, & p^{-1/2} (\mathbf{w}_{\text{SMDP}}^\top Y - \bar{X}_{\text{SMDP}}) - g_{\text{SMDP}} < 0. \end{cases} \quad (19)$$

Algorithm 2 Second Maximal Data Piling (SMDP) algorithm (Type II)

Require: Original training data matrix of the k th class \mathbf{X}_k for $k = 1, 2$.

Require: The number of repetitions K , estimated m

- 1: **for** $j = 1, \dots, K$ **do**
- 2: Randomly split \mathbf{X}_k into $\begin{cases} \mathbf{X}_{k,tr} = [X_{k1}, \dots, X_{kn_{k,tr}}] \\ \mathbf{X}_{k,te} = [X_{k1}^*, \dots, X_{kn_{k,te}}^*] \end{cases}$ so that $n_{k,te} > m_k$ ($k = 1, 2$)
- 3: Set $n_{tr} = n_{1,tr} + n_{2,tr}$, $\bar{\mathbf{X}}_{k,tr} = n_{k,tr}^{-1} \mathbf{X}_{k,tr} \mathbf{1}_{n_{k,tr}}$ and $\bar{\mathbf{X}}_{k,te} = \bar{\mathbf{X}}_{k,tr} \mathbf{1}_{n_{k,tr}}^\top$ ($k = 1, 2$)
- 4: Set $\mathbf{S}_{tr} = \sum_{k=1}^2 (\mathbf{X}_{k,tr} - \bar{\mathbf{X}}_{k,tr})(\mathbf{X}_{k,tr} - \bar{\mathbf{X}}_{k,tr})^\top$ and $\mathbf{d}_{tr} = \bar{\mathbf{X}}_{1,tr} - \bar{\mathbf{X}}_{2,tr}$
- 5: Write an eigen-decomposition of \mathbf{S}_{tr} by $\mathbf{S}_{tr} = \hat{\mathbf{U}} \hat{\mathbf{\Lambda}} \hat{\mathbf{U}}^\top = \hat{\mathbf{U}}_1 \hat{\mathbf{\Lambda}}_1 \hat{\mathbf{U}}_1^\top$ where $\hat{\mathbf{\Lambda}} = \text{Diag}(\hat{\lambda}_1, \dots, \hat{\lambda}_{n_{tr}-2}, 0, \dots, 0)$ arranged in descending order, and $\hat{\mathbf{U}} = [\hat{\mathbf{U}}_1, \hat{\mathbf{U}}_2]$ with $\hat{\mathbf{U}}_1 = [\hat{\mathbf{u}}_1, \dots, \hat{\mathbf{u}}_{n_{tr}-2}]$, $\hat{\mathbf{U}}_2 = [\hat{\mathbf{u}}_{n_{tr}-1}, \dots, \hat{\mathbf{u}}_p]$
- 6: Set $\mathbf{w}_{\text{MDP}} = \|\hat{\mathbf{U}}_2 \hat{\mathbf{U}}_2^\top \mathbf{d}_{tr}\|^{-1} \hat{\mathbf{U}}_2 \hat{\mathbf{U}}_2^\top \mathbf{d}_{tr}$ and $\kappa_{\text{MDP}} = p^{-1/2} \|\hat{\mathbf{U}}_2 \hat{\mathbf{U}}_2^\top \mathbf{d}_{tr}\|$
- 7: Set $\mathbf{V} = [\hat{\mathbf{u}}_1, \dots, \hat{\mathbf{u}}_{n_{tr}-2}, \mathbf{w}_{\text{MDP}}]$
- 8: Set $\bar{\mathbf{X}}_{k,te} = n_{k,te}^{-1} \mathbf{X}_{k,te} \mathbf{1}_{n_{k,te}}$ and $\bar{\mathbf{X}}_{k,te} = \bar{\mathbf{X}}_{k,te} \mathbf{1}_{n_{k,te}}^\top$ ($k = 1, 2$)
- 9: Set $\mathbf{S}_{te} = \sum_{k=1}^2 (\mathbf{X}_{k,te} - \bar{\mathbf{X}}_{k,te})(\mathbf{X}_{k,te} - \bar{\mathbf{X}}_{k,te})^\top$
- 10: Write an eigen-decomposition of $p^{-1} \mathbf{V}^\top \mathbf{S}_{te} \mathbf{V}$ by $p^{-1} \mathbf{V}^\top \mathbf{S}_{te} \mathbf{V} = \hat{\mathbf{Q}} \mathbf{H} \hat{\mathbf{Q}}^\top$ where $\mathbf{H} = \text{Diag}(h_1, \dots, h_{n_{tr}-1})$ arranged in descending order, and $\hat{\mathbf{Q}} = [\hat{\mathbf{Q}}_1, \hat{\mathbf{Q}}_2]$ with $\hat{\mathbf{Q}}_1 = [\hat{\mathbf{q}}_1, \dots, \hat{\mathbf{q}}_m]$ and $\hat{\mathbf{Q}}_2 = [\hat{\mathbf{q}}_{m+1}, \dots, \hat{\mathbf{q}}_{n_{tr}-1}]$
- 11: Set $\mathbf{a}_{j,\text{SMDP}} = \|\hat{\mathbf{Q}}_2 \hat{\mathbf{Q}}_2^\top \mathbf{e}_{\text{MDP}}\|^{-1} \hat{\mathbf{Q}}_2 \hat{\mathbf{Q}}_2^\top \mathbf{e}_{\text{MDP}}$ where $\mathbf{e}_{\text{MDP}} = (\mathbf{0}_{n-2}^\top, 1)^\top$
- 12: Set $\mathbf{w}_{j,\text{SMDP}} = \mathbf{V} \mathbf{a}_{j,\text{SMDP}}$
- 13: Apply Linear Discriminant Analysis to $p^{-1/2} \mathbf{w}_{j,\text{SMDP}}^\top \mathbf{X}_{te}$ where $\mathbf{X}_{te} = [\mathbf{X}_{1,te}, \mathbf{X}_{2,te}]$ and achieve a classification threshold b_j .
- 14: **end for**
- 15: Set $\mathbf{w}_{\text{SMDP}} = K^{-1} \sum_{j=1}^K \mathbf{w}_{j,\text{SMDP}}$
- 16: Set $b_{\text{SMDP}} = K^{-1} \sum_{j=1}^K b_j$
- 17: Use the following classification rule:

$$\phi_{\text{SMDP-II}}(Y; \mathcal{X}) = \begin{cases} 1, & p^{-1/2} \mathbf{w}_{\text{SMDP}}^\top Y \geq b_{\text{SMDP}}, \\ 2, & p^{-1/2} \mathbf{w}_{\text{SMDP}}^\top Y < b_{\text{SMDP}}. \end{cases} \quad (20)$$

$(\sqrt{8}\mathbf{1}_{p/8}, \mathbf{0}_{7p/8}^\top)^\top$, $\boldsymbol{\mu}_{(2)} = \mathbf{0}_p$. Note that in this case $\delta^2 = 1$. The population covariance matrices $\boldsymbol{\Sigma}_{(1)}$ and $\boldsymbol{\Sigma}_{(2)}$ will be given differently in each setting as follows.

Setting	$\boldsymbol{\Sigma}_{(1)}$	$\boldsymbol{\Sigma}_{(2)}$	(β_1, β_2)	(τ_1^2, τ_2^2)
I	$\sum_{i=1}^2 \sigma_{1,i}^2 \mathbf{u}_{(1),i} \mathbf{u}_{(1),i}^\top + \tau_1^2 \mathbf{I}_p$	$\sum_{i=1}^3 \sigma_{2,i}^2 \mathbf{u}_{(2),i} \mathbf{u}_{(2),i}^\top + \tau_2^2 \mathbf{I}_p$	$(1/2, 1/2)$	$(30, 15)$
II			$(1, 1)$	$(30, 30)$
III	$(1, 1)$		$(30, 15)$	
IV	$\sum_{i=1}^3 \sigma_{1,i}^2 \mathbf{u}_{(1),i} \mathbf{u}_{(1),i}^\top + \tau_1^2 \mathbf{I}_p$	$(1, 1)$	$(30, 30)$	
V		$(1, 1)$	$(30, 15)$	

We set $(\sigma_{1,1}^2, \sigma_{1,2}^2, \sigma_{1,3}^2) = (5p^{\beta_1}, 3p^{\beta_1}, 2p^{\beta_1})$, $(\sigma_{2,1}^2, \sigma_{2,2}^2, \sigma_{2,3}^2) = (5p^{\beta_2}, 3p^{\beta_2}, 2p^{\beta_2})$,

$$[\mathbf{u}_{(1),1}, \mathbf{u}_{(1),2}, \mathbf{u}_{(1),3}] = \frac{1}{\sqrt{p}} \begin{bmatrix} \sqrt{2}\mathbf{1}_{p/4} & \mathbf{0}_{p/4} & \mathbf{1}_{p/4} \\ \sqrt{2}\mathbf{1}_{p/4} & \mathbf{0}_{p/4} & -\mathbf{1}_{p/4} \\ \mathbf{0}_{p/4} & \sqrt{2}\mathbf{1}_{p/4} & \mathbf{1}_{p/4} \\ \mathbf{0}_{p/4} & \sqrt{2}\mathbf{1}_{p/4} & -\mathbf{1}_{p/4} \end{bmatrix},$$

and

$$[\mathbf{u}_{(2),1}, \mathbf{u}_{(2),2}, \mathbf{u}_{(2),3}] = \frac{1}{\sqrt{p}} \begin{bmatrix} \mathbf{1}_{p/4} & \sqrt{2}\mathbf{1}_{p/4} & \mathbf{0}_{p/4} \\ \mathbf{1}_{p/4} & \mathbf{0}_{p/4} & \sqrt{2}\mathbf{1}_{p/4} \\ \mathbf{1}_{p/4} & -\sqrt{2}\mathbf{1}_{p/4} & \mathbf{0}_{p/4} \\ \mathbf{1}_{p/4} & \mathbf{0}_{p/4} & -\sqrt{2}\mathbf{1}_{p/4} \end{bmatrix}.$$

Setting I corresponds to the case of weak spikes, while the other settings correspond to the case of strong spikes. Also, Settings II and III assume $m = m_2$, that is, $\mathcal{U} = \mathcal{U}_{(2)}$, while Settings IV and V assume $m > \max(m_1, m_2)$. Finally, Settings II and IV assume equal tail eigenvalues, while Settings III and V assume unequal tail eigenvalues for $\boldsymbol{\Sigma}_{(1)}$ and $\boldsymbol{\Sigma}_{(2)}$.

Independent test data of size $n_1^* = n_2^* = 500$ are generated from the same model with the training data. For each classification rule, we evaluate three metrics for our simulation study. First, we estimate the classification accuracy using independent test data. Next, we calculate the degree of second data piling defined as

$$\text{DegSDP}(\mathbf{w}) := \frac{\mathbf{w}^\top \mathbf{S}_B^* \mathbf{w}}{\mathbf{w}^\top \mathbf{S}_W^* \mathbf{w}} = \frac{\sum_{k=1}^2 n_k^* \{\mathbf{w}^\top (\bar{Y}_k - \bar{Y})\}^2}{\sum_{k=1}^2 \sum_{j=1}^{n_k^*} \{\mathbf{w}^\top (Y_{kj} - \bar{Y}_k)\}^2} \quad (21)$$

where \mathbf{w} is the normal vector of the classification rule, Y_{kj} is the j th observation of the test data for the k th class, $\bar{Y}_k = n_k^{*-1} \sum_{j=1}^{n_k^*} Y_{kj}$ and $\bar{Y} = (n_1^* + n_2^*)^{-1} \sum_{k=1}^2 n_k^* \bar{Y}_k$. Theoretically, $\text{DegSDP}(\mathbf{w}) \xrightarrow{P} \infty$ as $p \rightarrow \infty$ for any $\{\mathbf{w}\} \in \mathcal{A}$. For all settings except Setting I, we evaluate $\text{Angle}(\mathbf{w}, \mathcal{U})$, the angle between the normal vector \mathbf{w} of the classification rule and the common leading eigenspace \mathcal{U} . Recall that $\text{Angle}(\mathbf{w}, \mathcal{U}) \xrightarrow{P} \pi/2$ as $p \rightarrow \infty$ for any $\{\mathbf{w}\} \in \mathcal{A}$.

To clearly check performances of each classification rule, we use the true numbers of m_1 , m_2 and m for $\phi_{\text{PRD}, \hat{\alpha}}$, $\phi_{\text{b-PRD}, \hat{\alpha}_1}$, $\phi_{\text{b-PRD}, \hat{\alpha}_2}$ ($\hat{\alpha}$, $\hat{\alpha}_1$ and $\hat{\alpha}_2$ are defined in (14) and (9)), $\phi_{\text{SMDP-I}}$ and $\phi_{\text{SMDP-II}}$. Similarly, we use the true number of strongly spiked eigenvalues for

	Metric	ϕ_{MDP}	$\phi_{\text{PRD},\hat{\alpha}}$	$\phi_{\text{b-PRD},\hat{\alpha}_1}$	$\phi_{\text{b-PRD},\hat{\alpha}_2}$	$\phi_{\text{SMDP-I}}$	T-DBDA	DT	DWD
I	Accuracy	0.890 (0.028)	0.890 (0.028)	0.999 (0.001)	0.999 (0.001)	0.999 (0.001)	0.999 (0.001)	0.999 (0.001)	0.893 (0.027)
	DegSDP	12.819 (1.443)	12.819 (1.443)	12.819 (1.443)	12.819 (1.443)	12.574 (1.442)	12.535 (1.446)	12.956 (1.487)	12.596 (1.445)
II	Accuracy	0.846 (0.081)	0.996 (0.002)	0.996 (0.002)	0.996 (0.002)	0.993 (0.006)	0.926 (0.050)	0.705 (0.093)	0.784 (0.094)
	DegSDP	1.454 (1.356)	7.473 (0.948)	7.469 (0.946)	7.474 (0.952)	6.919 (1.100)	2.843 (1.639)	0.412 (0.625)	0.878 (1.021)
III	Angle(\mathbf{w}, \mathcal{U})	83.124 (3.476)	89.390 (0.301)	89.388 (0.299)	89.393 (0.304)	89.158 (0.500)	86.291 (1.708)	72.567 (8.394)	79.894 (4.997)
	Accuracy	0.712 (0.050)	0.602 (0.048)	0.876 (0.140)	0.998 (0.009)	0.999 (0.001)	0.939 (0.049)	0.708 (0.092)	0.702 (0.047)
IV	DegSDP	2.642 (2.414)	6.428 (4.013)	3.029 (3.392)	11.966 (2.178)	12.172 (1.747)	3.591 (2.354)	0.457 (0.952)	1.263 (1.568)
	Angle(\mathbf{w}, \mathcal{U})	84.662 (2.725)	86.947 (2.418)	82.721 (5.849)	89.370 (0.594)	89.386 (0.306)	85.905 (1.943)	70.853 (8.911)	80.412 (4.912)
V	Accuracy	0.786 (0.065)	0.980 (0.009)	0.980 (0.009)	0.980 (0.009)	0.974 (0.015)	0.858 (0.060)	0.671 (0.063)	0.731 (0.071)
	DegSDP	0.684 (0.504)	4.550 (0.705)	4.550 (0.705)	4.546 (0.707)	4.135 (0.843)	1.347 (0.684)	0.195 (0.169)	0.411 (0.365)
VI	Angle(\mathbf{w}, \mathcal{U})	80.471 (3.484)	89.138 (0.410)	89.138 (0.412)	89.138 (0.410)	88.832 (0.691)	84.489 (2.140)	67.875 (7.128)	76.374 (4.837)
	Accuracy	0.688 (0.041)	0.578 (0.050)	0.833 (0.155)	0.947 (0.046)	0.992 (0.010)	0.872 (0.065)	0.672 (0.064)	0.680 (0.035)
VII	DegSDP	1.003 (0.709)	3.071 (1.982)	1.826 (2.092)	3.956 (2.175)	7.113 (1.441)	1.598 (0.940)	0.189 (0.156)	0.492 (0.397)
	Angle(\mathbf{w}, \mathcal{U})	81.201 (3.417)	85.802 (2.353)	82.646 (5.877)	86.065 (2.660)	88.995 (0.609)	83.871 (2.468)	65.605 (7.510)	76.243 (4.896)

Table 3: Averaged estimates of classification accuracy, DegSDP in (21), and Angle(\mathbf{w}, \mathcal{U}) of each classification rule for each setting of the simulation study. Standard deviations are presented in parentheses.

T-DBDA. Using $\phi_{\text{b-PRD},\hat{\alpha}_1}$ and $\phi_{\text{b-PRD},\hat{\alpha}_2}$ requires correctly identifying \mathcal{D} , which is demanding when $\beta_1 = \beta_2 = 1$, $m > m_1$ and $\tau_1^2 > \tau_2^2$ as explained in Section 3.2 and Appendix B. In this case, we set $\mathcal{D} = \{1, \dots, m_1 + m_2, n_1, \dots, n_1 + m_2 - 1\}$, including all sample eigenvectors that can potentially capture the variability within \mathcal{U} in the signal subspace \mathcal{S} . It results in adding m_2 noisy directions to \mathbf{v}_α , but their influence becomes negligible as p increases when $\alpha := \hat{\alpha}_2$ is used. For $\phi_{\text{SMDP-I}}$ and $\phi_{\text{SMDP-II}}$, we set $n_{1,te} = n_{2,te} = 6$ so that \mathcal{X}_{te} consists of 30% of original training data \mathcal{X} and set the number of repetitions as $K = 10$.

We repeat this procedure 100 times and report the average of each metric in Table 3. These results are consistent with the theoretical findings in Section 4. We exclude results of SVM since the performances of ϕ_{MDP} and SVM are almost similar to each other. Also, we exclude results of $\phi_{\text{b-MDP}}$ since the performances of $\phi_{\text{b-PRD},\hat{\alpha}_1}$ or $\phi_{\text{b-PRD},\hat{\alpha}_2}$ are uniformly better than $\phi_{\text{b-MDP}}$. Moreover, we exclude results of $\phi_{\text{SMDP-II}}$ since the performances of $\phi_{\text{SMDP-I}}$ and $\phi_{\text{SMDP-II}}$ are almost similar to each other. For the case of weak spikes (Setting I), asymptotic perfect classification is possible by utilizing \mathbf{w}_{MDP} with the bias-correction

strategy. For the case of strong spikes with equal tail eigenvalues (Settings II and IV), all PRD classification rules and SMDP algorithms perform significantly better than the other classification rules. Moreover, the normal vector of each of these classification yields considerable DegSDP and is nearly orthogonal to \mathcal{U} . In contrast, for the case of strong spikes with unequal tail eigenvalues (Settings III and V), performances of PRD classification rules depend on the structure of leading eigenspaces. To be specific, in Setting III where $m = m_2 > m_1$, $\phi_{\text{b-PRD}, \hat{\alpha}_2}$ achieves nearly perfect classification while $\phi_{\text{PRD}, \hat{\alpha}}$ and $\phi_{\text{b-PRD}, \hat{\alpha}_1}$ do not. However, in Setting V where $m > \max(m_1, m_2)$, all PRD classification rules do not achieve nearly perfect classification.

Our results show that both $\phi_{\text{SMDP-I}}$ and $\phi_{\text{SMDP-II}}$ achieve successful classification performances in all of the settings. Note that in Setting V, only $\phi_{\text{SMDP-I}}$ and $\phi_{\text{SMDP-II}}$ achieve nearly perfect classification among the classification rules. Also, \mathbf{w}_{SMDP} yields a significant degree of second data piling and is nearly orthogonal to \mathcal{U} in all of the settings. These results confirm that our approach, projecting \mathbf{w}_{MDP} onto the nullspace of the common leading eigenspace, successfully works under various heterogeneous covariance models. Note that we also exclude results of DBDA, since T-DBDA shows better performances than these classification rules in all settings. It implies that the data transformation technique, which removes excessive variability within the leading eigenspace, contributes to achieve better classification performances when $\Sigma_{(1)}$ or $\Sigma_{(2)}$ has meaningfully diverging components.

5.2 Olivetti Faces Data Example

We use the Olivetti faces dataset (available at <http://cs.nyu.edu/~roweis/data.html>), which contains ten face images for each of 40 distinct subjects ($n = 400$) in $p = 64 \times 64 = 4096$ pixels. The pixel intensity values are represented as integers ranging from 0 to 255, which we normalize to the interval $[-1, 1]$. We focus on the binary classification problem of distinguishing between individuals wearing glasses and those not wearing glasses. There are 119 images of individuals wearing glasses ($n_1 = 119$) and 281 images of individuals not wearing glasses ($n_2 = 281$).

Figure 7 shows the scree plots of the eigenvalues for the data from each class, suggesting that it is reasonable to estimate the number of leading eigenvalues for each class as $m_1 = 3$ and $m_2 = 3$. For T-DBDA, we estimate the number of strongly spiked eigenvalues as described in Aoshima and Yata (2019), which also yields $m_1 = 3$ and $m_2 = 3$. Note that, in this case, the dimension of the common leading eigenspace, m , is between $\max(m_1, m_2) = 3$ and $m_1 + m_2 = 6$. Also, it can be checked that both classes have heterogeneous covariance structures. For $k = 1, 2$, let $\hat{\mathbf{U}}_{(k),1} = [\hat{\mathbf{u}}_{(k),1}, \dots, \hat{\mathbf{u}}_{(k),m_k}]$ where $\hat{\mathbf{u}}_{(k),i}$ is the i th eigenvector of the sample covariance matrix of the k th class and let $\hat{\mathcal{U}}_{(k)} = \text{span}(\hat{\mathbf{U}}_{(k),1})$. We find that the largest canonical angle between $\hat{\mathcal{U}}_{(1)}$ and $\hat{\mathcal{U}}_{(2)}$ is 49.198° .

We randomly split the data into training and test sets by 4:1. This experiment was repeated 100 times to calculate the average test error rates and DegSDP, which are presented in Tables 4 and 5, respectively. Our results indicate that $\phi_{\text{SMDP-II}}$ exhibits the lowest classification error rates for all choices of $m = 3, 4, 5, 6$. Moreover, the normal vector \mathbf{w}_{SMDP} of $\phi_{\text{SMDP-I}}$ and $\phi_{\text{SMDP-II}}$ yields the maximum DegSDP among the classification rules, which implies that the SMDP algorithms effectively identify a direction that yields second maximal data piling. Note that $\phi_{\text{SMDP-I}}$ also achieves competitive classification

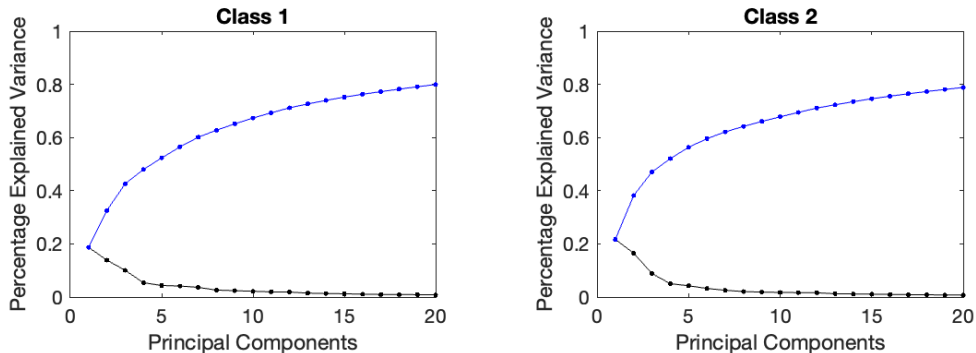


Figure 7: The proportion (black line) and cumulative proportion (blue line) of the total variance explained by each principal component for Class 1 (wearing glasses) and Class 2 (not wearing glasses) in the Olivetti dataset.

m	ϕ_{MDP}	$\phi_{\text{PRD},\hat{\alpha}}$	$\phi_{\text{SMDP-I}}$	$\phi_{\text{SMDP-II}}$	DBDA	T-DBDA	DT	DWD	SVM
3		0.057 (0.023)	0.040 (0.019)	0.016 (0.014)					
4	0.042 (0.020)	0.079 (0.028)	0.041 (0.019)	0.016 (0.015)	0.198 (0.045)	0.140 (0.042)	0.176 (0.040)	0.074 (0.028)	0.023 (0.013)
5		0.072 (0.027)	0.041 (0.018)	0.017 (0.015)					
6		0.068 (0.027)	0.041 (0.018)	0.016 (0.014)					

Table 4: Classification error rates of each classification rule applied to the binary classification of the Olivetti faces dataset. Standard deviations are presented in parentheses.

performance compared to other classification rules. However, $\phi_{\text{PRD},\hat{\alpha}}$ exhibits slightly worse performance than $\phi_{\text{SMDP-I}}$, $\phi_{\text{SMDP-II}}$ and even ϕ_{MDP} despite the fact that both classes have heterogeneous covariance structures. This highlights the impact of unequal tail eigenvalues of the covariance matrices on the second data piling phenomenon. Meanwhile, T-DBDA achieves the best classification performance among T-DBDA, DT, and DBDA, followed by DT and then DBDA. Note that T-DBDA removes the first three leading components, DT removes only the first leading component, and DBDA does not remove any leading components for each class in classification. This result is consistent with our observation that removing the leading eigenspace is beneficial.

Acknowledgments

m	ϕ_{MDP}	$\phi_{\text{PRD}, \hat{\alpha}}$	$\phi_{\text{SMDP-I}}$	$\phi_{\text{SMDP-II}}$	DBDA	T-DBDA	DT	DWD	SVM
3		3.492 (0.930)		5.377 (1.409)					
4	5.048 (1.323)	2.504 (0.734)		5.326 (1.469)	0.377 (0.169)	1.133 (0.262)	0.819 (0.287)	1.419 (0.468)	3.013 (0.584)
5		2.656 (0.770)		5.316 (1.476)					
6		2.761 (0.815)		5.316 (1.471)					

Table 5: DegSDP in (21) of each classification rule applied to the binary classification of the Olivetti faces dataset. Standard deviations are presented in parentheses.

This work was supported by National Research Foundation of Korea (NRF) grants funded by the Korea government (MSIT) (No. 2021R1A2C1093526, 2022M3J6A1063021, RS-2023-00218231, RS-2023-00301976, RS-2024-00333399).

Appendix A. Additional Assumptions

We introduce additional assumptions regarding the limiting angles between leading eigenvectors and the population mean difference vector $\boldsymbol{\mu}$. Assumption 4 specifies limiting angles between leading eigenvectors of each class and $\boldsymbol{\mu}$. Without loss of generality, we assume $\mathbf{u}_{(k),i}^\top \boldsymbol{\mu} \geq 0$ for all $k = 1, 2$ and $1 \leq i \leq m_k$.

Assumption 4 For $\theta_{k,i} \in [0, \pi/2]$, $\text{Angle}(\mathbf{u}_{(k),i}, \boldsymbol{\mu}) \rightarrow \theta_{k,i}$ as $p \rightarrow \infty$ for $1 \leq i \leq m_k$ and $k = 1, 2$.

Recall that we write an orthogonal basis of \mathcal{U} as $\mathbf{U}_1 = [\mathbf{u}_1, \dots, \mathbf{u}_m]$. Without loss of generality, we assume $\mathbf{u}_i^\top \boldsymbol{\mu} \geq 0$ for all $1 \leq i \leq m$. Note that there exist orthogonal matrices $\mathbf{R}_k^{(p)} \in \mathbb{R}^{m \times m_k}$ satisfying $\mathbf{U}_{(k),1} = \mathbf{U}_1 \mathbf{R}_k^{(p)}$ for $k = 1, 2$. The matrix $\mathbf{R}_k^{(p)}$ catches the angles between the m_k leading eigenvectors in $\mathbf{U}_{(k),1}$ and the m basis in \mathbf{U}_1 . We assume the following.

Assumption 5 For $\theta_i \in [0, \pi/2]$, $\text{Angle}(\mathbf{u}_i, \boldsymbol{\mu}) \rightarrow \theta_i$ as $p \rightarrow \infty$ for $1 \leq i \leq m$ and for an orthogonal matrix $\mathbf{R}_k \in \mathbb{R}^{m \times m_k}$, $\mathbf{R}_k^{(p)} \rightarrow \mathbf{R}_k$ as $p \rightarrow \infty$ for $k = 1, 2$. Moreover, $\mathbf{R} = [\mathbf{R}_1, \mathbf{R}_2] \in \mathbb{R}^{m \times (m_1 + m_2)}$ is of rank m .

Recall that φ denotes the limiting angle between $\boldsymbol{\mu}$ and \mathcal{U} . Then we have $\cos^2 \varphi = \sum_{i=1}^m \cos^2 \theta_i$. Similarly, let φ_k denote the limiting angle between $\boldsymbol{\mu}$ and $\mathcal{U}_{(k)}$ for $k = 1, 2$. Then we have $\cos^2 \varphi_1 = \sum_{i=1}^{m_1} \cos^2 \theta_{1,i}$, $\cos^2 \varphi_2 = \sum_{i=1}^{m_2} \cos^2 \theta_{2,i}$.

Appendix B. Asymptotic Properties of High-dimensional Sample Within-scatter Matrix

In this section, we investigate the asymptotic behavior of sample eigenvalues and eigenvectors of \mathbf{S}_W , which plays a critical role in characterizing the signal subspace \mathcal{S} in Section 3.2. Assume that $\beta_1 = \beta_2 = 1$ and $m_1, m_2 \geq 1$. For each $k = 1, 2$, denote the $n_k \times m_k$ matrix of the leading m_k principal component scores of the k th class as $\mathbf{W}_k = [\sigma_{k,1}\mathbf{z}_{k,1}, \dots, \sigma_{k,m_k}\mathbf{z}_{k,m_k}] \in \mathbb{R}^{n_k \times m_k}$. Also, denote the scaled covariance matrix of the principal component scores in the m_k leading eigenvectors $\{\mathbf{u}_{(k),i}\}_{i=1}^{m_k}$ of the k th class as

$$\Phi_k = \mathbf{W}_k^\top \left(\mathbf{I}_{n_k} - \frac{1}{n_k} \mathbf{J}_{n_k} \right) \mathbf{W}_k \in \mathbb{R}^{m_k \times m_k} \quad (22)$$

where \mathbf{J}_{n_k} is the matrix of size $n_k \times n_k$ whose all entries are 1. Let $\mathbf{W} = [\mathbf{R}_1 \mathbf{W}_1^\top, \mathbf{R}_2 \mathbf{W}_2^\top]^\top \in \mathbb{R}^{n \times m}$ and denote the scaled covariance matrix of the principal component scores in the m common leading eigenvectors $\{\mathbf{u}_i\}_{i=1}^m$ as

$$\Phi = \mathbf{W}^\top (\mathbf{I}_n - \mathbf{J}) \mathbf{W} \in \mathbb{R}^{m \times m} \quad (23)$$

where $\mathbf{J} = \begin{pmatrix} \frac{1}{n_1} \mathbf{J}_{n_1} & \mathbf{O}_{n_1 \times n_2} \\ \mathbf{O}_{n_2 \times n_1} & \frac{1}{n_2} \mathbf{J}_{n_2} \end{pmatrix}$. Finally, let

$$\Phi_{\tau_1, \tau_2} = \begin{pmatrix} \Phi_1 + \tau_1^2 \mathbf{I}_{m_1} & \Phi_1^{1/2} \mathbf{R}_1^\top \mathbf{R}_2 \Phi_2^{1/2} \\ \Phi_2^{1/2} \mathbf{R}_2^\top \mathbf{R}_1 \Phi_1^{1/2} & \Phi_2 + \tau_2^2 \mathbf{I}_{m_2} \end{pmatrix} \in \mathbb{R}^{(m_1+m_2) \times (m_1+m_2)}. \quad (24)$$

Note that Φ_{τ_1, τ_2} can be understood as a perturbed version of Φ with noises τ_1^2 and τ_2^2 . For any square matrix $\mathbf{M} \in \mathbb{R}^{l \times l}$ ($l \in \mathbb{N}$), let $\phi_i(\mathbf{M})$ and $v_i(\mathbf{M})$ denote the i th largest eigenvalue of \mathbf{M} and its corresponding eigenvector, respectively. If $\tau_1^2 = \tau_2^2 =: \tau^2$, then the eigenvalues of Φ and Φ_{τ_1, τ_2} are closely connected in the sense that

$$\phi_i(\Phi_{\tau_1, \tau_2}) = \begin{cases} \phi_i(\Phi) + \tau^2, & 1 \leq i \leq m, \\ \tau^2, & m+1 \leq i \leq m_1 + m_2. \end{cases} \quad (25)$$

However, (25) does not hold if $\tau_1^2 \neq \tau_2^2$. Both of Φ and Φ_{τ_1, τ_2} will play a critical role in explaining the asymptotic behavior of the eigenvalues and eigenvectors of \mathbf{S}_W , which is quite different depending on whether both covariance matrices have equal tail eigenvalues or unequal tail eigenvalues.

Lemma 16 shows that if $\tau_1^2 = \tau_2^2$, then the first m leading eigenvectors of \mathbf{S}_W explain the variation within the common leading eigenspace \mathcal{U} . The other sample eigenvectors are asymptotically orthogonal to \mathcal{U} , which implies that these eigenvectors do not capture the variability within \mathcal{U} .

Lemma 16 *Suppose Assumptions 1–5 hold. Also, assume $\beta_1 = \beta_2 = 1$, $\tau_1^2 = \tau_2^2 =: \tau^2$ and $m_1, m_2 \geq 1$. Then conditional to \mathbf{W}_1 and \mathbf{W}_2 , the following hold as $p \rightarrow \infty$.*

(i)

$$p^{-1}\hat{\lambda}_i \xrightarrow{P} \begin{cases} \phi_i(\mathbf{\Phi}) + \tau^2, & 1 \leq i \leq m, \\ \tau^2, & m+1 \leq i \leq n-2. \end{cases}$$

(ii)

$$\cos(\text{Angle}(\hat{\mathbf{u}}_i, \mathcal{U})) \xrightarrow{P} \begin{cases} C_i, & 1 \leq i \leq m, \\ 0, & m+1 \leq i \leq n-2 \end{cases}$$

where

$$C_i = \sqrt{\frac{\phi_i(\mathbf{\Phi})}{\phi_i(\mathbf{\Phi}) + \tau^2}} > 0. \quad (26)$$

In contrast to the case of $\tau_1^2 = \tau_2^2$, Lemma 17 shows that if $\tau_1^2 > \tau_2^2$, then some non-leading eigenvectors of \mathbf{S}_W may capture the variability within \mathcal{U} instead of leading eigenvectors.

Lemma 17 *Suppose Assumptions 1–5 hold. Also, assume $\beta_1 = \beta_2 = 1$ and $\tau_1^2 > \tau_2^2$ and $m_1, m_2 \geq 1$. Then conditional to \mathbf{W}_1 and \mathbf{W}_2 , the following hold as $p \rightarrow \infty$.*

(i)

$$p^{-1}\hat{\lambda}_i \xrightarrow{P} \begin{cases} \phi_i(\mathbf{\Phi}_{\tau_1, \tau_2}), & 1 \leq i \leq k_0, \\ \tau_1^2, & k_0 + 1 \leq i \leq k_0 + (n_1 - m_1 - 1), \\ \phi_{i-(n_1-m_1-1)}(\mathbf{\Phi}_{\tau_1, \tau_2}), & k_0 + (n_1 - m_1) \leq i \leq n_1 + m_2 - 1, \\ \tau_2^2, & n_1 + m_2 \leq i \leq n - 2, \end{cases}$$

where k_0 ($m_1 \leq k_0 \leq m_1 + m_2$) is an integer which satisfies $\phi_{k_0}(\mathbf{\Phi}_{\tau_1, \tau_2}) > \tau_1^2 \geq \phi_{k_0+1}(\mathbf{\Phi}_{\tau_1, \tau_2})$ where we use the convention of $\phi_{m_1+m_2+1}(\mathbf{\Phi}_{\tau_1, \tau_2}) = 0$.

(ii)

$$\cos(\text{Angle}(\hat{\mathbf{u}}_i, \mathcal{U})) \xrightarrow{P} \begin{cases} D_i, & 1 \leq i \leq k_0, \\ 0, & k_0 + 1 \leq i \leq k_0 + (n_1 - m_1 - 1), \\ D_{i-(n_1-m_1-1)}, & k_0 + (n_1 - m_1) \leq i \leq n_1 + m_2 - 1, \\ 0, & n_1 + m_2 \leq i \leq n - 2 \end{cases}$$

where k_0 is defined in Lemma 17 (i),

$$D_i = \sqrt{\frac{\|\sum_{k=1}^2 \mathbf{R}_k \mathbf{\Phi}_k^{1/2} \tilde{v}_{ik}(\mathbf{\Phi}_{\tau_1, \tau_2})\|_2^2}{\phi_i(\mathbf{\Phi}_{\tau_1, \tau_2})}} > 0 \quad (27)$$

and $v_i(\mathbf{\Phi}_{\tau_1, \tau_2}) = (\tilde{v}_{i1}(\mathbf{\Phi}_{\tau_1, \tau_2})^\top, \tilde{v}_{i2}(\mathbf{\Phi}_{\tau_1, \tau_2})^\top)^\top$ with $\tilde{v}_{ik}(\mathbf{\Phi}_{\tau_1, \tau_2}) \in \mathbb{R}^{m_k}$ for $k = 1, 2$.

Remark 6 If $\tau_1^2 = \tau_2^2 =: \tau^2$, then

$$D_i = \begin{cases} C_i, & 1 \leq i \leq m, \\ 0, & m + 1 \leq i \leq m_1 + m_2. \end{cases}$$

Thus, Lemma 16 can be seen as a special case of Lemma 17.

In Lemma 17, if $m = m_1$, we can check that $k_0 = m_1$ with probability 1. In contrast, if $m > m_1$, then k_0 is a random number depending on true leading principal component scores \mathbf{W}_1 and \mathbf{W}_2 , thus it is demanding to identify \mathcal{D} in this case.

Appendix C. Bias-corrected Projected Ridge Classification Rule

In this section, we provide a bias-corrected projected ridge classification rule, which is a bias-corrected version of $\phi_{\text{PRD},\alpha}$ in (15). For the case of strong spikes with unequal tail eigenvalues, when $m_1 = m_2 = 1$, Propositions 7 and 10 show that $\mathbf{v}_{\hat{\alpha}_k}$ is asymptotically orthogonal to $\mathbf{u}_{(k),1}$. These results can be extended to the general cases where $m_1 \geq 1$ and $m_2 \geq 1$. In general, Theorem 18 tells that $\mathbf{v}_{\hat{\alpha}_k}$ is asymptotically orthogonal to $\mathcal{U}_{(k)}$, which is the leading eigenspace of the k th class.

Theorem 18 Suppose Assumptions 1–5 hold and assume $\beta_1 = \beta_2 = 1$ and $\tau_1^2 > \tau_2^2$. Then for $\hat{\alpha}_k$ chosen as an HDLSS-consistent estimator of $-\tau_k^2$, $\text{Angle}(\mathbf{v}_{\hat{\alpha}_k}, \mathbf{u}_{(k),i,S}) \xrightarrow{P} \pi/2$ as $p \rightarrow \infty$ for $k = 1, 2$ and $1 \leq i \leq m_k$.

It implies that $P_{\mathbf{v}_{\hat{\alpha}_k}} \mathcal{Y}_k$ converges to a single point as p increases for each $k = 1, 2$. Hence, in cases where $\mathcal{U}_{(1)}$ includes $\mathcal{U}_{(2)}$ (or $\mathcal{U}_{(2)}$ includes $\mathcal{U}_{(1)}$), both of \mathcal{Y}_1 and \mathcal{Y}_2 are piled on $\mathbf{v}_{\hat{\alpha}_1}$ (or $\mathbf{v}_{\hat{\alpha}_2}$), respectively.

Theorem 19 Suppose Assumptions 1–5 hold and assume $\beta_1 = \beta_2 = 1$, $\tau_1^2 > \tau_2^2$. Also, for $1 \leq k \neq s \leq 2$, further assume that $m = m_k \geq m_s$ (that is, $\mathcal{U}_{(k)}$ includes $\mathcal{U}_{(s)}$). Then for any independent observation $Y \in \mathcal{Y}$,

$$\frac{1}{\sqrt{p}} \mathbf{v}_{\hat{\alpha}_k}^\top (Y - \bar{X}) \xrightarrow{P} \begin{cases} \gamma_k (\eta_2 (1 - \cos^2 \varphi) \delta^2 - (\tau_1^2 - \tau_2^2)/n), & \pi(Y) = 1, \\ \gamma_k (-\eta_1 (1 - \cos^2 \varphi) \delta^2 - (\tau_1^2 - \tau_2^2)/n), & \pi(Y) = 2 \end{cases}$$

as $p \rightarrow \infty$ where γ_k is a strictly positive random variable depending on the true principal component scores of \mathcal{X} .

Note that Theorem 19 is a generalized version of Proposition 7 (iii). For the case of strong spikes with unequal eigenvalues, when $m = m_k$, Theorem 19 tells that projections of independent test data are asymptotically piled on two distinct points on $\mathbf{v}_{\hat{\alpha}_k}$ for each $k = 1, 2$. Hence, a classification rule utilizing $\mathbf{v}_{\hat{\alpha}_k}$ can also achieve asymptotic perfect classification in such cases. In the following, we propose the bias-corrected projected ridge classification rule.

Bias-corrected projected ridge classification rule We define the bias-corrected projected ridge classification rule as

$$\phi_{\text{b-PRD},\alpha}(Y; \mathcal{X}) = \begin{cases} 1, & p^{-1/2} \mathbf{v}_\alpha^\top (Y - \bar{X}) - (\hat{\alpha}_1 - \hat{\alpha}_2) / (n \|\tilde{\mathbf{v}}_\alpha\|) \geq 0, \\ 2, & p^{-1/2} \mathbf{v}_\alpha^\top (Y - \bar{X}) - (\hat{\alpha}_1 - \hat{\alpha}_2) / (n \|\tilde{\mathbf{v}}_\alpha\|) < 0, \end{cases} \quad (28)$$

where $\tilde{\mathbf{v}}_\alpha$ is given as

$$\tilde{\mathbf{v}}_\alpha = \sum_{i \in \mathcal{D}} \frac{\alpha_p}{\hat{\lambda}_i + \alpha_p} \hat{\mathbf{u}}_i \left(\frac{1}{\sqrt{p}} \hat{\mathbf{u}}_i^\top \mathbf{d} \right) + \frac{1}{\sqrt{p}} \hat{\mathbf{U}}_2 \hat{\mathbf{U}}_2^\top \mathbf{d}.$$

Note that $\mathbf{v}_\alpha \propto \tilde{\mathbf{v}}_\alpha$. It can be shown that $\|\tilde{\mathbf{v}}_{\hat{\alpha}_k}\| \xrightarrow{P} \gamma_k^{-1}$ as $p \rightarrow \infty$ where γ_k ($k = 1, 2$) is defined in Theorem 19, and $\phi_{\text{b-PRD},\hat{\alpha}_k}$ achieves asymptotic perfect classification if $m = m_k$ for $k = 1, 2$.

In practice, $\phi_{\text{b-PRD},\alpha}$ requires identifying \mathcal{D} and determining the signal subspace \mathcal{S} onto which the ridged linear discriminant vector \mathbf{w}_α is projected. In case of $m = m_1$, we have seen in Lemma 17 that $k_0 = m_1$ with probability 1 and thus can set $\mathcal{D} = \{1, \dots, m_1, n_1, \dots, n_1 + m_2 - 1\}$. However, this becomes challenging when $m = m_2 > m_1$ as explained in Section 3.2 and Appendix B. In this case, one possible approach to circumvent this difficulty is to set $\mathcal{D} = \{1, \dots, m_1 + m_2, n_1, \dots, n_1 + m_2 - 1\}$, including all sample eigenvectors that may capture the variability within \mathcal{U} in the signal subspace \mathcal{S} . Even if the resulting \mathbf{v}_α is affected by m_2 additional noisy directions, their influence becomes negligible as p increases when $\alpha := \hat{\alpha}_2$ (defined in (9)) is used. Moreover, $\mathbf{v}_{\hat{\alpha}_2}$ yields second data piling and $\phi_{\text{b-PRD},\hat{\alpha}_2}$ achieves asymptotic perfect classification. The simulation results of Setting III in Section 5.1 numerically confirm the validity of this approach.

Appendix D. Double Data Piling for the Case of Strong and Weak Spikes

In this section, we discuss the double data piling phenomenon for the cases where (i) $\beta_1 = 1$ and $\beta_2 < 1$ or (ii) $\beta_1 < 1$ and $\beta_2 = 1$. Recall that in the main article, we assumed $\beta_1 = \beta_2 = 1$ and defined the common leading subspace $\mathcal{U} = \text{span}([\mathbf{U}_{(1),1}, \mathbf{U}_{(2),1}])$. However, if $\beta_1 = 1$ and $\beta_2 < 1$ (or $\beta_1 < 1$ and $\beta_2 = 1$), it is more natural to define \mathcal{U} as the subspace spanned by leading eigenspace of the first (or second) class, respectively. That is, if (i) $\beta_1 = 1$ and $\beta_2 < 1$, we define $\mathcal{U} = \mathcal{U}_{(1)}$ and $m = m_1$. On the other hand, if (ii) $\beta_1 < 1$ and $\beta_2 = 1$, we define $\mathcal{U} = \mathcal{U}_{(2)}$ and $m = m_2$. Lemmas 20 and 21 give the asymptotic limits of the sample eigenvalues and eigenvectors under the assumption of (i) and (ii), respectively. As in the main article, we assume $\tau_1^2 \geq \tau_2^2$.

Lemma 20 *Suppose Assumptions 1–5 hold. Also, assume $\beta_1 = 1$, $0 \leq \beta_2 < 1$ and $\tau_1^2 \geq \tau_2^2$. Then conditional to \mathbf{W}_1 and \mathbf{W}_2 , as $p \rightarrow \infty$,*

$$p^{-1} \hat{\lambda}_i \xrightarrow{P} \begin{cases} \phi_i(\Phi_1) + \tau_1^2, & 1 \leq i \leq m_1, \\ \tau_1^2, & m_1 + 1 \leq i \leq n_1 - 1, \\ \tau_2^2, & n_1 \leq i \leq n - 2 \end{cases}$$

and $\cos(\text{Angle}(\hat{\mathbf{u}}_i, \mathcal{U})) \xrightarrow{P} \begin{cases} A_i & 1 \leq i \leq m_1, \\ 0, & m_1 + 1 \leq i \leq n - 2 \end{cases}$ where $A_i = \sqrt{\phi_i(\Phi_1) / (\phi_i(\Phi_1) + \tau_1^2)}$.

β_1, β_2	τ_1^2, τ_2^2	\mathcal{D}	$ \mathcal{D} $
$\beta_1 = 1$ $\beta_2 < 1$	$\tau_1^2 \geq \tau_2^2$	$\{1, \dots, m\}$	m
$\beta_1 < 1$ $\beta_2 = 1$	$\tau_1^2 \geq \tau_2^2$	$\{1, \dots, k_1, k_1 + n_1, \dots, n_1 + m - 1\}$	m

Table 6: The index set \mathcal{D} for each case. k_1 is a random number depending on the true principal component scores of training data \mathcal{X} defined in Lemma 21.

Lemma 21 *Suppose Assumptions 1–5 hold. Also, assume $0 \leq \beta_1 < 1$, $\beta_2 = 1$ and $\tau_1^2 \geq \tau_2^2$. Then conditional to \mathbf{W}_1 and \mathbf{W}_2 , as $p \rightarrow \infty$,*

$$p^{-1} \hat{\lambda}_i \xrightarrow{P} \begin{cases} \phi_i(\Phi_2) + \tau_2^2, & 1 \leq i \leq k_1, \\ \tau_1^2, & k_1 + 1 \leq i \leq k_1 + (n_1 - 1), \\ \phi_{i-(n_1-1)}(\Phi_2) + \tau_2^2, & k_1 + n_1 \leq i \leq n_1 + m_2 - 1, \\ \tau_2^2, & n_1 + m_2 \leq i \leq n - 2, \end{cases}$$

where k_1 ($0 \leq k_1 \leq m_2$) is an integer which satisfies $\phi_{k_1}(\Phi_2) + \tau_2^2 > \tau_1^2 \geq \phi_{k_1+1}(\Phi_2) + \tau_2^2$ where we use the convention that $\phi_0(\Phi_2) = \infty$ and $\phi_{m_2+1}(\Phi_2) = 0$. Moreover,

$$\cos(\text{Angle}(\hat{\mathbf{u}}_i, \mathcal{U})) \xrightarrow{P} \begin{cases} B_i, & 1 \leq i \leq k_1, \\ 0, & k_1 + 1 \leq i \leq k_1 + (n_1 - 1), \\ B_{i-(n_1-1)}, & k_1 + n_1 \leq i \leq n_1 + m_2 - 1, \\ 0, & n_1 + m_2 \leq i \leq n - 2 \end{cases}$$

where $B_i = \sqrt{\phi_i(\Phi_2) / (\phi_i(\Phi_2) + \tau_2^2)}$.

If (i) $\beta_1 = 1$ and $0 \leq \beta_2 < 1$, then the leading $m = m_1$ sample eigenvectors can always explain the variation within $\mathcal{U} = \mathcal{U}_{(1)}$ in the data from the first class, while the other sample eigenvectors are strongly inconsistent with \mathcal{U} .

In contrast, if (ii) $0 \leq \beta_1 < 1$ and $\beta_2 = 1$, then $m = m_2$ sample eigenvectors explain the variation within $\mathcal{U} = \mathcal{U}_{(2)}$ in the second class, but some non-leading sample eigenvectors may capture the variability instead of some of the leading m_2 sample eigenvectors. For example, if $m_2 = 1$ and $\tau_1^2 = \tau_2^2$, then $k_1 = 1$ with probability 1 and $\hat{\mathbf{u}}_1$ always accounts for the variation along \mathcal{U} . However, if $m_2 = 1$ and $\tau_1^2 > \tau_2^2$, then k_1 is either 0 or 1, which means that either $\hat{\mathbf{u}}_1$ or $\hat{\mathbf{u}}_{n_1}$ can capture the variability along \mathcal{U} .

Let $\mathcal{S} = \text{span}(\{\hat{\mathbf{u}}_i\}_{i \in \mathcal{D}}, \mathbf{w}_{\text{MDP}})$ with \mathcal{D} be given in Table 6 for each case. It can be shown that Theorem 3 also holds for the case of (i) $\beta_1 = 1, \beta_2 < 1$ or (ii) $\beta_1 < 1, \beta_2 = 1$, that is, projections of \mathcal{Y} onto \mathcal{S} are distributed along parallel affine subspaces, one for each class. More precisely, projections of \mathcal{Y}_k onto \mathcal{S} tend to lie on an m -dimensional affine subspace \mathcal{L}_k if $\beta_k = 1$, or a point in \mathcal{L}_k if $\beta_k < 1$. See Figure 8 for an illustration.

Furthermore, we can show that the projected ridged linear discriminant vector \mathbf{v}_α defined in (11) with a negative ridge parameter can also be a second maximal data piling

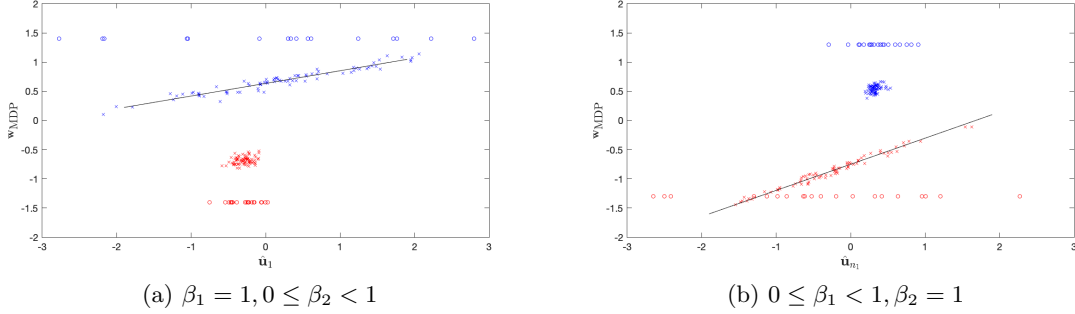


Figure 8: 2-dimensional projections of training data \mathcal{X} (class 1: blue circles, class 2: red circles) and independent test data \mathcal{Y} (class 1: blue crosses, class 2: red crosses) onto (a) $\mathcal{S}_1 = \text{span}(\hat{\mathbf{u}}_1, \mathbf{w}_{\text{MDP}})$ and (b) $\mathcal{S}_{n_1} = \text{span}(\hat{\mathbf{u}}_{n_1}, \mathbf{w}_{\text{MDP}})$.

direction for these cases. Theorem 22 shows that $\mathbf{v}_{-\tau_1^2}$ (or $\mathbf{v}_{-\tau_2^2}$) yields second data piling if (i) $\beta_1 = 1, \beta_2 < 1$ (or (ii) $\beta_1 < 1, \beta_2 = 1$), respectively.

Theorem 22 *Suppose Assumptions 1–5 hold and assume $\beta_k = 1, \beta_s < 1$ ($1 \leq k \neq s \leq 2$). Then for $\hat{\alpha}_k$ chosen as an HDLSS-consistent estimator of $-\tau_k^2$, $\text{Angle}(\mathbf{v}_{\hat{\alpha}_k}, \mathbf{u}_{(k),i,\mathcal{S}}) \xrightarrow{P} \pi/2$ as $p \rightarrow \infty$ for all $1 \leq i \leq m_k$. Moreover, for any independent observation $Y \in \mathcal{Y}$,*

$$\frac{1}{\sqrt{p}} \mathbf{v}_{\hat{\alpha}_k}^\top (Y - \bar{X}) \xrightarrow{P} \begin{cases} \gamma_{A,k}(\eta_2(1 - \cos^2 \varphi)\delta^2 - (\tau_1^2 - \tau_2^2)/n), & \pi(Y) = 1, \\ \gamma_{A,k}(-\eta_1(1 - \cos^2 \varphi)\delta^2 - (\tau_1^2 - \tau_2^2)/n), & \pi(Y) = 2 \end{cases} \quad (29)$$

as $p \rightarrow \infty$ where $\gamma_{A,k}$ is a strictly positive random variable depending on the true principal component scores of \mathcal{X} .

Similarly to the case of strong spikes with equal tail eigenvalues in Section 4.2, we can show that $\{\mathbf{w}\} \in \mathcal{A}$ is asymptotically close to the subspace spanned by $\mathbf{v}_{\hat{\alpha}_1}$ (or $\mathbf{v}_{\hat{\alpha}_2}$) and $\{\hat{\mathbf{u}}_i\}_{i \in \{1, \dots, n-2\} \setminus \mathcal{D}}$ for case (i) (or (ii)), respectively. This naturally implies that $\mathbf{v}_{\hat{\alpha}_1}$ (or $\mathbf{v}_{\hat{\alpha}_2}$) is a second maximal data piling direction. Furthermore, it can be shown that the bias-corrected projected ridge classification rule $\phi_{\text{b-PRD},\alpha}$ in (28) achieves perfect classification only at the negative ridge parameter $\alpha = -\tau_k^2$ if $\beta_k = 1, \beta_s < 1$ ($1 \leq k \neq s \leq 2$) with a regularizing condition on the distribution of $(\mathbf{z}_{k,1}, \dots, \mathbf{z}_{k,m_k})^\top$ as in Theorem 3.7 of Chang et al. (2021).

As seen in Appendix C, the use of \mathbf{v}_α requires correctly identifying \mathcal{D} and determining the signal subspace \mathcal{S} . This becomes challenging when $\beta_1 < 1, \beta_2 = 1$ and $\tau_1^2 > \tau_2^2$ as shown in Lemma 21. Similarly done in Appendix C for the case of strong spikes, we can set $\mathcal{D} = \{1, \dots, m_2, n_1, \dots, n_1 + m_2 - 1\}$. Even if \mathbf{v}_α is affected by m_2 additional noisy directions, it can still yield second data piling when using $\alpha := \hat{\alpha}_2$, and $\phi_{\text{b-PRD},\hat{\alpha}_2}$ achieves asymptotic perfect classification.

Appendix E. Proofs of Main Results

In this section, we give the proofs of main lemmas and theorems. Unless otherwise stated, we only give the proofs for the case of $\beta_1 = \beta_2 = 1$, $\tau_1^2 > \tau_2^2$. The proofs for the other cases are quite similar to, but much simpler than, those for this case.

For any vector $\mathbf{v} \in \mathbb{R}^l$ ($l \in \mathbb{N}$), let $[\mathbf{v}]_i$ denote the i th element of \mathbf{v} . For any matrix $\mathbf{M} \in \mathbb{R}^{l \times l'}$ ($l, l' \in \mathbb{N}$), let $[\mathbf{M}]_i$ and $[\mathbf{M}]^j$ denote the i th row and the j th column of \mathbf{M} , respectively. Also, let $[\mathbf{M}]_{i,j}$ denote the (i, j) -coordinate of \mathbf{M} . Let $\mathbf{1}_l \in \mathbb{R}^l$ (and $\mathbf{0}_l \in \mathbb{R}^l$) denote a vector whose all entries are 1 (and 0, respectively). Write an $(l \times l)$ identity matrix as \mathbf{I}_l , and an $(l \times l')$ matrix whose entries are all zero as $\mathbf{O}_{l \times l'}$. Also, for $k = 1, 2$, let \mathbf{J}_{n_k} be the matrix of size $n_k \times n_k$ whose all entries are 1 and $\mathbf{J} = \begin{pmatrix} \frac{1}{n_1} \mathbf{J}_{n_1} & \mathbf{O}_{n_1 \times n_2} \\ \mathbf{O}_{n_2 \times n_1} & \frac{1}{n_2} \mathbf{J}_{n_2} \end{pmatrix}$.

E.1 Preliminary Lemmas

Recall that the matrix of true principal component scores of $\mathbf{X}_k = [X_{k1}, \dots, X_{kn_k}]$ is $\mathbf{Z}_k = \Lambda_{(k)}^{-\frac{1}{2}} \mathbf{U}_{(k)}^\top (\mathbf{X}_k - \boldsymbol{\mu}_{(k)} \mathbf{1}_{n_k}^\top) = [\mathbf{z}_{k,1}, \dots, \mathbf{z}_{k,p}]^\top \in \mathbb{R}^{p \times n_k}$ where $\mathbf{z}_{k,j}$ is a vector of j th principal component scores of the k th class. We write $\bar{\mathbf{z}}_{k,i} = n_k^{-1} \mathbf{z}_{k,i}^\top \mathbf{1}_{n_k}$. Also, denote a vector of true principal component scores of independent observation Y by $\boldsymbol{\zeta} = (\zeta_1, \dots, \zeta_p)^\top$. Then each element of \mathbf{Z}_k and $\boldsymbol{\zeta}$ is uncorrelated, and has mean zero and unit variance. The following lemma follows directly from Lemma C.1 of Chang et al. (2021).

Lemma 23 *Suppose Assumptions 1–5 hold. For $k = 1, 2$, the following hold as $p \rightarrow \infty$.*

$$\begin{aligned}
 (i) \quad & p^{-1} \boldsymbol{\mu}^\top \mathbf{U}_{(k)} \Lambda_{(k)}^{1/2} \boldsymbol{\zeta} \xrightarrow{P} \begin{cases} \sum_{i=1}^{m_k} \sigma_{k,i} \cos \theta_{k,i} \delta \zeta_i, & \beta_k = 1, \\ 0, & 0 \leq \beta_k < 1. \end{cases} \\
 (ii) \quad & p^{-1} \boldsymbol{\mu}^\top \mathbf{U}_{(k)} \Lambda_{(k)}^{1/2} \mathbf{Z}_k \xrightarrow{P} \begin{cases} \sum_{i=1}^{m_k} \sigma_{k,i} \cos \theta_{k,i} \delta \mathbf{z}_{k,i}^\top, & \beta_k = 1, \\ 0, & 0 \leq \beta_k < 1. \end{cases} \\
 (iii) \quad & p^{-1} \mathbf{Z}_k^\top \Lambda_{(k)} \boldsymbol{\zeta} \xrightarrow{P} \begin{cases} \sum_{i=1}^{m_k} \sigma_{k,i}^2 z_{k,i} \zeta_i, & \beta_k = 1, \\ 0, & 0 \leq \beta_k < 1. \end{cases} \\
 (iv) \quad & p^{-1} \mathbf{Z}_k^\top \Lambda_{(k)} \mathbf{Z}_k \xrightarrow{P} \begin{cases} \sum_{i=1}^{m_k} \sigma_{k,i}^2 z_{k,i} z_{k,i}^\top + \tau_k^2 \mathbf{I}_{n_k}, & \beta_k = 1, \\ \tau_k^2 \mathbf{I}_{n_k}, & 0 \leq \beta_k < 1. \end{cases}
 \end{aligned}$$

We will investigate asymptotic properties of the sample within-scatter matrix $\mathbf{S}_W = (\mathbf{X} - \bar{\mathbf{X}})(\mathbf{X} - \bar{\mathbf{X}})^\top = \sum_{i=1}^{n-2} \hat{\lambda}_i \hat{\mathbf{u}}_i \hat{\mathbf{u}}_i^\top$ where $\mathbf{X} = [\mathbf{X}_1, \mathbf{X}_2]$ and $\bar{\mathbf{X}} = [\bar{\mathbf{X}}_1, \bar{\mathbf{X}}_2]$. Since the dimension of \mathbf{S}_W grows as $p \rightarrow \infty$, we instead use the $n \times n$ dual matrix, $\mathbf{S}_D = (\mathbf{X} - \bar{\mathbf{X}})^\top (\mathbf{X} - \bar{\mathbf{X}})$, which shares its nonzero eigenvalues with \mathbf{S}_W . We write the singular-value-decomposition of $\mathbf{X} - \bar{\mathbf{X}} = \hat{\mathbf{U}}_1 \mathbf{D}_1 \hat{\mathbf{V}}_1^\top = \sum_{i=1}^{n-2} d_i \hat{\mathbf{u}}_i \hat{\mathbf{v}}_i^\top$, where $\hat{\mathbf{u}}_i$ is the i th eigenvector of \mathbf{S}_W , d_i is the i th largest nonzero singular value, and $\hat{\mathbf{v}}_i$ is the vector of normalized sample principal component scores. Write $\hat{\mathbf{v}}_i = (\hat{\mathbf{v}}_{i,1}^\top, \hat{\mathbf{v}}_{i,2}^\top)^\top$ where $\hat{\mathbf{v}}_{i,1} \in \mathbb{R}^{n_1}$ and $\hat{\mathbf{v}}_{i,2} \in \mathbb{R}^{n_2}$. Then for $1 \leq i \leq n-2$, we can write

$$\hat{\mathbf{u}}_i = d_i^{-1} (\mathbf{X} - \bar{\mathbf{X}}) \hat{\mathbf{v}}_i = \hat{\lambda}_i^{-1/2} \sum_{k=1}^2 \mathbf{U}_{(k)} \Lambda_{(k)}^{1/2} \mathbf{Z}_k \left(\mathbf{I}_{n_k} - \frac{1}{n_k} \mathbf{J}_{n_k} \right) \hat{\mathbf{v}}_{i,k}. \quad (30)$$

Recall that $\mathbf{W}_k = [\sigma_{k,1}\mathbf{z}_{k,1}, \dots, \sigma_{k,m_k}\mathbf{z}_{k,m_k}]$ is $n_k \times m_k$ matrix of the leading m_k principal component scores of the k th class for each $k = 1, 2$.

Lemma 24 *Suppose Assumptions 1–5 hold. Then,*

$$p^{-1}\mathbf{S}_D \xrightarrow{P} \mathbf{S}_0 := \begin{pmatrix} \mathbf{S}_{0,11} & \mathbf{S}_{0,12} \\ \mathbf{S}_{0,21} & \mathbf{S}_{0,22} \end{pmatrix}$$

as $p \rightarrow \infty$ where

$$\mathbf{S}_{0,ii} = \begin{cases} (\mathbf{I}_{n_i} - \frac{1}{n_i}\mathbf{J}_{n_i})(\mathbf{W}_i\mathbf{W}_i^\top + \tau_i^2\mathbf{I}_{n_i})(\mathbf{I}_{n_i} - \frac{1}{n_i}\mathbf{J}_{n_i}), & \beta_i = 1, \\ \tau_i^2(\mathbf{I}_{n_i} - \frac{1}{n_i}\mathbf{J}_{n_i}), & 0 \leq \beta_i < 1 \end{cases}$$

for $i = 1, 2$ and

$$\mathbf{S}_{0,ij} = \begin{cases} (\mathbf{I}_{n_i} - \frac{1}{n_i}\mathbf{J}_{n_i})(\mathbf{W}_i\mathbf{R}_i^\top\mathbf{R}_j\mathbf{W}_j^\top)(\mathbf{I}_{n_j} - \frac{1}{n_j}\mathbf{J}_{n_j}), & \beta_1 = \beta_2 = 1, \\ \mathbf{O}_{n_i \times n_j}, & o.w \end{cases}$$

for $1 \leq i \neq j \leq 2$.

Proof Observe that $\mathbf{X} - \bar{\mathbf{X}} = \mathbf{X}(\mathbf{I}_n - \mathbf{J}) = [\mathbf{U}_{(1)}\mathbf{\Lambda}_{(1)}^{1/2}\mathbf{Z}_1, \mathbf{U}_{(2)}\mathbf{\Lambda}_{(2)}^{1/2}\mathbf{Z}_2](\mathbf{I}_n - \mathbf{J})$ and

$$\frac{\mathbf{S}_D}{p} = (\mathbf{I}_n - \mathbf{J}) \begin{pmatrix} p^{-1}\mathbf{Z}_1^\top\mathbf{\Lambda}_{(1)}\mathbf{Z}_1 & p^{-1}\mathbf{Z}_1^\top\mathbf{\Lambda}_{(1)}^{1/2}\mathbf{U}_{(1)}^\top\mathbf{U}_{(2)}\mathbf{\Lambda}_{(2)}^{1/2}\mathbf{Z}_2 \\ p^{-1}\mathbf{Z}_2^\top\mathbf{\Lambda}_{(2)}^{1/2}\mathbf{U}_{(2)}^\top\mathbf{U}_{(1)}\mathbf{\Lambda}_{(1)}^{1/2}\mathbf{Z}_1 & p^{-1}\mathbf{Z}_2^\top\mathbf{\Lambda}_{(2)}\mathbf{Z}_2 \end{pmatrix} (\mathbf{I}_n - \mathbf{J}).$$

By Lemma 23 (iv), we have $p^{-1}\mathbf{Z}_i^\top\mathbf{\Lambda}_{(i)}\mathbf{Z}_i \xrightarrow{P} \begin{cases} \mathbf{W}_i\mathbf{W}_i^\top + \tau_i^2\mathbf{I}_{n_i}, & \beta_i = 1, \\ \tau_i^2\mathbf{I}_{n_i}, & 0 \leq \beta_i < 1 \end{cases}$ as $p \rightarrow \infty$.

Thus, it suffices to show that

$$p^{-1}\mathbf{Z}_1^\top\mathbf{\Lambda}_{(1)}^{1/2}\mathbf{U}_{(1)}^\top\mathbf{U}_{(2)}\mathbf{\Lambda}_{(2)}^{1/2}\mathbf{Z}_2 \xrightarrow{P} \begin{cases} \mathbf{W}_1\mathbf{R}_1^\top\mathbf{R}_2\mathbf{W}_2^\top, & \beta_1 = \beta_2 = 1, \\ \mathbf{O}_{n_1 \times n_2}, & o.w \end{cases}$$

as $p \rightarrow \infty$. Let $\mathbf{A}_{ij} = \mathbf{Z}_{1,i}^\top\mathbf{\Lambda}_{(1),i}^{1/2}\mathbf{U}_{(1),i}^\top\mathbf{U}_{(2),j}\mathbf{\Lambda}_{(2),j}^{1/2}\mathbf{Z}_{2,j}$ for $i, j = 1, 2$ where $\mathbf{U}_{(k),1} = [\mathbf{u}^{(k),1}, \dots, \mathbf{u}^{(k),m_k}]$, $\mathbf{U}_{(k),2} = [\mathbf{u}^{(k),m_k+1}, \dots, \mathbf{u}^{(k),p}]$, $\mathbf{\Lambda}_{(k),1} = \text{Diag}(\{\lambda^{(k),i}\}_{i=1}^{m_k})$, $\mathbf{\Lambda}_{(k),2} = \text{Diag}(\{\lambda^{(k),i}\}_{i=m_k+1}^p)$, $\mathbf{Z}_{k,1} = [\mathbf{z}_{k,1}, \dots, \mathbf{z}_{k,m_k}]^\top$ and $\mathbf{Z}_{k,2} = [\mathbf{z}_{k,m_k+1}, \dots, \mathbf{z}_{k,p}]^\top$. Then, we can decompose $\mathbf{Z}_1^\top\mathbf{\Lambda}_{(1)}^{1/2}\mathbf{U}_{(1)}^\top\mathbf{U}_{(2)}\mathbf{\Lambda}_{(2)}^{1/2}\mathbf{Z}_2 = \sum_{i,j=1}^2 \mathbf{A}_{ij}$. By Assumption 2, there exists $M_k < \infty$ such that $\tau_{k,i} \leq M_k$ for all i . Thus,

$$\begin{aligned} p^{-2}\mathbb{E}\|\mathbf{A}_{12}\|_F^2 &= p^{-2}\mathbb{E}\text{trace}(\mathbf{A}_{12}^\top\mathbf{A}_{12}) = p^{-2}n_1n_2\text{trace}(\mathbf{U}_{(2),2}^\top\mathbf{U}_{(1),1}\mathbf{\Lambda}_{(1),1}\mathbf{U}_{(1),1}^\top\mathbf{U}_{(2),2}\mathbf{\Lambda}_{(2),2}) \\ &= p^{-2}n_1n_2 \sum_{l=1}^{m_1} \sum_{l'=m_2+1}^p (p^{\beta_1}\sigma_{1,l}^2 + \tau_{1,l}^2)\tau_{2,l'}^2(\mathbf{u}_{(1),l}^\top\mathbf{u}_{(2),l'})^2 \leq p^{-2}n_1n_2m_1(p^{\beta_1}\sigma_{1,1}^2 + M_1^2)M_2^2 \rightarrow 0 \end{aligned}$$

as $p \rightarrow \infty$ where $\|\cdot\|_F$ denotes the Frobenius norm of a matrix. Thus, $p^{-1}\mathbf{A}_{12} \xrightarrow{P} \mathbf{O}_{n_1 \times n_2}$ as $p \rightarrow \infty$, and $p^{-1}\mathbf{A}_{21}, p^{-1}\mathbf{A}_{22} \xrightarrow{P} \mathbf{O}_{n_1 \times n_2}$ can be shown in a similar manner. Then it

suffices to show that $p^{-1}\mathbf{A}_{11} \xrightarrow{P} \mathbf{W}_1\mathbf{R}_1^\top\mathbf{R}_2\mathbf{W}_2^\top$ if $\beta_1 = \beta_2 = 1$ and $p^{-1}\mathbf{A}_{11} \xrightarrow{P} \mathbf{O}_{n_1 \times n_2}$ otherwise as $p \rightarrow \infty$. If $\beta_1 < 1$ or $\beta_2 < 1$, then

$$\begin{aligned} p^{-2}\mathbb{E}\|\mathbf{A}_{11}\|_F^2 &= p^{-2}n_1n_2 \sum_{l=1}^{m_1} \sum_{l'=1}^{m_2} (p^{\beta_1}\sigma_{1,l}^2 + \tau_{1,l}^2)(p^{\beta_2}\sigma_{2,l'}^2 + \tau_{2,l'}^2)(\mathbf{u}_{(1),l}^\top\mathbf{u}_{(2),l'})^2 \\ &\leq p^{-2}n_1n_2m_1m_2(p^{\beta_1}\sigma_{1,1}^2 + M_1^2)(p^{\beta_2}\sigma_{2,1}^2 + M_2^2) \rightarrow 0 \end{aligned}$$

and $p^{-1}\mathbf{A}_{11} \xrightarrow{P} \mathbf{O}_{n_1 \times n_2}$ as $p \rightarrow \infty$ since $\beta_1 + \beta_2 < 2$. If $\beta_1 = \beta_2 = 1$, then $p^{-1}\mathbf{A}_{11} = p^{-1}\mathbf{Z}_{1,1}^\top\mathbf{\Lambda}_{(1),1}^{1/2}\mathbf{R}_1^{(p)\top}\mathbf{R}_2\mathbf{\Lambda}_{(2),1}^{1/2}\mathbf{Z}_{2,1} \xrightarrow{P} \mathbf{W}_1\mathbf{R}_1^\top\mathbf{R}_2\mathbf{W}_2^\top$ as $p \rightarrow \infty$. \blacksquare

E.2 Proof of Lemmas 16 and 17

Lemmas 23 and 24 play an important role in the proof of Lemmas 16 and 17. Recall that for any square matrix \mathbf{M} , $\phi_i(\mathbf{M})$ and $v_i(\mathbf{M})$ denote the i th largest eigenvalue of \mathbf{M} and its corresponding eigenvector, respectively. Also, let $v_{ij}(\mathbf{M})$ be the j th coefficient of $v_i(\mathbf{M})$. For \mathbf{S}_0 defined in Lemma 24, write $v_i(\mathbf{S}_0) = (\tilde{v}_{i1}(\mathbf{S}_0)^\top, \tilde{v}_{i2}(\mathbf{S}_0)^\top)^\top$ where $\tilde{v}_{i1}(\mathbf{S}_0) \in \mathbb{R}^{n_1}$ and $\tilde{v}_{i2}(\mathbf{S}_0) \in \mathbb{R}^{n_2}$. Also, for $\mathbf{\Phi}_{\tau_1, \tau_2}$ defined in (24), write $v_i(\mathbf{\Phi}_{\tau_1, \tau_2}) = (\tilde{v}_{i1}(\mathbf{\Phi}_{\tau_1, \tau_2})^\top, \tilde{v}_{i2}(\mathbf{\Phi}_{\tau_1, \tau_2})^\top)^\top$ where $\tilde{v}_{i1}(\mathbf{\Phi}_{\tau_1, \tau_2}) \in \mathbb{R}^{m_1}$ and $\tilde{v}_{i2}(\mathbf{\Phi}_{\tau_1, \tau_2}) \in \mathbb{R}^{m_2}$.

Proof The proof of Lemma 16 closely follows those of Lemmas C.2 and C.3 of Chang et al. (2021). To prove Lemma 17, assume $\beta_1 = \beta_2 = 1$ and $\tau_1^2 > \tau_2^2$. By Lemma 24, as $p \rightarrow \infty$,

$$\frac{1}{p}\mathbf{S}_D \xrightarrow{P} \mathbf{S}_0 = (\mathbf{I}_n - \mathbf{J}) \begin{pmatrix} \mathbf{W}_1\mathbf{W}_1^\top + \tau_1^2\mathbf{I}_{n_1} & \mathbf{W}_1\mathbf{R}_1^\top\mathbf{R}_2\mathbf{W}_2^\top \\ \mathbf{W}_2\mathbf{R}_2^\top\mathbf{R}_1\mathbf{W}_1^\top & \mathbf{W}_2\mathbf{W}_2^\top + \tau_2^2\mathbf{I}_{n_2} \end{pmatrix} (\mathbf{I}_n - \mathbf{J}).$$

To show (i), recall that \mathbf{S}_W shares its nonzero eigenvalues with \mathbf{S}_D , and since ϕ_i is a continuous function of elements of a symmetric matrix, we have $p^{-1}\phi_i(\mathbf{S}_W) \xrightarrow{P} \phi_i(\mathbf{S}_0)$ as $p \rightarrow \infty$ for $1 \leq i \leq n - 2$. First, let $\mathbf{h}_0 = (\mathbf{h}_{01}^\top, \mathbf{0}_{n_2}^\top)^\top \in \mathbb{R}^n$ be a unit vector satisfying

$$\mathbf{W}_1^\top \left(\mathbf{I}_{n_1} - \frac{1}{n_1}\mathbf{J}_{n_1} \right) \mathbf{h}_{01} = \mathbf{0}_{m_1} \quad (31)$$

and $\mathbf{1}_{n_1}^\top \mathbf{h}_{01} = 0$. Then, $\mathbf{S}_0\mathbf{h}_0 = \tau_1^2\mathbf{h}_0$. It implies that \mathbf{S}_0 has an eigenvalue τ_1^2 of multiplicity $(n_1 - m_1 - 1)$. Likewise, we can show that \mathbf{S}_0 has an eigenvalue τ_2^2 of multiplicity $(n_2 - m_2 - 1)$. Lastly, let $\mathbf{h}_i = (\mathbf{h}_{i1}^\top, \mathbf{h}_{i2}^\top)^\top \in \mathbb{R}^n$ ($1 \leq i \leq m_1 + m_2$) be a unit vector with

$$\mathbf{h}_{ik} = \left(\mathbf{I}_{n_k} - \frac{1}{n_k}\mathbf{J}_{n_k} \right) \mathbf{W}_k\mathbf{\Phi}_k^{-1/2}\tilde{v}_{ik}(\mathbf{\Phi}_{\tau_1, \tau_2}) \quad (32)$$

for $k = 1, 2$. Then, $\mathbf{S}_0\mathbf{h}_i = \phi_i(\mathbf{\Phi}_{\tau_1, \tau_2})\mathbf{h}_i$ for all $1 \leq i \leq m_1 + m_2$. Thus, \mathbf{S}_0 has eigenvalues $\phi_i(\mathbf{\Phi}_{\tau_1, \tau_2})$ for $1 \leq i \leq m_1 + m_2$. In summary, \mathbf{S}_0 has $(n - 2)$ non-negative eigenvalues with τ_1^2 of multiplicity $(n_1 - m_1 - 1)$, τ_2^2 of multiplicity $(n_2 - m_2 - 1)$ and $\phi_i(\mathbf{\Phi}_{\tau_1, \tau_2})$ for $1 \leq i \leq m_1 + m_2$. Note that $\phi_{m_1}(\mathbf{\Phi}_{\tau_1, \tau_2}) > \tau_1^2$ and $\phi_{m_1+m_2}(\mathbf{\Phi}_{\tau_1, \tau_2}) > \tau_2^2$ can be shown by Weyl's inequality and the positive definiteness of $\mathbf{\Phi}_1$ and $\mathbf{\Phi}_2$ (with probability 1). Hence, $\mathbb{P}(m_1 \leq k_0 \leq m_1 + m_2) = 1$ where k_0 is an integer which satisfies $\phi_{k_0}(\mathbf{\Phi}_{\tau_1, \tau_2}) > \tau_1^2 \geq \phi_{k_0+1}(\mathbf{\Phi}_{\tau_1, \tau_2})$ where we use the convention of $\phi_{m_1+m_2+1}(\mathbf{\Phi}_{\tau_1, \tau_2}) = 0$.

To show (ii), we will show that

$$\hat{\mathbf{u}}_i^\top \mathbf{u}_j \xrightarrow{P} \begin{cases} D_{i,j}, & 1 \leq i \leq k_0, \\ 0, & k_0 + 1 \leq i \leq k_0 + (n_1 - m_1 - 1), \\ D_{i-(n_1-m_1-1),j}, & k_0 + (n_1 - m_1) \leq i \leq n_1 + m_2 - 1, \\ 0, & n_1 + m_2 \leq i \leq n - 2 \end{cases} \quad (33)$$

where k_0 ($m_1 \leq k_0 \leq m_1 + m_2$) is defined in (i) and

$$D_{i,j} := \frac{1}{\sqrt{\phi_i(\Phi_{\tau_1, \tau_2})}} \sum_{k=1}^2 [\mathbf{R}_k]_j \Phi_k^{1/2} \tilde{v}_{ik}(\Phi_{\tau_1, \tau_2}) \quad (34)$$

for $1 \leq i \leq m_1 + m_2$ and $1 \leq j \leq m$. Using (30), we can write

$$\mathbf{u}_j^\top \hat{\mathbf{u}}_i = \left(\frac{\hat{\lambda}_i}{p} \right)^{-1/2} \sum_{k=1}^2 \frac{1}{\sqrt{p}} \mathbf{u}_j^\top \mathbf{U}_{(k)} \Lambda_{(k)}^{1/2} \mathbf{Z}_k \left(\mathbf{I}_{n_k} - \frac{1}{n_k} \mathbf{J}_{n_k} \right) \hat{\mathbf{v}}_{i,k}.$$

Note that $p^{-1/2} \mathbf{u}_j^\top \mathbf{U}_{(k)} \Lambda_{(k)}^{1/2} \mathbf{Z}_k$ can be decomposed into two terms:

$$\frac{1}{\sqrt{p}} \mathbf{u}_j^\top \mathbf{U}_{(k)} \Lambda_{(k)}^{1/2} \mathbf{Z}_k = \sum_{i=1}^{m_k} \frac{1}{\sqrt{p}} \mathbf{u}_j^\top \mathbf{u}_{(k),i} \lambda_{(k),i}^{1/2} \mathbf{z}_{k,i}^\top + \sum_{i=m_k+1}^p \frac{1}{\sqrt{p}} \mathbf{u}_j^\top \mathbf{u}_{(k),i} \lambda_{(k),i}^{1/2} \mathbf{z}_{k,i}^\top$$

for $1 \leq j \leq m$. The first term converges to $[\mathbf{R}_k]_j \mathbf{W}_k^\top$ in probability as $p \rightarrow \infty$. The second term converges to zero in probability since for any $\epsilon > 0$,

$$\begin{aligned} \mathbb{P} \left(\left\| \sum_{i=m_k+1}^p \frac{1}{\sqrt{p}} \mathbf{u}_j^\top \mathbf{u}_{(k),i} \lambda_{(k),i}^{1/2} \mathbf{z}_{k,i}^\top \right\| > \epsilon \right) &\leq \frac{1}{p\epsilon^2} \mathbb{E} \left(\left\| \sum_{i=m_k+1}^p \mathbf{u}_j^\top \mathbf{u}_{(k),i} \tau_{k,i} \mathbf{z}_{k,i}^\top \right\|^2 \right) \\ &= \frac{1}{p\epsilon^2} \mathbb{E} \left(\sum_{i=m_k+1}^p (\mathbf{u}_j^\top \mathbf{u}_{(k),i})^2 \tau_{k,i}^2 \mathbf{z}_{k,i}^\top \mathbf{z}_{k,i} \right) \leq \frac{n_k M_k^2}{p\epsilon^2} \rightarrow 0 \end{aligned} \quad (35)$$

as $p \rightarrow \infty$. Then we have $p^{-1/2} \mathbf{u}_j^\top \mathbf{U}_{(k)} \Lambda_{(k)}^{1/2} \mathbf{Z}_k \xrightarrow{P} [\mathbf{R}_k]_j \mathbf{W}_k^\top$ as $p \rightarrow \infty$ for $k = 1, 2$. Note that for $i \in \mathcal{D} = \{1, \dots, k_0, k_0 + (n_1 - m_1), \dots, n_1 + m_2 - 1\}$, $\hat{\mathbf{v}}_i = (\hat{\mathbf{v}}_{i,1}, \hat{\mathbf{v}}_{i,2})^\top \xrightarrow{P} v_i(\mathbf{S}_0)$ as $p \rightarrow \infty$. Hence, for $i \in \mathcal{D}$ and $1 \leq j \leq m$, $\mathbf{u}_j^\top \hat{\mathbf{u}}_i \xrightarrow{P} \phi_i(\mathbf{S}_0)^{-1/2} \mathbf{e}_j^\top \mathbf{W}^\top (\mathbf{I}_n - \mathbf{J}) v_i(\mathbf{S}_0)$ as $p \rightarrow \infty$ where $\mathbf{e}_j \in \mathbb{R}^m$ is a vector whose j th coordinate is 1 and other coordinates are zero. Using (32), we have $\mathbf{u}_j^\top \hat{\mathbf{u}}_i \xrightarrow{P} D_{i,j}$ for $1 \leq i \leq k_0$ and $\mathbf{u}_j^\top \hat{\mathbf{u}}_i \xrightarrow{P} D_{i-(n_1-m_1-1),j}$ for $k_0 + (n_1 - m_1) \leq i \leq n_1 + m_2 - 1$ as $p \rightarrow \infty$. In contrast, for $i \in \{1, \dots, n - 2\} \setminus \mathcal{D}$, (31) gives $\mathbf{W}_1^\top (\mathbf{I}_{n_1} - n_1^{-1} \mathbf{J}_{n_1}) \hat{\mathbf{v}}_{i,1} = o_p(1)$ and $\mathbf{W}_2^\top (\mathbf{I}_{n_2} - n_2^{-1} \mathbf{J}_{n_2}) \hat{\mathbf{v}}_{i,2} = o_p(1)$, which imply that $\mathbf{W}^\top (\mathbf{I}_n - \mathbf{J}) \hat{\mathbf{v}}_i = o_p(1)$ and $\mathbf{u}_j^\top \hat{\mathbf{u}}_i \xrightarrow{P} 0$ as $p \rightarrow \infty$. Now the limit of $\cos(\text{Angle}(\hat{\mathbf{u}}_i, \mathcal{U})) = \sqrt{\sum_{j=1}^m (\hat{\mathbf{u}}_i^\top \mathbf{u}_j)^2}$ can be obtained by (33). \blacksquare

Note that Lemmas 16 and 17 can also be used to investigate the asymptotic behavior of $\hat{\mathbf{u}}_i^\top \mathbf{d}$, where \mathbf{d} is the sample mean difference vector. Lemma 25 will be used frequently in the proof of main theorems.

Lemma 25 *Suppose Assumptions 1–5 hold. Then conditional to \mathbf{W}_1 and \mathbf{W}_2 , the following hold as $p \rightarrow \infty$.*

(i) *If $\beta_1 = \beta_2 = 1$ and $\tau_1^2 = \tau_2^2 =: \tau^2$, then*

$$p^{-1/2} \mathbf{d}^\top \hat{\mathbf{u}}_i \xrightarrow{P} \begin{cases} \sum_{j=1}^m r_j C_{i,j}, & 1 \leq i \leq m, \\ 0, & m+1 \leq i \leq n-2 \end{cases}$$

for $1 \leq j \leq m$ where $r_j := \cos \theta_j \delta + \sum_{k=1}^{m_1} [\mathbf{R}_1]_{jk} \sigma_{1,k} \bar{\mathbf{z}}_{1,k} - \sum_{k=1}^{m_2} [\mathbf{R}_2]_{jk} \sigma_{2,k} \bar{\mathbf{z}}_{2,k}$ and $C_{i,j} := \sqrt{\phi_i(\Phi) / (\phi_i(\Phi) + \tau^2)} v_{ij}(\Phi)$.

(ii) *If $\beta_1 = \beta_2 = 1$ and $\tau_1^2 > \tau_2^2$, then*

$$p^{-1/2} \mathbf{d}^\top \hat{\mathbf{u}}_i \xrightarrow{P} \begin{cases} \sum_{j=1}^m r_j D_{i,j}, & 1 \leq i \leq k_0, \\ 0, & k_0 + 1 \leq i \leq k_0 + (n_1 - m_1 - 1), \\ \sum_{j=1}^m r_j D_{i-(n_1-m_1-1),j}, & k_0 + (n_1 - m_1) \leq i \leq n_1 + m_2 - 1, \\ 0, & n_1 + m_2 \leq i \leq n - 2 \end{cases}$$

for $1 \leq j \leq m$ where k_0 is defined in Lemma 17 (i), r_j is defined in Lemma 25 (i) and $D_{i,j}$ is defined in (34).

Proof Observe that $\mathbf{d} = \bar{X}_1 - \bar{X}_2 = \boldsymbol{\mu} + \frac{1}{n_1} \mathbf{U}_{(1)} \boldsymbol{\Lambda}_{(1)}^{1/2} \mathbf{Z}_1 \mathbf{1}_{n_1} - \frac{1}{n_2} \mathbf{U}_{(2)} \boldsymbol{\Lambda}_{(2)}^{1/2} \mathbf{Z}_2 \mathbf{1}_{n_2}$ and

$$\frac{1}{\sqrt{p}} \mathbf{d}^\top \hat{\mathbf{u}}_i = \frac{1}{\sqrt{p}} \boldsymbol{\mu}^\top \hat{\mathbf{u}}_i + \frac{1}{n_1 \sqrt{p}} \mathbf{1}_{n_1}^\top \mathbf{Z}_1^\top \boldsymbol{\Lambda}_{(1)}^{1/2} \mathbf{U}_{(1)}^\top \hat{\mathbf{u}}_i - \frac{1}{n_2 \sqrt{p}} \mathbf{1}_{n_2}^\top \mathbf{Z}_2^\top \boldsymbol{\Lambda}_{(2)}^{1/2} \mathbf{U}_{(2)}^\top \hat{\mathbf{u}}_i.$$

Using (30), we can write

$$\frac{1}{\sqrt{p}} \boldsymbol{\mu}^\top \hat{\mathbf{u}}_i = \left(\frac{\hat{\lambda}_i}{p} \right)^{-1/2} \left(\frac{\boldsymbol{\mu}^\top \mathbf{U}_{(1)} \boldsymbol{\Lambda}_{(1)}^{1/2} \mathbf{Z}_1}{p}, \frac{\boldsymbol{\mu}^\top \mathbf{U}_{(2)} \boldsymbol{\Lambda}_{(2)}^{1/2} \mathbf{Z}_2}{p} \right) (\mathbf{I}_n - \mathbf{J}) \hat{\mathbf{v}}_i.$$

Write $\mathbf{c} = (\cos \theta_1, \dots, \cos \theta_m)^\top \in \mathbb{R}^m$ and $\mathbf{c}_k = (\cos \theta_{k,1}, \dots, \cos \theta_{k,m_k})^\top \in \mathbb{R}^{m_k}$. Then we have $p^{-1} \boldsymbol{\mu}^\top \mathbf{U}_{(k)} \boldsymbol{\Lambda}_{(k)}^{1/2} \mathbf{Z}_k \xrightarrow{P} \mathbf{c}_k^\top \mathbf{W}_k^\top \delta$ as $p \rightarrow \infty$ from Lemma 23 (ii). Thus,

$$\frac{1}{\sqrt{p}} \boldsymbol{\mu}^\top \hat{\mathbf{u}}_i \xrightarrow{P} \begin{cases} \phi_i(\mathbf{S}_0)^{-1/2} \delta \mathbf{c}^\top \mathbf{W}^\top (\mathbf{I}_n - \mathbf{J}) v_i(\mathbf{S}_0), & i \in \mathcal{D}, \\ 0, & o.w \end{cases} \quad (36)$$

as $p \rightarrow \infty$. Also, combining Lemma 23 (iv) and Lemma 24 gives

$$\frac{1}{n_k \sqrt{p}} \mathbf{1}_{n_k}^\top \mathbf{Z}_k^\top \boldsymbol{\Lambda}_{(k)}^{1/2} \mathbf{U}_{(k)}^\top \hat{\mathbf{u}}_i \xrightarrow{P} \begin{cases} \phi_i(\mathbf{S}_0)^{-1/2} n_k^{-1} \mathbf{1}_{n_k}^\top \mathbf{W}_k \mathbf{R}_k^\top \mathbf{W}^\top (\mathbf{I}_n - \mathbf{J}) v_i(\mathbf{S}_0), & i \in \mathcal{D}, \\ 0, & o.w \end{cases} \quad (37)$$

as $p \rightarrow \infty$ for $k = 1, 2$. Hence, combining (36) and (37) gives

$$\frac{1}{\sqrt{p}} \mathbf{d}^\top \hat{\mathbf{u}}_i \xrightarrow{P} \phi_i(\mathbf{S}_0)^{-1/2} (\delta \mathbf{c}^\top + n_1^{-1} \mathbf{1}_{n_1}^\top \mathbf{W}_1 \mathbf{R}_1^\top - n_2^{-1} \mathbf{1}_{n_2}^\top \mathbf{W}_2 \mathbf{R}_2^\top) \mathbf{W}^\top (\mathbf{I}_n - \mathbf{J}) v_i(\mathbf{S}_0)$$

for $i \in \mathcal{D}$ and $p^{-1/2} \mathbf{d}^\top \hat{\mathbf{u}}_i \xrightarrow{P} 0$ otherwise as $p \rightarrow \infty$. ■

E.3 Proof of Theorem 3

Proof For $Y \in \mathcal{Y}$, assume $\pi(Y) = 1$. Recall that if $\beta_1 = \beta_2 = 1$ and $\tau_1^2 > \tau_2^2$, then

$$\mathcal{D} = \{i : 1 \leq i \leq k_0, k_0 + (n_1 - m_1) \leq i \leq n_1 + m_2 - 1\}$$

where k_0 is defined in Lemma 17 (i) and $\mathcal{S} = \text{span}(\{\hat{\mathbf{u}}_i\}_{i \in \mathcal{D}}, \mathbf{w}_{\text{MDP}})$. For notational simplicity, we write $\mathcal{D} = \{i_1, \dots, i_{m_1+m_2}\}$ so that $i_l < i_{l'}$ if $l < l'$. Let $\mathbf{t}^0 = (t_1, \dots, t_m)^\top \in \mathbb{R}^m$ with $t_j = \eta_2 \cos \theta_j \delta + \sum_{k=1}^{m_1} [\mathbf{R}_1]_{jk} \sigma_{1,k} (\zeta_k - \eta_1 \bar{\mathbf{z}}_{1,k}) - \eta_2 \sum_{k=1}^{m_2} [\mathbf{R}_2]_{jk} \sigma_{2,k} \bar{\mathbf{z}}_{2,k}$ for $1 \leq j \leq m$ and $\boldsymbol{\nu}^0 = \mathbf{U}_{1,\mathcal{S}} \mathbf{t}^0 + \nu_1 \mathbf{w}_{\text{MDP}} + \bar{X}_{\mathcal{S}}$. Note that $\boldsymbol{\nu}^0 \in \mathcal{L}_1$. We claim that $\|Y_{\mathcal{S}} - \boldsymbol{\nu}^0\| \xrightarrow{P} 0$ as $p \rightarrow \infty$. For this, we need to show that (a) $\hat{\mathbf{u}}_i^\top (Y_{\mathcal{S}} - \boldsymbol{\nu}^0) \xrightarrow{P} 0$ for $1 \leq i \leq m$ and (b) $\mathbf{w}_{\text{MDP}}^\top (Y_{\mathcal{S}} - \boldsymbol{\nu}^0) \xrightarrow{P} 0$ as $p \rightarrow \infty$.

First, we show that (a) $\hat{\mathbf{u}}_i^\top (Y_{\mathcal{S}} - \boldsymbol{\nu}^0) = p^{-1/2} \hat{\mathbf{u}}_i^\top (Y - \bar{X}) - \hat{\mathbf{u}}_i^\top \mathbf{U}_{1,\mathcal{S}} \mathbf{t}^0 \xrightarrow{P} 0$ for $1 \leq i \leq m$ as $p \rightarrow \infty$. Note that

$$\begin{aligned} \frac{1}{\sqrt{p}} \hat{\mathbf{u}}_i^\top (Y - \bar{X}) &= \frac{1}{\sqrt{p}} \hat{\mathbf{u}}_i^\top \left\{ \eta_2 \boldsymbol{\mu} + \mathbf{U}_{(1)} \boldsymbol{\Lambda}_{(1)}^{1/2} \left(\zeta - \frac{1}{n} \mathbf{Z}_1 \mathbf{1}_{n_1} \right) - \frac{1}{n} \mathbf{U}_{(2)} \boldsymbol{\Lambda}_{(2)}^{1/2} \mathbf{Z}_2 \mathbf{1}_{n_2} \right\} \\ &= \frac{\eta_2}{\sqrt{p}} \hat{\mathbf{u}}_i^\top \boldsymbol{\mu} + \sum_{k=1}^{m_1} \hat{\mathbf{u}}_i^\top \mathbf{u}_{(1),k} \sigma_{1,k} (\zeta_k - \eta_1 \bar{\mathbf{z}}_{1,k}) - \eta_2 \sum_{k=1}^{m_2} \hat{\mathbf{u}}_i^\top \mathbf{u}_{(2),k} \sigma_{2,k} \bar{\mathbf{z}}_{2,k} + o_p(1). \end{aligned} \quad (38)$$

Using (33) and (36), we have

$$\frac{1}{\sqrt{p}} \hat{\mathbf{u}}_i^\top (Y - \bar{X}) \xrightarrow{P} \frac{1}{\sqrt{\phi_l(\boldsymbol{\Phi}_{\tau_1, \tau_2})}} \sum_{j=1}^m t_j \boldsymbol{\Phi}_{lj} \quad (39)$$

where $\boldsymbol{\Phi}_{lj} = \sum_{k=1}^2 [\mathbf{R}_k]_j \boldsymbol{\Phi}_k^{1/2} \tilde{v}_{lk}(\boldsymbol{\Phi}_{\tau_1, \tau_2})$ for $1 \leq l \leq m_1 + m_2$ and $1 \leq j \leq m$ and $\hat{\mathbf{u}}_i^\top \mathbf{U}_{1,\mathcal{S}} \mathbf{t}^0 \xrightarrow{P} (\phi_l(\boldsymbol{\Phi}_{\tau_1, \tau_2}))^{-1/2} \sum_{j=1}^m t_j \boldsymbol{\Phi}_{lj}$ as $p \rightarrow \infty$. Hence, $\hat{\mathbf{u}}_i^\top (Y_{\mathcal{S}} - \boldsymbol{\nu}^0) = p^{-1/2} \hat{\mathbf{u}}_i^\top (Y - \bar{X}) - \hat{\mathbf{u}}_i^\top \mathbf{U}_{1,\mathcal{S}} \mathbf{t}^0 \xrightarrow{P} 0$ as $p \rightarrow \infty$ for $1 \leq l \leq m_1 + m_2$.

Next, we show that (b) $\mathbf{w}_{\text{MDP}}^\top (Y_{\mathcal{S}} - \boldsymbol{\nu}^0) = p^{-1/2} \mathbf{w}_{\text{MDP}}^\top (Y - \bar{X}) - \mathbf{w}_{\text{MDP}}^\top \mathbf{U}_{1,\mathcal{S}} \mathbf{t}^0 - \nu_1 \xrightarrow{P} 0$ as $p \rightarrow \infty$. We decompose $p^{-1/2} \mathbf{w}_{\text{MDP}}^\top (Y - \bar{X})$ into the two terms:

$$\frac{1}{\sqrt{p}} \mathbf{w}_{\text{MDP}}^\top (Y - \bar{X}) = \frac{\sqrt{p}}{\|\hat{\mathbf{U}}_2 \hat{\mathbf{U}}_2^\top \mathbf{d}\|} \left(\frac{\mathbf{d}^\top (Y - \bar{X})}{p} - \frac{(\hat{\mathbf{U}}_1 \hat{\mathbf{U}}_1^\top \mathbf{d})^\top (Y - \bar{X})}{p} \right) = \frac{1}{\kappa_{\text{MDP}}} (K_1 - K_2)$$

where $K_1 = \mathbf{d}^\top (Y - \bar{X})/p$ and $K_2 = (\hat{\mathbf{U}}_1 \hat{\mathbf{U}}_1^\top \mathbf{d})^\top (Y - \bar{X})/p$. By Lemmas 23 and 24,

$$\begin{aligned} K_1 &= \frac{1}{p} \left(\boldsymbol{\mu} + \frac{1}{n_1} \mathbf{U}_{(1)} \boldsymbol{\Lambda}_{(1)}^{1/2} \mathbf{Z}_1 \mathbf{1}_{n_1} - \frac{1}{n_2} \mathbf{U}_{(2)} \boldsymbol{\Lambda}_{(2)}^{1/2} \mathbf{Z}_2 \mathbf{1}_{n_2} \right)^\top \\ &\quad \left\{ \eta_2 \boldsymbol{\mu} + \mathbf{U}_{(1)} \boldsymbol{\Lambda}_{(1)}^{1/2} \left(\zeta - \frac{1}{n} \mathbf{Z}_1 \mathbf{1}_{n_1} \right) - \frac{1}{n} \mathbf{U}_{(2)} \boldsymbol{\Lambda}_{(2)}^{1/2} \mathbf{Z}_2 \mathbf{1}_{n_2} \right\} \\ &\xrightarrow{P} \eta_2 (1 - \cos^2 \varphi) \delta^2 - \frac{\tau_1^2 - \tau_2^2}{n} + \sum_{j=1}^m t_j r_j \end{aligned} \quad (40)$$

as $p \rightarrow \infty$ where r_j is defined in Lemma 25. Using Lemma 25, we also obtain

$$\begin{aligned} K_2 &= \frac{(\hat{\mathbf{U}}_1 \hat{\mathbf{U}}_1^\top \mathbf{d})^\top (Y - \bar{X})}{p} = \sum_{i \in \mathcal{D}} \left(\frac{1}{\sqrt{p}} \hat{\mathbf{u}}_i^\top \mathbf{d} \right) \left(\frac{1}{\sqrt{p}} \hat{\mathbf{u}}_i^\top (Y - \bar{X}) \right) + o_p(1) \\ &\xrightarrow{P} \sum_{l=1}^{m_1+m_2} \sum_{j=1}^m \sum_{j'=1}^m \frac{1}{\phi_l(\Phi_{\tau_1, \tau_2})} t_j r_{j'} \Phi_{lj} \Phi_{lj'}. \end{aligned} \quad (41)$$

as $p \rightarrow \infty$. Note that the limit of κ_{MDP}^2 can be obtained from the limit of $p^{-1} \|\mathbf{d}\|^2$ and $p^{-1} \|\hat{\mathbf{U}}_1 \hat{\mathbf{U}}_1^\top \mathbf{d}\|^2$:

$$\begin{aligned} \kappa_{\text{MDP}}^2 &= \frac{1}{p} \|\mathbf{d}\|^2 - \frac{1}{p} \|\hat{\mathbf{U}}_1 \hat{\mathbf{U}}_1^\top \mathbf{d}\|^2 \\ &\xrightarrow{P} (1 - \cos^2 \varphi) \delta^2 + \frac{\tau_1^2}{n_1} + \frac{\tau_2^2}{n_2} + \sum_{j=1}^m \sum_{j'=1}^m r_j r_{j'} \left(I_{jj'} - \sum_{l=1}^{m_1+m_2} \frac{1}{\phi_l(\Phi_{\tau_1, \tau_2})} \Phi_{lj} \Phi_{lj'} \right) \\ &= (1 - \cos^2 \varphi) \delta^2 + \frac{\tau_1^2}{n_1} + \frac{\tau_2^2}{n_2} + \mathbf{r}^\top \left(\mathbf{I}_m - \left(\mathbf{R}_1 \Phi_1^{1/2} \mathbf{R}_2 \Phi_2^{1/2} \right) \Phi_{\tau_1, \tau_2}^{-1} \begin{pmatrix} \Phi_1^{1/2} \mathbf{R}_1^\top \\ \Phi_2^{1/2} \mathbf{R}_2^\top \end{pmatrix} \right) \mathbf{r} \\ &=: \kappa^2 \end{aligned} \quad (42)$$

as $p \rightarrow \infty$ where $\mathbf{r} = (r_1, \dots, r_m)^\top$ and $I_{jj'} = I(j = j')$. Note that $\kappa^2 \geq (1 - \cos^2 \varphi) \delta^2 + \tau_1^2/n_1 + \tau_2^2/n_2 > 0$. Combining (40), (41) and (42) gives

$$\begin{aligned} \frac{1}{\sqrt{p}} \mathbf{w}_{\text{MDP}}^\top (Y - \bar{X}) &= \frac{1}{\kappa_{\text{MDP}}} (K_1 - K_2) \\ &\xrightarrow{P} \frac{1}{\kappa} \left\{ \eta_2 (1 - \cos^2 \varphi) \delta^2 - \frac{\tau_1^2 - \tau_2^2}{n} + \sum_{j=1}^m \sum_{j'=1}^m t_j r_{j'} \left(I_{jj'} - \sum_{l=1}^{m_1+m_2} \frac{1}{\phi_l(\Phi_{\tau_1, \tau_2})} \Phi_{lj} \Phi_{lj'} \right) \right\} \end{aligned} \quad (43)$$

as $p \rightarrow \infty$. Also, Lemma 25 and (33) lead to

$$\begin{aligned} \mathbf{w}_{\text{MDP}}^\top \mathbf{U}_{1, \mathbf{S}} \mathbf{t}^0 &= \sum_{j=1}^m t_j \mathbf{w}_{\text{MDP}}^\top \mathbf{u}_j = \frac{1}{\kappa_{\text{MDP}}} \sum_{j=1}^m t_j \left\{ \frac{1}{\sqrt{p}} \mathbf{u}_j^\top \mathbf{d} - \mathbf{u}_j^\top \hat{\mathbf{U}}_1 \left(\frac{1}{\sqrt{p}} \hat{\mathbf{U}}_1^\top \mathbf{d} \right) \right\} \\ &\xrightarrow{P} \frac{1}{\kappa} \sum_{j=1}^m \sum_{j'=1}^m t_j r_{j'} \left(I_{jj'} - \sum_{l=1}^{m_1+m_2} \frac{1}{\phi_l(\Phi_{\tau_1, \tau_2})} \Phi_{lj} \Phi_{lj'} \right) \end{aligned} \quad (44)$$

as $p \rightarrow \infty$. From (43) and (44), we have $\mathbf{w}_{\text{MDP}}^\top (Y_{\mathcal{S}} - \boldsymbol{\nu}^0) \xrightarrow{P} 0$ as $p \rightarrow \infty$. Hence, from (a) and (b), we have $\|Y_{\mathcal{S}} - \boldsymbol{\nu}^0\| \xrightarrow{P} 0$ as $p \rightarrow \infty$ for $Y \in \mathcal{Y}$ with $\pi(Y) = 1$. Using similar arguments, we can show for $Y \in \mathcal{Y}$ with $\pi(Y) = 2$. \blacksquare

E.4 Proof of Theorem 4

Proof Write

$$\tilde{\mathbf{w}}_\alpha = \sum_{i=1}^{n-2} \frac{\alpha_p}{\hat{\lambda}_i + \alpha_p} \hat{\mathbf{u}}_i \left(\frac{1}{\sqrt{p}} \hat{\mathbf{u}}_i^\top \mathbf{d} \right) + \frac{1}{\sqrt{p}} \|\hat{\mathbf{U}}_2 \hat{\mathbf{U}}_2^\top \mathbf{d}\| \mathbf{w}_{\text{MDP}}.$$

Then $\mathbf{w}_\alpha \propto \tilde{\mathbf{w}}_\alpha$ for any $\alpha \in \mathbb{R}$ where \mathbf{w}_α is defined. Also, note that $\text{Angle}(\mathbf{w}_\alpha, \mathcal{S}) = \arccos(\|P_{\mathcal{S}}\tilde{\mathbf{w}}_\alpha\|/\|\tilde{\mathbf{w}}_\alpha\|)$. We decompose $\|\tilde{\mathbf{w}}_\alpha\|^2$ into the two terms:

$$\|\tilde{\mathbf{w}}_\alpha\|^2 = \|P_{\mathcal{S}}\tilde{\mathbf{w}}_\alpha\|^2 + \sum_{i \in \{1, \dots, n-2\} \setminus \mathcal{D}} \left(\frac{\alpha_p}{\hat{\lambda}_i + \alpha_p} \right)^2 \left(\frac{1}{\sqrt{p}} \hat{\mathbf{u}}_i^\top \mathbf{d} \right)^2. \quad (45)$$

Using Lemmas 16 and 25, the second term in (45) converges to zero in probability for $\alpha \in \mathbb{R} \setminus \{-\tau_1^2, -\tau_2^2\}$. Then it suffices to show that $\|P_{\mathcal{S}}\tilde{\mathbf{w}}_\alpha\|$ is stochastically bounded. Note that

$$\|P_{\mathcal{S}}\tilde{\mathbf{w}}_\alpha\|^2 = \sum_{i \in \mathcal{D}} \left(\frac{\alpha_p}{\hat{\lambda}_i + \alpha_p} \right)^2 \left(\frac{1}{\sqrt{p}} \hat{\mathbf{u}}_i^\top \mathbf{d} \right)^2 + \kappa_{\text{MDP}}^2.$$

Again from Lemmas 16 and 25, the first term converges in probability since

$$\sum_{i \in \mathcal{D}} \left(\frac{\alpha_p}{\hat{\lambda}_i + \alpha_p} \right)^2 \left(\frac{1}{\sqrt{p}} \hat{\mathbf{u}}_i^\top \mathbf{d} \right)^2 \xrightarrow{P} \sum_{l=1}^{m_1+m_2} \left(\frac{\alpha}{\phi_l(\Phi_{\tau_1, \tau_2}) + \alpha} \right)^2 \left(\sum_{j=1}^m \frac{1}{\sqrt{\phi_l(\Phi_{\tau_1, \tau_2})}} r_j \Phi_{lj} \right)^2$$

as $p \rightarrow \infty$ where $\Phi_{lj} = \sum_{k=1}^2 [\mathbf{R}_k]_j \Phi_k^{1/2} \tilde{v}_{lk}(\Phi_{\tau_1, \tau_2})$. We have already shown that κ_{MDP}^2 converges to $\kappa^2 > 0$ in the proof of Theorem 3. These complete the proof. \blacksquare

E.5 Proof of Theorems 5 and 6

Proof Using Lemmas 16 and 25, the proofs closely follow those of Theorems 3.2–3.4 of Chang et al. (2021). \blacksquare

E.6 Proof of Theorem 18

Proof For notational simplicity, we write $\mathcal{D} = \{i_1, \dots, i_{m_1+m_2}\}$ so that $i_l < i_{l'}$ if $l < l'$. Write

$$\tilde{\mathbf{v}}_\alpha = \sum_{l=1}^{m_1+m_2} \frac{\alpha}{\hat{\lambda}_{i_l}/p + \alpha} \left(\frac{1}{\sqrt{p}} \hat{\mathbf{u}}_{i_l}^\top \mathbf{d} \right) \hat{\mathbf{u}}_{i_l} + \frac{1}{\sqrt{p}} \|\hat{\mathbf{U}}_2 \hat{\mathbf{U}}_2^\top \mathbf{d}\| \mathbf{w}_{\text{MDP}}. \quad (46)$$

Assume that for each $k = 1, 2$, $\hat{\alpha}_k$ is an HDLSS-consistent estimator of $-\tau_k^2$. First, we shall show that $\text{Angle}(\mathbf{v}_{\hat{\alpha}_1}, \mathbf{u}_{(1), \iota, \mathcal{S}}) \xrightarrow{P} \pi/2$ as $p \rightarrow \infty$ for $1 \leq \iota \leq m_1$. Using Lemmas 16, 17 and 25, the inner product between $\tilde{\mathbf{v}}_{\hat{\alpha}_1}$ and $\mathbf{u}_{(1), \iota, \mathcal{S}}$ becomes

$$\begin{aligned} \tilde{\mathbf{v}}_{\hat{\alpha}_1}^\top \mathbf{u}_{(1), \iota, \mathcal{S}} &= \sum_{l=1}^{m_1+m_2} \frac{\hat{\alpha}_1}{\hat{\lambda}_{i_l}/p + \hat{\alpha}_1} \left(\frac{1}{\sqrt{p}} \hat{\mathbf{u}}_{i_l}^\top \mathbf{d} \right) (\mathbf{u}_{(1), \iota}^\top \hat{\mathbf{u}}_{i_l}) + \frac{1}{\sqrt{p}} \|\hat{\mathbf{U}}_2 \hat{\mathbf{U}}_2^\top \mathbf{d}\| (\mathbf{u}_{(1), \iota}^\top \mathbf{w}_{\text{MDP}}) \\ &= \sum_{j=1}^m \left\{ \sum_{l=1}^{m_1+m_2} \frac{\hat{\alpha}_1}{\hat{\lambda}_{i_l}/p + \hat{\alpha}_1} \left(\frac{1}{\sqrt{p}} \hat{\mathbf{u}}_{i_l}^\top \mathbf{d} \right) (\mathbf{u}_j^\top \hat{\mathbf{u}}_{i_l}) + \frac{1}{\sqrt{p}} \|\hat{\mathbf{U}}_2 \hat{\mathbf{U}}_2^\top \mathbf{d}\| (\mathbf{u}_j^\top \mathbf{w}_{\text{MDP}}) \right\} [\mathbf{R}_1^{(p)}]_{j\iota} \end{aligned}$$

$$\begin{aligned}
 & \xrightarrow{P} \sum_{j=1}^m \left[\sum_{j'=1}^m \sum_{l=1}^{m_1+m_2} \frac{-\tau_1^2}{(\phi_l(\mathbf{\Phi}_{\tau_1, \tau_2}) - \tau_1^2) \phi_l(\mathbf{\Phi}_{\tau_1, \tau_2})} r_{j'} \mathbf{\Phi}_{lj} \mathbf{\Phi}_{lj'} \right. \\
 & \quad \left. + \kappa \times \frac{1}{\kappa} \left\{ \sum_{j'=1}^m r_{j'} \left(I_{jj'} - \sum_{l=1}^{m_1+m_2} \frac{1}{\phi_l(\mathbf{\Phi}_{\tau_1, \tau_2})} \mathbf{\Phi}_{lj} \mathbf{\Phi}_{lj'} \right) \right\} \right] [\mathbf{R}_1]_{j\iota} \\
 & = \sum_{j=1}^m \sum_{j'=1}^m r_{j'} \left(I_{jj'} - \sum_{l=1}^{m_1+m_2} \frac{1}{\phi_l(\mathbf{\Phi}_{\tau_1, \tau_2}) - \tau_1^2} \mathbf{\Phi}_{lj} \mathbf{\Phi}_{lj'} \right) [\mathbf{R}_1]_{j\iota}
 \end{aligned}$$

as $p \rightarrow \infty$ where r_j is defined in Lemma 25, $I_{jj'} = I(j = j')$ and $\mathbf{\Phi}_{lj} = \sum_{k=1}^2 [\mathbf{R}_k]_j \mathbf{\Phi}_k^{1/2} \tilde{v}_{lk}(\mathbf{\Phi}_{\tau_1, \tau_2})$. Write

$$\begin{aligned}
 \mathbf{D}(\mathbf{\Phi}_{\tau_1, \tau_2}) &= \text{Diag}(\phi_1(\mathbf{\Phi}_{\tau_1, \tau_2}), \dots, \phi_{m_1+m_2}(\mathbf{\Phi}_{\tau_1, \tau_2})) \\
 \tilde{\mathbf{V}}_i(\mathbf{\Phi}_{\tau_1, \tau_2}) &= [\tilde{v}_{1i}(\mathbf{\Phi}_{\tau_1, \tau_2}), \dots, \tilde{v}_{(m_1+m_2)i}(\mathbf{\Phi}_{\tau_1, \tau_2})] \\
 \mathbf{V}(\mathbf{\Phi}_{\tau_1, \tau_2}) &= [v_1(\mathbf{\Phi}_{\tau_1, \tau_2}), \dots, v_{m_1+m_2}(\mathbf{\Phi}_{\tau_1, \tau_2})] = [\tilde{\mathbf{V}}_1(\mathbf{\Phi}_{\tau_1, \tau_2})^\top, \tilde{\mathbf{V}}_2(\mathbf{\Phi}_{\tau_1, \tau_2})^\top]^\top.
 \end{aligned}$$

Then we can write

$$\begin{aligned}
 \tilde{\mathbf{v}}_{\hat{\alpha}_1}^\top \mathbf{u}_{1, \iota, \mathcal{S}} & \xrightarrow{P} \mathbf{r}^\top \{ \mathbf{I}_m - (\mathbf{R}_1 \mathbf{\Phi}_1^{1/2} \tilde{\mathbf{V}}_1(\mathbf{\Phi}_{\tau_1, \tau_2}) + \mathbf{R}_2 \mathbf{\Phi}_2^{1/2} \tilde{\mathbf{V}}_2(\mathbf{\Phi}_{\tau_1, \tau_2})) (\mathbf{D}(\mathbf{\Phi}_{\tau_1, \tau_2}) - \tau_1^2 \mathbf{I}_{m_1+m_2})^{-1} \\
 & \quad (\mathbf{R}_1 \mathbf{\Phi}_1^{1/2} \tilde{\mathbf{V}}_1(\mathbf{\Phi}_{\tau_1, \tau_2}) + \mathbf{R}_2 \mathbf{\Phi}_2^{1/2} \tilde{\mathbf{V}}_2(\mathbf{\Phi}_{\tau_1, \tau_2}))^\top \} [\mathbf{R}_1]^\iota
 \end{aligned} \tag{47}$$

as $p \rightarrow \infty$ where $\mathbf{r} = (r_1, \dots, r_m)^\top$. Note that $\tilde{\mathbf{V}}_k(\mathbf{\Phi}_{\tau_1, \tau_2}) \tilde{\mathbf{V}}_k(\mathbf{\Phi}_{\tau_1, \tau_2})^\top = \mathbf{I}_{m_k}$ for $k = 1, 2$ and $\tilde{\mathbf{V}}_1(\mathbf{\Phi}_{\tau_1, \tau_2}) \tilde{\mathbf{V}}_2(\mathbf{\Phi}_{\tau_1, \tau_2})^\top = \mathbf{O}_{m_1 \times m_2}$. Also, since $\mathbf{\Phi}_{\tau_1, \tau_2} \mathbf{V}(\mathbf{\Phi}_{\tau_1, \tau_2}) = \mathbf{V}(\mathbf{\Phi}_{\tau_1, \tau_2}) \mathbf{D}(\mathbf{\Phi}_{\tau_1, \tau_2})$, we have $\mathbf{\Phi}_1 \tilde{\mathbf{V}}_1(\mathbf{\Phi}_{\tau_1, \tau_2}) + \mathbf{\Phi}_1^{1/2} \mathbf{R}_1^\top \mathbf{R}_2 \mathbf{\Phi}_2^{1/2} \tilde{\mathbf{V}}_2(\mathbf{\Phi}_{\tau_1, \tau_2}) = \tilde{\mathbf{V}}_1(\mathbf{\Phi}_{\tau_1, \tau_2}) (\mathbf{D}(\mathbf{\Phi}_{\tau_1, \tau_2}) - \tau_1^2 \mathbf{I}_{m_1+m_2})$. Hence,

$$\begin{aligned}
 & (\mathbf{R}_1 \mathbf{\Phi}_1^{1/2} \tilde{\mathbf{V}}_1(\mathbf{\Phi}_{\tau_1, \tau_2}) + \mathbf{R}_2 \mathbf{\Phi}_2^{1/2} \tilde{\mathbf{V}}_2(\mathbf{\Phi}_{\tau_1, \tau_2}))^\top \mathbf{R}_1 \\
 & = (\mathbf{D}(\mathbf{\Phi}_{\tau_1, \tau_2}) - \tau_1^2 \mathbf{I}_{m_1+m_2}) \tilde{\mathbf{V}}_1(\mathbf{\Phi}_{\tau_1, \tau_2})^\top \mathbf{\Phi}_1^{-1/2}.
 \end{aligned} \tag{48}$$

Combining (47) and (48) gives

$$\begin{aligned}
 \tilde{\mathbf{v}}_{\hat{\alpha}_1}^\top \mathbf{u}_{(1), \iota, \mathcal{S}} & \xrightarrow{P} \mathbf{r}^\top [\mathbf{R}_1 - (\mathbf{R}_1 \mathbf{\Phi}_1^{1/2} \tilde{\mathbf{V}}_1(\mathbf{\Phi}_{\tau_1, \tau_2}) + \mathbf{R}_2 \mathbf{\Phi}_2^{1/2} \tilde{\mathbf{V}}_2(\mathbf{\Phi}_{\tau_1, \tau_2})) \tilde{\mathbf{V}}_1(\mathbf{\Phi}_{\tau_1, \tau_2})^\top \mathbf{\Phi}_1^{-1/2}]^\iota \\
 & = \mathbf{r}^\top [\mathbf{R}_1 - \mathbf{R}_1]^\iota = \mathbf{r}^\top [\mathbf{O}^{m \times m_1}]^\iota = 0
 \end{aligned} \tag{49}$$

as $p \rightarrow \infty$ for all $1 \leq \iota \leq m_1$. We can easily check that $\|\tilde{\mathbf{v}}_{\hat{\alpha}_1}\|$ and $\|\mathbf{u}_{(1), \iota, \mathcal{S}}\|$ converge to strictly positive random variables. In particular,

$$\|\tilde{\mathbf{v}}_{\hat{\alpha}_1}\|^2 \xrightarrow{P} \sum_{l=1}^{m_1+m_2} \frac{\tau_1^4}{(\phi_l(\mathbf{\Phi}_{\tau_1, \tau_2}) - \tau_1^2)^2 \phi_l(\mathbf{\Phi}_{\tau_1, \tau_2})} \left(\sum_{j=1}^m r_j \mathbf{\Phi}_{lj} \right)^2 + \kappa^2 =: \frac{1}{\gamma_1^2} > 0. \tag{50}$$

Hence, $\text{Angle}(\mathbf{v}_{\hat{\alpha}_1}, \mathbf{u}_{(1), \iota, \mathcal{S}}) \xrightarrow{P} \pi/2$ as $p \rightarrow \infty$ for all $1 \leq \iota \leq m_1$. We will make use of γ_1 in the proof of Theorem 19. Similarly, we can show that $\text{Angle}(\mathbf{v}_{\hat{\alpha}_2}, \mathbf{u}_{(2), \iota, \mathcal{S}}) \xrightarrow{P} \pi/2$ as $p \rightarrow \infty$ for all $1 \leq \iota \leq m_2$ and

$$\|\tilde{\mathbf{v}}_{\hat{\alpha}_2}\|^2 \xrightarrow{P} \sum_{l=1}^{m_1+m_2} \frac{\tau_2^4}{(\phi_l(\mathbf{\Phi}_{\tau_1, \tau_2}) - \tau_2^2)^2 \phi_l(\mathbf{\Phi}_{\tau_1, \tau_2})} \left(\sum_{j=1}^m r_j \mathbf{\Phi}_{lj} \right)^2 + \kappa^2 =: \frac{1}{\gamma_2^2} > 0. \tag{51}$$

We will also make use of γ_2 in the proof of Theorem 19. ■

E.7 Proof of Theorem 19

Proof We continue to use the same notations as in Theorem 18. For $k = 1, 2$, assume that $\pi(Y_k) = k$ for $Y_k \in \mathcal{Y}$ and denote $M_k(\alpha) = p^{-1/2} \tilde{\mathbf{v}}_\alpha^\top (Y_k - \bar{X})$. Assume $m = m_1$. Using Lemmas 16, 17 and 25 with equations (39) and (43), we have

$$\begin{aligned}
 M_1(\hat{\alpha}_1) &= \frac{1}{\sqrt{p}} \tilde{\mathbf{v}}_{\hat{\alpha}_1}^\top (Y_1 - \bar{X}) \\
 &= \sum_{l=1}^{m_1+m_2} \frac{\hat{\alpha}_1}{\hat{\lambda}_{i_l}/p + \hat{\alpha}_1} \left(\frac{1}{\sqrt{p}} \hat{\mathbf{u}}_{i_l}^\top \mathbf{d} \right) \left\{ \frac{1}{\sqrt{p}} \hat{\mathbf{u}}_{i_l}^\top (Y_1 - \bar{X}) \right\} + \frac{1}{\sqrt{p}} \|\hat{\mathbf{U}}_2 \hat{\mathbf{U}}_2^\top \mathbf{d}\| \left\{ \frac{1}{\sqrt{p}} \mathbf{w}_{\text{MDP}}^\top (Y_1 - \bar{X}) \right\} \\
 &\xrightarrow{P} \sum_{l=1}^{m_1+m_2} \sum_{j=1}^m \sum_{j'=1}^m \frac{-\tau_1^2}{(\phi_l(\Phi_{\tau_1, \tau_2}) - \tau_1^2) \phi_l(\Phi_{\tau_1, \tau_2})} t_j r_{j'} \Phi_{lj} \Phi_{lj'} \\
 &\quad + \kappa \times \frac{1}{\kappa} \left\{ \eta_2 (1 - \cos^2 \varphi) \delta^2 - \frac{\tau_1^2 - \tau_2^2}{n} + \sum_{j=1}^m \sum_{j'=1}^m t_j r_{j'} \left(I_{jj'} - \sum_{l=1}^{m_1+m_2} \frac{1}{\phi_l(\Phi_{\tau_1, \tau_2})} \Phi_{lj} \Phi_{lj'} \right) \right\} \\
 &= \eta_2 (1 - \cos^2 \varphi) \delta^2 - \frac{\tau_1^2 - \tau_2^2}{n} + \sum_{j=1}^m \sum_{j'=1}^m t_j r_{j'} \left(I_{jj'} - \sum_{l=1}^{m_1+m_2} \frac{1}{\phi_l(\Phi_{\tau_1, \tau_2}) - \tau_1^2} \Phi_{lj} \Phi_{lj'} \right)
 \end{aligned}$$

as $p \rightarrow \infty$. Note that in this case \mathbf{R}_1 is invertible since $m = m_1$. Then using (49), we have

$$I_{jj'} - \sum_{l=1}^{m_1+m_2} \frac{1}{\phi_l(\Phi_{\tau_1, \tau_2}) - \tau_1^2} \Phi_{lj} \Phi_{lj'} = 0$$

for all $1 \leq j, j' \leq m$. Therefore, we have

$$\frac{1}{\sqrt{p}} \mathbf{v}_{\hat{\alpha}_1}^\top (Y_1 - \bar{X}) = \frac{1}{\|\tilde{\mathbf{v}}_{\hat{\alpha}_1}\|} \frac{1}{\sqrt{p}} \tilde{\mathbf{v}}_{\hat{\alpha}_1}^\top (Y_1 - \bar{X}) \xrightarrow{P} \gamma_1 \left(\eta_2 (1 - \cos^2 \varphi) \delta^2 - \frac{\tau_1^2 - \tau_2^2}{n} \right)$$

as $p \rightarrow \infty$ where γ_1 is defined in (50). In a similar way, we can show that

$$\begin{aligned}
 M_2(\hat{\alpha}_1) &= \frac{1}{\sqrt{p}} \tilde{\mathbf{v}}_{\hat{\alpha}_1}^\top (Y_2 - \bar{X}) \\
 &\xrightarrow{P} -\eta_1 (1 - \cos^2 \varphi) \delta^2 - \frac{\tau_1^2 - \tau_2^2}{n} + \sum_{j=1}^m \sum_{j'=1}^m s_j r_{j'} \left(I_{jj'} - \sum_{l=1}^{m_1+m_2} \frac{1}{\phi_l(\Phi_{\tau_1, \tau_2}) - \tau_1^2} \Phi_{lj} \Phi_{lj'} \right) \\
 &= -\eta_1 (1 - \cos^2 \varphi) \delta^2 - \frac{\tau_1^2 - \tau_2^2}{n}
 \end{aligned}$$

as $p \rightarrow \infty$ where $s_j = -\eta_1 \cos \theta_j \delta - \eta_1 \sum_{k=1}^{m_1} [\mathbf{R}_1]_{jk} \sigma_{1,k} \bar{\mathbf{z}}_{1,k} + \sum_{k=1}^{m_2} [\mathbf{R}_2]_{jk} \sigma_{2,k} (\zeta_k - \eta_2 \bar{\mathbf{z}}_{2,k})$ for $1 \leq j \leq m$. Hence, we have

$$\frac{1}{\sqrt{p}} \mathbf{v}_{\hat{\alpha}_1}^\top (Y_2 - \bar{X}) = \frac{1}{\|\tilde{\mathbf{v}}_{\hat{\alpha}_1}\|} \frac{1}{\sqrt{p}} \tilde{\mathbf{v}}_{\hat{\alpha}_1}^\top (Y_2 - \bar{X}) \xrightarrow{P} \gamma_1 \left(-\eta_1 (1 - \cos^2 \varphi) \delta^2 - \frac{\tau_1^2 - \tau_2^2}{n} \right)$$

as $p \rightarrow \infty$. Using similar arguments, we can show the results for the case of $m = m_2$. \blacksquare

E.8 Proof of Proposition 7

Proof Assume further that $m_1 = m_2 = m = 1$ (that is, $\mathbf{u}_{(1),1} = \mathbf{u}_{(2),1} = \mathbf{u}_1$). (i) is a special case of Theorem 18. To show (ii), note that for any given $\alpha \in \mathbb{R}$, $\{\mathbf{v}_\alpha\} \in \mathcal{A}$ if and only if $\mathbf{v}_\alpha^\top \mathbf{u}_1 \xrightarrow{P} 0$ as $p \rightarrow \infty$. From Lemmas 16, 17 and 25, we have $\tilde{\mathbf{v}}_\alpha^\top \mathbf{u}_1 \xrightarrow{P} r_1 \left(1 - \sum_{l=1}^2 (\phi_l(\Phi_{\tau_1, \tau_2}) + \alpha)^{-1} \Phi_{l1}^2\right)$ as $p \rightarrow \infty$. Using (i), we have

$$r_1 \left(1 - \sum_{l=1}^2 \frac{1}{\phi_l(\Phi_{\tau_1, \tau_2}) - \tau_l^2} \Phi_{l1}^2\right) = 0 \text{ and } r_1 \left(1 - \sum_{l=1}^2 \frac{1}{\phi_l(\Phi_{\tau_1, \tau_2}) - \tau_2^2} \Phi_{l1}^2\right) = 0. \quad (52)$$

Hence,

$$\tilde{\mathbf{v}}_\alpha^\top \mathbf{u}_1 \xrightarrow{P} \frac{r_1(\alpha + \tau_1^2)(\alpha + \tau_2^2)}{(\alpha + \phi_1(\Phi_{\tau_1, \tau_2}))(\alpha + \phi_2(\Phi_{\tau_1, \tau_2}))}$$

as $p \rightarrow \infty$. Since $\|\tilde{\mathbf{v}}_\alpha\|$ is stochastically bounded, $\mathbf{v}_\alpha^\top \mathbf{u}_1 \xrightarrow{P} 0$ as $p \rightarrow \infty$ if and only if $\alpha = -\tau_1^2$ or $\alpha = -\tau_2^2$. (iii) is a special case of Theorem 19. \blacksquare

E.9 Proof of Theorem 8

Proof Assume further that $m_1 = m_2 = m = 1$ (that is, $\mathbf{u}_{(1),1} = \mathbf{u}_{(2),1} = \mathbf{u}_1$). From Proposition 7, we can check that $D(\mathbf{v}_{\hat{\alpha}_k})$, the asymptotic distance between $P_{\mathbf{v}_{\hat{\alpha}_k}} \mathcal{Y}_1$ and $P_{\mathbf{v}_{\hat{\alpha}_k}} \mathcal{Y}_2$, is $\gamma_k(1 - \cos^2 \varphi)\delta^2$ for each $k = 1, 2$, where γ_1 and γ_2 are defined in (50) and (51), respectively. To be specific, when $m_1 = m_2 = m = 1$,

$$\gamma_k = \left(r_1^2 \sum_{l=1}^2 \frac{\tau_k^4}{(\phi_l(\Phi_{\tau_1, \tau_2}) - \tau_k^2)^2 \phi_l(\Phi_{\tau_1, \tau_2})} \Phi_{l1}^2 + \kappa^2 \right)^{-1/2} \quad (53)$$

as $p \rightarrow \infty$ where $r_1 = \cos \theta_1 \delta + \sigma_{1,1} \bar{\mathbf{z}}_{1,1} - \sigma_{2,1} \bar{\mathbf{z}}_{2,1}$, $\Phi_{11} = \Phi_1^{1/2} v_{11}(\Phi_{\tau_1, \tau_2}) + \Phi_2^{1/2} v_{12}(\Phi_{\tau_1, \tau_2})$ and $\Phi_{21} = \Phi_1^{1/2} v_{21}(\Phi_{\tau_1, \tau_2}) + \Phi_2^{1/2} v_{22}(\Phi_{\tau_1, \tau_2})$. It can be checked that

$$\begin{aligned} \Phi_{11}^2 &= \phi_1(\Phi_{\tau_1, \tau_2}) - \tau_2^2 - v_{11}^2(\Phi_{\tau_1, \tau_2})(\tau_1^2 - \tau_2^2) \\ \Phi_{21}^2 &= \phi_2(\Phi_{\tau_1, \tau_2}) - \tau_1^2 - v_{22}^2(\Phi_{\tau_1, \tau_2})(\tau_2^2 - \tau_1^2) \end{aligned} \quad (54)$$

and

$$\begin{aligned} v_{11}^2(\Phi_{\tau_1, \tau_2}) &= v_{22}^2(\Phi_{\tau_1, \tau_2}) = \frac{(\phi_1(\Phi_{\tau_1, \tau_2}) - \tau_2^2)(\tau_1^2 - \phi_2(\Phi_{\tau_1, \tau_2}))}{(\tau_1^2 - \tau_2^2)(\phi_1(\Phi_{\tau_1, \tau_2}) - \phi_2(\Phi_{\tau_1, \tau_2}))} \\ &= \frac{1}{2} + \frac{\Phi_1 - \Phi_2 + \tau_1^2 - \tau_2^2}{2\sqrt{(\Phi_1 - \Phi_2 + \tau_1^2 - \tau_2^2)^2 + 4\Phi_1\Phi_2}}. \end{aligned} \quad (55)$$

Combining (54) and (55) gives

$$\begin{aligned}
 D(\mathbf{v}_{\hat{\alpha}_1}) \leq D(\mathbf{v}_{\hat{\alpha}_2}) &\Leftrightarrow \gamma_1^2 \leq \gamma_2^2 \\
 &\Leftrightarrow \sum_{l=1}^2 \frac{\tau_1^4}{(\phi_l(\Phi_{\tau_1, \tau_2}) - \tau_1^2)^2 \phi_l(\Phi_{\tau_1, \tau_2})} \Phi_{l1}^2 \geq \sum_{l=1}^2 \frac{\tau_2^4}{(\phi_l(\Phi_{\tau_1, \tau_2}) - \tau_2^2)^2 \phi_l(\Phi_{\tau_1, \tau_2})} \Phi_{l1}^2 \\
 &\Leftrightarrow \tau_1^4 \left(\frac{\phi_2(\Phi_{\tau_1, \tau_2})(\phi_1(\Phi_{\tau_1, \tau_2}) - \tau_2^2)}{\phi_1(\Phi_{\tau_1, \tau_2}) - \tau_1^2} + \frac{\phi_1(\Phi_{\tau_1, \tau_2})(\tau_2^2 - \phi_2(\Phi_{\tau_1, \tau_2}))}{\phi_2(\Phi_{\tau_1, \tau_2}) - \tau_1^2} \right) \\
 &\geq \tau_2^4 \left(\frac{\phi_2(\Phi_{\tau_1, \tau_2})(\phi_1(\Phi_{\tau_1, \tau_2}) - \tau_1^2)}{\phi_1(\Phi_{\tau_1, \tau_2}) - \tau_2^2} + \frac{\phi_1(\Phi_{\tau_1, \tau_2})(\tau_1^2 - \phi_2(\Phi_{\tau_1, \tau_2}))}{\phi_2(\Phi_{\tau_1, \tau_2}) - \tau_2^2} \right) \\
 &\Leftrightarrow \tau_1^4 \left(\frac{\Phi_2 + \tau_2^2}{\Phi_1} \right) \geq \tau_2^4 \left(\frac{\Phi_1 + \tau_1^2}{\Phi_2} \right) \Leftrightarrow \frac{\Phi_2}{\tau_2^2} \geq \frac{\Phi_1}{\tau_1^2}.
 \end{aligned}$$

Now, assume further that $X|\pi(X) = k \sim \mathcal{N}_p(\boldsymbol{\mu}_{(k)}, \boldsymbol{\Sigma}_{(k)})$. For each $k = 1, 2$, note that $\Phi_k = \mathbf{W}_k^\top (\mathbf{I}_{n_k} - n_k^{-1} \mathbf{J}_{n_k}) \mathbf{W}_k \sim \sigma_{k,1}^2 V_k$ where $V_k \sim \chi^2(n_k - 1)$ and V_1 and V_2 are independent to each other. Then,

$$\begin{aligned}
 \zeta &= \mathbb{P}(D(\mathbf{v}_{\hat{\alpha}_1}) \leq D(\mathbf{v}_{\hat{\alpha}_2})) = \mathbb{P}(\tau_1^{-2} \Phi_1 \leq \tau_2^{-2} \Phi_2) \\
 &= \mathbb{P} \left(\frac{(n_1 - 1)^{-1} V_1}{(n_2 - 1)^{-1} V_2} \leq \frac{(n_2 - 1) \tau_2^{-2} \sigma_{2,1}^2}{(n_1 - 1) \tau_1^{-2} \sigma_{1,1}^2} \right) = \mathbb{P} \left(F \leq \frac{(n_2 - 1) \tau_2^{-2} \sigma_{2,1}^2}{(n_1 - 1) \tau_1^{-2} \sigma_{1,1}^2} \right)
 \end{aligned}$$

where $F \sim F(n_1 - 1, n_2 - 1)$. ■

E.10 Proof of Proposition 9

Proof Assume further that $m_1 = m_2 = m = 1$ (that is, $\mathbf{u}_{(1),1} = \mathbf{u}_{(2),1} = \mathbf{u}_1$). Recall that in this case $\mathcal{D} = \{1, n_1\}$ and $\mathcal{S} = \text{span}(\hat{\mathbf{u}}_1, \hat{\mathbf{u}}_{n_1}, \mathbf{w}_{\text{MDP}})$. (i) Let $\tilde{\mathbf{f}}_1 = (-\hat{\mathbf{u}}_{n_1}^\top \mathbf{u}_1) \hat{\mathbf{u}}_1 + (\hat{\mathbf{u}}_1^\top \mathbf{u}_1) \hat{\mathbf{u}}_{n_1}$. Note that $\mathbf{f}_1 = \tilde{\mathbf{f}}_1 / \|\tilde{\mathbf{f}}_1\| \in \mathcal{S}$ and \mathbf{f}_1 is orthogonal to $\mathbf{u}_{1,\mathcal{S}}$ and \mathbf{w}_{MDP} for all p . By (33), $\|\tilde{\mathbf{f}}_1\|^2 = (\hat{\mathbf{u}}_{n_1}^\top \mathbf{u}_1)^2 + (\hat{\mathbf{u}}_1^\top \mathbf{u}_1)^2$ converges to some strictly positive random variable v_1^{-2} as $p \rightarrow \infty$. For $Y \in \mathcal{Y}$, assume $\pi(Y) = 1$. Then using (33) and (39), we have

$$\begin{aligned}
 \frac{1}{\sqrt{p}} \mathbf{f}_1^\top (Y - \bar{X}) &= \frac{1}{\|\tilde{\mathbf{f}}_1\|} \left\{ (-\hat{\mathbf{u}}_{n_1}^\top \mathbf{u}_1) \frac{1}{\sqrt{p}} \hat{\mathbf{u}}_1^\top (Y - \bar{X}) + (\hat{\mathbf{u}}_1^\top \mathbf{u}_1) \frac{1}{\sqrt{p}} \hat{\mathbf{u}}_{n_1}^\top (Y - \bar{X}) \right\} \\
 &\xrightarrow{P} v_1 \left(-\frac{t_1 \Phi_{11} \Phi_{21}}{\sqrt{\phi_1(\Phi_{\tau_1, \tau_2}) \phi_2(\Phi_{\tau_1, \tau_2})}} + \frac{t_1 \Phi_{11} \Phi_{21}}{\sqrt{\phi_1(\Phi_{\tau_1, \tau_2}) \phi_2(\Phi_{\tau_1, \tau_2})}} \right) = 0
 \end{aligned}$$

as $p \rightarrow \infty$. Similarly, we can show that $p^{-1/2} \mathbf{f}_1^\top (Y - \bar{X}) \xrightarrow{P} 0$ as $p \rightarrow \infty$ for $Y \in \mathcal{Y}$ with $\pi(Y) = 2$. (ii) Let $\tilde{\mathbf{f}}_0 = -(\hat{\mathbf{u}}_1^\top \mathbf{u}_1)(\mathbf{w}_{\text{MDP}}^\top \mathbf{u}_1) \hat{\mathbf{u}}_1 - (\hat{\mathbf{u}}_{n_1}^\top \mathbf{u}_1)(\mathbf{w}_{\text{MDP}}^\top \mathbf{u}_1) \hat{\mathbf{u}}_{n_1} + \{(\hat{\mathbf{u}}_1^\top \mathbf{u}_1)^2 + (\hat{\mathbf{u}}_{n_1}^\top \mathbf{u}_1)^2\} \mathbf{w}_{\text{MDP}}$. Note that $\mathbf{f}_0 = \tilde{\mathbf{f}}_0 / \|\tilde{\mathbf{f}}_0\| \in \mathcal{S}$ and \mathbf{f}_0 is orthogonal to both of $\mathbf{u}_{1,\mathcal{S}}$ and \mathbf{f}_1 . Using (33) and (44), $\|\tilde{\mathbf{f}}_0\|^2$ converges to a strictly positive random variable \tilde{v}_0^{-2} :

$$\|\tilde{\mathbf{f}}_0\|^2 = \{(\hat{\mathbf{u}}_1^\top \mathbf{u}_1)^2 + (\hat{\mathbf{u}}_{n_1}^\top \mathbf{u}_1)^2 + (\mathbf{w}_{\text{MDP}}^\top \mathbf{u}_1)^2\} \{(\hat{\mathbf{u}}_1^\top \mathbf{u}_1)^2 + (\hat{\mathbf{u}}_{n_1}^\top \mathbf{u}_1)^2\}$$

$$\begin{aligned} & \xrightarrow{P} \left\{ \frac{\Phi_{11}^2}{\phi_1(\Phi_{\tau_1, \tau_2})} + \frac{\Phi_{21}^2}{\phi_2(\Phi_{\tau_1, \tau_2})} + \frac{r_1^2}{\kappa^2} \left(1 - \frac{\Phi_{11}^2}{\phi_1(\Phi_{\tau_1, \tau_2})} - \frac{\Phi_{21}^2}{\phi_2(\Phi_{\tau_1, \tau_2})} \right)^2 \right\} \left(\frac{\Phi_{11}^2}{\phi_1(\Phi_{\tau_1, \tau_2})} + \frac{\Phi_{21}^2}{\phi_2(\Phi_{\tau_1, \tau_2})} \right) \\ & =: \tilde{v}_0^{-2}. \end{aligned}$$

For $Y \in \mathcal{Y}$, assume $\pi(Y) = 1$. Using (33), (39), (43) and (44), we have

$$\begin{aligned} & \frac{1}{\sqrt{p}} \mathbf{f}_0^\top (Y - \bar{X}) = \frac{1}{\|\tilde{\mathbf{f}}_0\|} \frac{1}{\sqrt{p}} \tilde{\mathbf{f}}_0^\top (Y - \bar{X}) \\ & \xrightarrow{P} \frac{\tilde{v}_0}{\kappa} \left(\frac{\Phi_{11}^2}{\phi_1(\Phi_{\tau_1, \tau_2})} + \frac{\Phi_{21}^2}{\phi_2(\Phi_{\tau_1, \tau_2})} \right) \left\{ \eta_2 (1 - \cos^2 \varphi) \delta^2 - \frac{\tau_1^2 - \tau_2^2}{n} \right\} \\ & =: v_0 \left\{ \eta_2 (1 - \cos^2 \varphi) \delta^2 - \frac{\tau_1^2 - \tau_2^2}{n} \right\} \end{aligned}$$

as $p \rightarrow \infty$ where

$$v_0 = \left\{ r_1^2 \left(1 - \frac{\Phi_{11}^2}{\phi_1(\Phi_{\tau_1, \tau_2})} - \frac{\Phi_{21}^2}{\phi_2(\Phi_{\tau_1, \tau_2})} \right)^2 \left(\frac{\Phi_{11}^2}{\phi_1(\Phi_{\tau_1, \tau_2})} + \frac{\Phi_{21}^2}{\phi_2(\Phi_{\tau_1, \tau_2})} \right)^{-1} + \kappa^2 \right\}^{-1/2} \quad (56)$$

is a strictly positive random variable. Similarly, we can show that $p^{-1/2} \mathbf{f}_0^\top (Y - \bar{X}) \xrightarrow{P} v_0 \{ -\eta_1 (1 - \cos^2 \varphi) \delta^2 - (\tau_1^2 - \tau_2^2)/n \}$ as $p \rightarrow \infty$ for $Y \in \mathcal{Y}$ with $\pi(Y) = 2$. (iii) To show that v_0 defined in (56) is greater than γ_1 and γ_2 defined in (53), it suffices to show that

$$\begin{aligned} & \left(1 - \frac{\Phi_{11}^2}{\phi_1(\Phi_{\tau_1, \tau_2})} - \frac{\Phi_{21}^2}{\phi_2(\Phi_{\tau_1, \tau_2})} \right)^2 \left(\frac{\Phi_{11}^2}{\phi_1(\Phi_{\tau_1, \tau_2})} + \frac{\Phi_{21}^2}{\phi_2(\Phi_{\tau_1, \tau_2})} \right)^{-1} \\ & < \frac{\tau_k^4 \Phi_{11}^2}{(\phi_1(\Phi_{\tau_1, \tau_2}) - \tau_k^2)^2 \phi_1(\Phi_{\tau_1, \tau_2})} + \frac{\tau_k^4 \Phi_{21}^2}{(\phi_2(\Phi_{\tau_1, \tau_2}) - \tau_k^2)^2 \phi_2(\Phi_{\tau_1, \tau_2})} \end{aligned}$$

for $k = 1, 2$. From (52), we have

$$1 - \frac{\Phi_{11}^2}{\phi_1(\Phi_{\tau_1, \tau_2}) - \tau_k^2} - \frac{\Phi_{21}^2}{\phi_2(\Phi_{\tau_1, \tau_2}) - \tau_k^2} = 0$$

for $k = 1, 2$ and thus

$$\begin{aligned} & \left(1 - \frac{\Phi_{11}^2}{\phi_1(\Phi_{\tau_1, \tau_2})} - \frac{\Phi_{21}^2}{\phi_2(\Phi_{\tau_1, \tau_2})} \right)^2 = \tau_k^4 \left\{ \sum_{i=1}^2 \frac{\Phi_{i1}^2}{\phi_i(\Phi_{\tau_1, \tau_2}) (\phi_i(\Phi_{\tau_1, \tau_2}) - \tau_k^2)} \right\}^2 \\ & \leq \tau_k^4 \left(\sum_{i=1}^2 \frac{\Phi_{i1}^2}{\phi_i(\Phi_{\tau_1, \tau_2})} \right) \left\{ \sum_{i=1}^2 \frac{\Phi_{i1}^2}{(\phi_i(\Phi_{\tau_1, \tau_2}) - \tau_k^2)^2 \phi_i(\Phi_{\tau_1, \tau_2})} \right\} \end{aligned}$$

by Cauchy-Schwarz inequality. Note that the equality does not hold with probability 1 since $\phi_1(\Phi_{\tau_1, \tau_2}) > \phi_2(\Phi_{\tau_1, \tau_2})$. Hence, $v_0 > \gamma_k$ for all $k = 1, 2$ with probability 1. \blacksquare

E.11 Proof of Proposition 10

Proof Assume further that $m_1 = m_2 = 1$ and $m = 2$ (that is, $\mathbf{u}_{(1),1} \neq \mathbf{u}_{(2),1}$). For any given $\alpha \in \mathbb{R}$, $\{\mathbf{v}_\alpha\} \in \mathcal{A}$ if and only if $\mathbf{v}_\alpha^\top \mathbf{u}_{(1),1} \xrightarrow{P} 0$ and $\mathbf{v}_\alpha^\top \mathbf{u}_{(2),1} \xrightarrow{P} 0$ as $p \rightarrow \infty$. Since $\|\tilde{\mathbf{v}}_\alpha\|$ (defined in (46)) is stochastically bounded for all $\alpha \in \mathbb{R}$ where $\tilde{\mathbf{v}}_\alpha$ is defined, it suffices to show that there is no ridge parameter $\alpha \in \mathbb{R}$ such that both of $\tilde{\mathbf{v}}_\alpha^\top \mathbf{u}_{(1),1}$ and $\tilde{\mathbf{v}}_\alpha^\top \mathbf{u}_{(2),1}$ converge to zero as $p \rightarrow \infty$. It can be checked that

$$v_{11}^2(\Phi_{\tau_1, \tau_2}) = v_{22}^2(\Phi_{\tau_1, \tau_2}) = \frac{1}{2} + \frac{\Phi_1 - \Phi_2 + \tau_1^2 - \tau_2^2}{2\sqrt{(\Phi_1 - \Phi_2 + \tau_1^2 - \tau_2^2)^2 + 4(\mathbf{R}_1^\top \mathbf{R}_2)^2 \Phi_1 \Phi_2}} \quad (57)$$

and

$$v_{11}(\Phi_{\tau_1, \tau_2})v_{12}(\Phi_{\tau_1, \tau_2}) = \frac{(\mathbf{R}_1^\top \mathbf{R}_2)\Phi_1^{1/2}\Phi_2^{1/2}}{\sqrt{(\Phi_1 - \Phi_2 + \tau_1^2 - \tau_2^2)^2 + 4(\mathbf{R}_1^\top \mathbf{R}_2)\Phi_1\Phi_2}}. \quad (58)$$

Combining (48), (57) and (58) gives

$$\begin{aligned} \tilde{\mathbf{v}}_\alpha^\top \mathbf{u}_{1,1} &\xrightarrow{P} \mathbf{r}^\top \{\mathbf{I}_2 - (\mathbf{R}_1 \Phi_1^{1/2} \tilde{\mathbf{V}}_1(\Phi_{\tau_1, \tau_2}) + \mathbf{R}_2 \Phi_2^{1/2} \tilde{\mathbf{V}}_2(\Phi_{\tau_1, \tau_2}))(\mathbf{D}(\Phi_{\tau_1, \tau_2}) + \alpha \mathbf{I}_2)^{-1} \\ &\quad (\mathbf{R}_1 \Phi_1^{1/2} \tilde{\mathbf{V}}_1(\Phi_{\tau_1, \tau_2}) + \mathbf{R}_2 \Phi_2^{1/2} \tilde{\mathbf{V}}_2(\Phi_{\tau_1, \tau_2}))^\top\} \mathbf{R}_1 \\ &= \frac{(\mathbf{r}^\top \mathbf{R}_1)(\alpha + \tau_1^2)(\alpha + \phi_1(\Phi_{\tau_1, \tau_2}))v_{21}^2(\Phi_{\tau_1, \tau_2}) + \phi_2(\Phi_{\tau_1, \tau_2})v_{11}^2(\Phi_{\tau_1, \tau_2})}{(\alpha + \phi_1(\Phi_{\tau_1, \tau_2}))(\alpha + \phi_2(\Phi_{\tau_1, \tau_2}))} \\ &\quad - \frac{(\mathbf{r}^\top \mathbf{R}_2)(\alpha + \tau_1^2)\{\Phi_1^{-1/2}\Phi_2^{1/2}(\phi_1(\Phi_{\tau_1, \tau_2}) - \phi_2(\Phi_{\tau_1, \tau_2}))v_{11}(\Phi_{\tau_1, \tau_2})v_{12}(\Phi_{\tau_1, \tau_2})\}}{(\alpha + \phi_1(\Phi_{\tau_1, \tau_2}))(\alpha + \phi_2(\Phi_{\tau_1, \tau_2}))} \\ &= \frac{(\mathbf{r}^\top \mathbf{R}_1)(\alpha + \tau_1^2)\{\alpha + \Phi_2 + \tau_2^2 - (\mathbf{r}^\top \mathbf{R}_1)^{-1}(\mathbf{r}^\top \mathbf{R}_2)(\mathbf{R}_1^\top \mathbf{R}_2)\Phi_2\}}{(\alpha + \phi_1(\Phi_{\tau_1, \tau_2}))(\alpha + \phi_2(\Phi_{\tau_1, \tau_2}))} \end{aligned}$$

as $p \rightarrow \infty$ where $\mathbf{r} = (r_1, r_2)^\top$ with r_i ($i = 1, 2$) defined in Lemma 25. Hence, $\tilde{\mathbf{v}}_\alpha^\top \mathbf{u}_{(1),1} \xrightarrow{P} 0$ as $p \rightarrow \infty$ if and only if $\alpha = -\tau_1^2$ and $\alpha = -\Phi_2 - \tau_2^2 + (\mathbf{r}^\top \mathbf{R}_1)^{-1}(\mathbf{r}^\top \mathbf{R}_2)(\mathbf{R}_1^\top \mathbf{R}_2)\Phi_2$. Similarly,

$$\tilde{\mathbf{v}}_\alpha^\top \mathbf{u}_{(2),1} \xrightarrow{P} \frac{(\mathbf{r}^\top \mathbf{R}_2)(\alpha + \tau_2^2)\{\alpha + \Phi_1 + \tau_1^2 - (\mathbf{r}^\top \mathbf{R}_2)^{-1}(\mathbf{r}^\top \mathbf{R}_1)(\mathbf{R}_1^\top \mathbf{R}_2)\Phi_1\}}{(\alpha + \phi_1(\Phi_{\tau_1, \tau_2}))(\alpha + \phi_2(\Phi_{\tau_1, \tau_2}))}$$

as $p \rightarrow \infty$. Hence, $\tilde{\mathbf{v}}_\alpha^\top \mathbf{u}_{(2),1} \xrightarrow{P} 0$ as $p \rightarrow \infty$ if and only if $\alpha = -\tau_2^2$ and $\alpha = -\Phi_1 - \tau_1^2 + (\mathbf{r}^\top \mathbf{R}_2)^{-1}(\mathbf{r}^\top \mathbf{R}_1)(\mathbf{R}_1^\top \mathbf{R}_2)\Phi_1$ and there is no ridge parameter $\alpha \in \mathbb{R}$ such that both of $\tilde{\mathbf{v}}_\alpha^\top \mathbf{u}_{(1),1}$ and $\tilde{\mathbf{v}}_\alpha^\top \mathbf{u}_{(2),1}$ converge to zero as $p \rightarrow \infty$. \blacksquare

E.12 Proof of Theorem 11

Proof For notational simplicity, we write $\mathcal{D} = \{i_1, \dots, i_{m_1+m_2}\}$ so that $i_l < i_{l'}$ if $l < l'$. Let $\hat{\mathbf{V}}_1 = [\hat{\mathbf{u}}_{i_1}, \dots, \hat{\mathbf{u}}_{i_{m_1+m_2}}]$ and $\tilde{\mathbf{V}} = [\hat{\mathbf{V}}_1, \mathbf{w}_{\text{MDP}}]$ so that the columns of $\tilde{\mathbf{V}}$ form an orthonormal basis of \mathcal{S} . Write $\mathbf{K} = \hat{\mathbf{V}}_1^\top \mathbf{U}_1 \in \mathbb{R}^{(m_1+m_2) \times m}$ and $\mathbf{k}^\top = \mathbf{w}_{\text{MDP}}^\top \mathbf{U}_1 \in \mathbb{R}^{1 \times m}$. From (33), we get $\mathbf{K} \xrightarrow{P} \tilde{\mathbf{\Omega}}_1$ as $p \rightarrow \infty$, which is a $(m_1 + m_2) \times m$ matrix such that

$$[\tilde{\mathbf{\Omega}}_1]_{i,j} = \frac{1}{\sqrt{\phi_i(\Phi_{\tau_1, \tau_2})}} \Phi_{ij} \quad (59)$$

where $\Phi_{ij} = \sum_{k=1}^2 [\mathbf{R}_k]_j \Phi_k^{1/2} \tilde{v}_{ik}(\Phi_{\tau_1, \tau_2})$ for $1 \leq i \leq m_1 + m_2$ and $1 \leq j \leq m$. Also, from (44), we get $\mathbf{k} \xrightarrow{P} \boldsymbol{\omega}_1$, which is a $m \times 1$ vector such that

$$\boldsymbol{\omega}_1 = \frac{1}{\kappa} (\mathbf{I}_m - \tilde{\boldsymbol{\Omega}}_1^\top \tilde{\boldsymbol{\Omega}}_1) \mathbf{r} \quad (60)$$

where $\mathbf{r} = (r_1, \dots, r_m)^\top$ with r_j defined in Lemma 25. Lastly, write $\tilde{\boldsymbol{\Omega}} = [\tilde{\boldsymbol{\Omega}}_1^\top, \boldsymbol{\omega}_1^\top]^\top$. Note that $\tilde{\boldsymbol{\Omega}}_1$ and $\tilde{\boldsymbol{\Omega}}$ are of rank m .

(i) For any given $\{\mathbf{w}\} \in \mathcal{T}$, $\mathbf{w} \in \mathcal{T}_p = \text{span}(\{\hat{\mathbf{u}}_i\}_{i \in \mathcal{D}}) \cap \text{span}(\mathbf{U}_{1, \mathcal{S}}^\perp)$ for each p . That is, $\mathbf{w} \in \mathcal{T}_p$ can be expressed as $\mathbf{w} = \hat{\mathbf{V}}_1 \mathbf{a}_1$ for some $\mathbf{a}_1 \in \mathbb{R}^{m_1 + m_2}$ such that $\mathbf{K}^\top \mathbf{a}_1 = \mathbf{0}_m$. Hence, $\mathbf{a}_1^\top [\tilde{\boldsymbol{\Omega}}_1]^j = o_p(1)$ for all $1 \leq j \leq m$. For $Y \in \mathcal{Y}$, assume $\pi(Y) = 1$. From (39), we have

$$\frac{1}{\sqrt{p}} \mathbf{w}^\top (Y - \bar{X}) = \mathbf{a}_1^\top \frac{1}{\sqrt{p}} \hat{\mathbf{V}}_1^\top (Y - \bar{X}) = \sum_{j=1}^m t_j \mathbf{a}_1^\top [\tilde{\boldsymbol{\Omega}}_1]^j + o_p(1) \xrightarrow{P} 0$$

as $p \rightarrow \infty$ where t_j is defined in the proof of Theorem 3. Similarly, we can show the same result for $Y \in \mathcal{Y}$ with $\pi(Y) = 2$.

(ii) Recall that $\mathcal{S} = \text{span}(\mathbf{U}_{1, \mathcal{S}}) \oplus \mathcal{T}_p \oplus \text{span}(\mathbf{f}_0)$. Write $\mathbf{f}_0 = \tilde{\mathbf{V}} \mathbf{a}$ where $\mathbf{a} = (\mathbf{a}_{0,1}, a_{0, \text{MDP}})^\top \in \mathbb{R}^{m_1 + m_2 + 1}$ with $\mathbf{a}_{0,1} \in \mathbb{R}^{m_1 + m_2}$ and $a_{0, \text{MDP}} \in \mathbb{R}$. Since \mathbf{f}_0 is orthogonal to \mathcal{T}_p , $\mathbf{a}_{0,1} = \mathbf{K} \mathbf{p}$ for some $\mathbf{p} \in \mathbb{R}^m$. Also, since \mathbf{f}_0 is orthogonal to $\text{span}(\mathbf{U}_{1, \mathcal{S}})$, $\mathbf{U}_1^\top \mathbf{f}_0 = \mathbf{K}^\top \mathbf{a}_{0,1} + \mathbf{k} a_{0, \text{MDP}} = \mathbf{K}^\top \mathbf{K} \mathbf{p} + \mathbf{k} a_{0, \text{MDP}} = \mathbf{0}_m$. Lastly, since \mathbf{f}_0 is a unit vector, $\|\mathbf{K} \mathbf{p}\|_2^2 + a_{0, \text{MDP}}^2 = 1$. Then $\mathbf{a}_{0,1} = \mathbf{K} \mathbf{p} = -\mathbf{K}(\mathbf{K}^\top \mathbf{K})^{-1} \mathbf{k} a_{0, \text{MDP}}$ and $a_{0, \text{MDP}}^2 = \{\mathbf{k}^\top (\mathbf{K}^\top \mathbf{K})^{-1} \mathbf{k} + 1\}^{-1}$. Moreover,

$$\mathbf{a}_{0,1} \xrightarrow{P} \boldsymbol{\psi}_{0,1} := \frac{\psi_{0, \text{MDP}}}{\kappa} \tilde{\boldsymbol{\Omega}}_1 (\mathbf{I}_m - (\tilde{\boldsymbol{\Omega}}_1^\top \tilde{\boldsymbol{\Omega}}_1)^{-1}) \mathbf{r}$$

and

$$a_{0, \text{MDP}} \xrightarrow{P} \psi_{0, \text{MDP}} := \frac{\kappa}{\sqrt{\kappa^2 + \mathbf{r}^\top (\mathbf{I}_m - \tilde{\boldsymbol{\Omega}}_1^\top \tilde{\boldsymbol{\Omega}}_1) (\tilde{\boldsymbol{\Omega}}_1^\top \tilde{\boldsymbol{\Omega}}_1)^{-1} (\mathbf{I}_m - \tilde{\boldsymbol{\Omega}}_1^\top \tilde{\boldsymbol{\Omega}}_1) \mathbf{r}}} \quad (61)$$

as $p \rightarrow \infty$. Note that $\boldsymbol{\psi}_0 = (\boldsymbol{\psi}_{0,1}^\top, \psi_{0, \text{MDP}})^\top$ satisfies $\boldsymbol{\psi}_0^\top [\tilde{\boldsymbol{\Omega}}]^j = 0$ for all $1 \leq j \leq m$. Now, for $Y \in \mathcal{Y}$, assume $\pi(Y) = 1$. Combining (39) and (43) gives

$$\begin{aligned} \frac{1}{\sqrt{p}} \mathbf{f}_0^\top (Y - \bar{X}) &= \mathbf{a}_{0,1}^\top \frac{1}{\sqrt{p}} \hat{\mathbf{V}}_1^\top (Y - \bar{X}) + a_{0, \text{MDP}} \frac{1}{\sqrt{p}} \mathbf{w}_{\text{MDP}}^\top (Y - \bar{X}) \\ &\xrightarrow{P} \sum_{j=1}^m t_j \boldsymbol{\psi}_0^\top [\tilde{\boldsymbol{\Omega}}]^j + \frac{\psi_{0, \text{MDP}}}{\kappa} \left\{ \eta_2 (1 - \cos^2 \varphi) \delta^2 - \frac{\tau_1^2 - \tau_2^2}{n} \right\} \\ &= \frac{\psi_{0, \text{MDP}}}{\kappa} \left\{ \eta_2 (1 - \cos^2 \varphi) \delta^2 - \frac{\tau_1^2 - \tau_2^2}{n} \right\} =: v_0 \left\{ \eta_2 (1 - \cos^2 \varphi) \delta^2 - \frac{\tau_1^2 - \tau_2^2}{n} \right\} \end{aligned}$$

as $p \rightarrow \infty$ where

$$v_0 = \left\{ \kappa^2 + \mathbf{r}^\top (\mathbf{I}_m - \tilde{\boldsymbol{\Omega}}_1^\top \tilde{\boldsymbol{\Omega}}_1) (\tilde{\boldsymbol{\Omega}}_1^\top \tilde{\boldsymbol{\Omega}}_1)^{-1} (\mathbf{I}_m - \tilde{\boldsymbol{\Omega}}_1^\top \tilde{\boldsymbol{\Omega}}_1) \mathbf{r} \right\}^{-1/2} \quad (62)$$

is a strictly positive random variable. Note that v_0 in (56) is a special case of (62) when $m_1 = m_2 = m = 1$. Similarly, we can show that $p^{-1/2} \mathbf{f}_0^\top (Y - \bar{X}) \xrightarrow{P} v_0 \{-\eta_1 (1 - \cos^2 \varphi) \delta^2 - (\tau_1^2 - \tau_2^2)/n\}$ as $p \rightarrow \infty$ for $Y \in \mathcal{Y}$ with $\pi(Y) = 2$. \blacksquare

E.13 Proof of Theorem 12

Proof We will use the same notations as in the proof of Theorem 11.

(i) For each p , let $\{\mathbf{f}_i\}_{i=1}^{m_1+m_2-m}$ forms an orthonormal basis of \mathcal{T}_p . Also, choose $\{\mathbf{g}_i\}_{i=1}^m$ so that $\{\mathbf{f}_0\} \cup \{\mathbf{f}_i\}_{i=1}^{m_1+m_2-m} \cup \{\mathbf{g}_i\}_{i=1}^m$ forms an orthonormal basis of \mathcal{S} . Then $\{\mathbf{f}_0\} \cup \{\mathbf{f}_i\}_{i=1}^{m_1+m_2-m} \cup \{\mathbf{g}_i\}_{i=1}^m \cup \{\hat{\mathbf{u}}_i\}_{i \in \{1, \dots, n-2\} \setminus \mathcal{D}}$ forms an orthonormal basis of $\mathcal{S}_{\mathcal{X}}$.

Write $\mathcal{B}_p = \text{span}(\mathbf{f}_0) \oplus \mathcal{T}_p \oplus \text{span}(\{\hat{\mathbf{u}}_i\}_{i \in \{1, \dots, n-2\} \setminus \mathcal{D}})$. For any given $\{\mathbf{w}\} \in \mathcal{A}$, write $\mathbf{w} = a_0 \mathbf{f}_0 + \sum_{i=1}^{m_1+m_2-m} a_i \mathbf{f}_i + \sum_{i=1}^m b_i \mathbf{g}_i + \sum_{i \in \{1, \dots, n-2\} \setminus \mathcal{D}} c_i \hat{\mathbf{u}}_i$. Note that for all $0 \leq i \leq m_1 + m_2 - m$, \mathbf{f}_i is orthogonal to \mathbf{u}_j for $1 \leq j \leq m$. Also, from (33) we have $\hat{\mathbf{u}}_i^\top \mathbf{u}_j \xrightarrow{P} 0$ as $p \rightarrow \infty$ for $i \in \{1, \dots, n-2\} \setminus \mathcal{D}$ and $1 \leq j \leq m$. Using Lemma 3.3 (i) of Chang et al. (2021), it can be shown that $\{\mathbf{w}\} \in \mathcal{A}$ is equivalent to $\mathbf{w}^\top \mathbf{u}_j \xrightarrow{P} 0$ as $p \rightarrow \infty$ for $1 \leq j \leq m$. Hence, $b_i = o_p(1)$ for $1 \leq i \leq m$. Let $\{\mathbf{v}\} \in \mathcal{B}_p$ with $\mathbf{v} = P_{\mathcal{B}_p} \mathbf{w} / \|P_{\mathcal{B}_p} \mathbf{w}\| \in \mathcal{B}_p$ for all p . Then $\|\mathbf{w} - \mathbf{v}\| \xrightarrow{P} 0$ since $\|P_{\mathcal{B}_p} \mathbf{w}\|^2 = \|\mathbf{w}\|^2 - \sum_{i=1}^m b_i^2 \xrightarrow{P} 1$ as $p \rightarrow \infty$.

(ii) Theorem 11 tells that $D(\mathbf{f}_i) = 0$ for all $1 \leq i \leq m_1 + m_2 - m$ while $D(\mathbf{f}_0) > 0$. Also, since $p^{-1/2} \mathbf{w}^\top \boldsymbol{\mu} \xrightarrow{P} D(\mathbf{w})$ as $p \rightarrow \infty$ for any $\{\mathbf{w}\} \in \mathcal{A}$ such that $D(\mathbf{w})$ exists, (36) leads to $D(\hat{\mathbf{u}}_i) = 0$ for $i \in \{1, \dots, n-2\} \setminus \mathcal{D}$. Then $p^{-1/2} \mathbf{w}^\top (Y_1 - Y_2) \leq |a_0| D(\mathbf{f}_0) + o_p(1)$ for $Y_i \in \mathcal{Y}$ with $\pi(Y_i) = i$ ($i = 1, 2$). Now $|a_0| \leq 1$ implies that $D(\mathbf{w}) \leq D(\mathbf{f}_0)$ and the equality holds if and only if $a_0 \xrightarrow{P} 1$ as $p \rightarrow \infty$. \blacksquare

E.14 Proof of Theorem 13

To distinguish between the notations for the training dataset \mathcal{X} and the independent test dataset \mathcal{Y} in Section 4.5, we use a superscript for the latter. Specifically, any quantity defined with a superscript $*$ refers to the independent test dataset \mathcal{Y} , whereas quantities without the superscript pertain to the training dataset \mathcal{X} . For example, \mathbf{S}_W^* is the within-class scatter matrix of \mathcal{Y} and $\hat{\mathbf{u}}_i^*$ is the i th eigenvector of \mathbf{S}_W^* . Also, $\mathcal{D}^* \subset \{1, \dots, n^* - 2\}$ is the index set collecting the indices of the sample eigenvectors of \mathbf{S}_W^* capable of explaining variations contained in the common leading eigenspace \mathcal{U} . For notational simplicity, we write $\mathcal{D} = \{i_1, \dots, i_{m_1+m_2}\}$ and $\mathcal{D}^* = \{j_1, \dots, j_{m_1+m_2}\}$ so that $i_l < i_{l'}$ and $j_l < j_{l'}$ if $l < l'$. **Proof** First, we shall find the probability limit of $\hat{\mathbf{u}}_i^\top \hat{\mathbf{u}}_j^*$ ($1 \leq i \leq n-2$ and $1 \leq j \leq n^*-2$). Using equation (30) and Lemmas 16, 17 and 24, we have

$$\hat{\mathbf{u}}_i^\top \hat{\mathbf{u}}_j^* \xrightarrow{P} \begin{cases} (\phi_i(\mathbf{S}_0) \phi_j(\mathbf{S}_0^*))^{-1/2} \{\mathbf{W}^\top (\mathbf{I}_n - \mathbf{J}) v_i(\mathbf{S}_0)\}^\top \{\mathbf{W}^{*\top} (\mathbf{I}_{n^*} - \mathbf{J}^*) v_j(\mathbf{S}_0^*)\}, & i \in \mathcal{D}, j \in \mathcal{D}^* \\ 0, & o.w \end{cases}$$

as $p \rightarrow \infty$ where \mathbf{S}_0^* is the probability limit of $p^{-1} (\mathbf{Y} - \bar{\mathbf{Y}})^\top (\mathbf{Y} - \bar{\mathbf{Y}})$, which is the scaled dual matrix of \mathbf{S}_W^* . To be specific, for $i_l \in \mathcal{D}$ and $j_{l'} \in \mathcal{D}^*$ ($1 \leq l, l' \leq m_1 + m_2$), we have

$$\hat{\mathbf{u}}_{i_l}^\top \hat{\mathbf{u}}_{j_{l'}}^* \xrightarrow{P} \frac{1}{\sqrt{\phi_l(\boldsymbol{\Phi}_{\tau_1, \tau_2}) \phi_{l'}(\boldsymbol{\Phi}_{\tau_1, \tau_2}^*)}} \sum_{k=1}^m \boldsymbol{\Phi}_{lk} \boldsymbol{\Phi}_{l'k}^* \quad (63)$$

as $p \rightarrow \infty$ where $\boldsymbol{\Phi}_{lk} = \sum_{i=1}^2 [\mathbf{R}_i]_k \boldsymbol{\Phi}_i^{1/2} \tilde{v}_{li}(\boldsymbol{\Phi}_{\tau_1, \tau_2})$ and $\boldsymbol{\Phi}_{l'k}^* = \sum_{i=1}^2 [\mathbf{R}_i]_k \boldsymbol{\Phi}_i^{*1/2} \tilde{v}_{l'i}(\boldsymbol{\Phi}_{\tau_1, \tau_2}^*)$ ($k = 1, \dots, m$).

Next, to obtain the probability limit of $\mathbf{w}_{\text{MDP}}^\top \hat{\mathbf{u}}_j^*$, note that

$$\mathbf{w}_{\text{MDP}}^\top \hat{\mathbf{u}}_j^* = \hat{\mathbf{u}}_j^{*\top} \frac{\hat{\mathbf{U}}_2 \hat{\mathbf{U}}_2^\top \mathbf{d}}{\|\hat{\mathbf{U}}_2 \hat{\mathbf{U}}_2^\top \mathbf{d}\|} = \frac{1}{\kappa_{\text{MDP}}} \left(\frac{1}{\sqrt{p}} \hat{\mathbf{u}}_j^{*\top} \mathbf{d} - \frac{1}{\sqrt{p}} \hat{\mathbf{u}}_j^{*\top} \hat{\mathbf{U}}_1 \hat{\mathbf{U}}_1^\top \mathbf{d} \right).$$

Using similar arguments to the proof of Lemma 25, for $j_{l'} \in \mathcal{D}^*$, we have

$$\frac{1}{\sqrt{p}} \hat{\mathbf{u}}_{j_{l'}}^{*\top} \mathbf{d} \xrightarrow{P} \frac{1}{\sqrt{\phi_{l'}(\Phi_{\tau_1, \tau_2}^*)}} \sum_{k=1}^m r_k \Phi_{l'k}^* \quad (64)$$

and

$$\begin{aligned} \frac{1}{\sqrt{p}} \hat{\mathbf{u}}_{j_{l'}}^{*\top} \hat{\mathbf{U}}_1 \hat{\mathbf{U}}_1^\top \mathbf{d} &= \sum_{i \in \mathcal{D}} (\hat{\mathbf{u}}_{j_{l'}}^{*\top} \hat{\mathbf{u}}_i) \left(\frac{1}{\sqrt{p}} \hat{\mathbf{u}}_i^\top \mathbf{d} \right) + o_p(1) \\ &\xrightarrow{P} \frac{1}{\sqrt{\phi_{l'}(\Phi_{\tau_1, \tau_2}^*)}} \sum_{i=1}^{m_1+m_2} \sum_{k=1}^m \sum_{k'=1}^m \frac{1}{\phi_i(\Phi_{\tau_1, \tau_2}^*)} r_{k'} \Phi_{ik} \Phi_{ik'} \Phi_{l'k}^* \end{aligned} \quad (65)$$

as $p \rightarrow \infty$ where r_k is defined in Lemma 25. Combining (64) and (65) gives

$$\mathbf{w}_{\text{MDP}}^\top \hat{\mathbf{u}}_{j_{l'}}^* \xrightarrow{P} \frac{1}{\kappa \sqrt{\phi_{l'}(\Phi_{\tau_1, \tau_2}^*)}} \sum_{k=1}^m \sum_{k'=1}^m \left(I_{kk'} - \sum_{i=1}^{m_1+m_2} \frac{1}{\phi_i(\Phi_{\tau_1, \tau_2}^*)} \Phi_{ik} \Phi_{ik'} \right) r_{k'} \Phi_{l'k}^* \quad (66)$$

as $p \rightarrow \infty$ where $I_{kk'} = I(k = k')$. In contrast, for $j \notin \mathcal{D}^*$, we can show that $\mathbf{w}_{\text{MDP}}^\top \hat{\mathbf{u}}_j^* \xrightarrow{P} 0$ as $p \rightarrow \infty$.

Let $\xi_{i,j}$ be the probability limit of $\hat{\mathbf{u}}_i^\top \hat{\mathbf{u}}_j^*$ and $\xi_{\text{MDP},j}$ be the probability limit of $\mathbf{w}_{\text{MDP}}^\top \hat{\mathbf{u}}_j^*$, and write $\boldsymbol{\xi}_j = (\xi_{1,j}, \dots, \xi_{n-2,j}, \xi_{\text{MDP},j})^\top$ for $1 \leq j \leq m$. Also, let $\mathbf{V} = [\hat{\mathbf{u}}_1, \dots, \hat{\mathbf{u}}_{n-2}, \mathbf{w}_{\text{MDP}}]$ and denote the probability limit of the $(n-1) \times (n-1)$ matrix $p^{-1} \mathbf{V}^\top \mathbf{S}_W^* \mathbf{V}$ by \mathbf{L} . Since $\hat{\mathbf{u}}_i^\top \hat{\mathbf{u}}_j^* \xrightarrow{P} 0$ and $\mathbf{w}_{\text{MDP}}^\top \hat{\mathbf{u}}_j^* \xrightarrow{P} 0$ as $p \rightarrow \infty$ for $j \notin \mathcal{D}^*$, we have $\boldsymbol{\xi}_j = \mathbf{0}_{n-1}$ for $j \notin \mathcal{D}^*$ and $\mathbf{L} = \sum_{l'=1}^{m_1+m_2} \phi_{l'}(\Phi_{\tau_1, \tau_2}^*) \boldsymbol{\xi}_{j_{l'}} \boldsymbol{\xi}_{j_{l'}}^\top$. Recall that $\phi_{l'}(\Phi_{\tau_1, \tau_2}^*) > 0$ for all $l' = 1, \dots, m_1+m_2$. Now, we define the $(n-2) \times m$ matrix $\boldsymbol{\Omega}_1$ such that

$$[\boldsymbol{\Omega}_1]_{i,j} = [\tilde{\boldsymbol{\Omega}}_1]_{l,j} \quad (67)$$

for $1 \leq l \leq m_1+m_2$ and $1 \leq j \leq m$ where $\tilde{\boldsymbol{\Omega}}_1$ is defined in (59), and $[\boldsymbol{\Omega}_1]_{i,j} = 0$ for $i \notin \mathcal{D}$ and $1 \leq j \leq m$. Also, we define the $(n-1) \times m$ matrix $\boldsymbol{\Omega} = [\boldsymbol{\Omega}_1^\top, \boldsymbol{\omega}_1]^\top$ where $\boldsymbol{\omega}_1$ is the $m \times 1$ vector defined in (60). Lastly, we define the $(m_1+m_2) \times m$ matrix $\tilde{\boldsymbol{\Omega}}_1^*$ such that

$$[\tilde{\boldsymbol{\Omega}}_1^*]_{i,j} = \frac{1}{\sqrt{\phi_i(\Phi_{\tau_1, \tau_2}^*)}} \Phi_{ij}^* \quad (68)$$

for $1 \leq i \leq m_1+m_2$ and $1 \leq j \leq m$. Then from (63) and (66),

$$\boldsymbol{\Xi} := [\boldsymbol{\xi}_{j_1}, \dots, \boldsymbol{\xi}_{j_{m_1+m_2}}] = \boldsymbol{\Omega} \tilde{\boldsymbol{\Omega}}_1^{*\top} \in \mathbb{R}^{(n-1) \times (m_1+m_2)}. \quad (69)$$

Since both of $\boldsymbol{\Omega}$ and $\tilde{\boldsymbol{\Omega}}_1^*$ are of rank m , we have $\text{rank}(\mathbf{L}) = \text{rank}(\boldsymbol{\Xi}) = m$. \blacksquare

E.15 Proof of Theorem 14

Proof (i) For any given $\{\mathbf{w}\} \in \bar{\mathcal{A}}$, we have already seen that there exists $\{\mathbf{v}\}$ such that $\mathbf{v} \in \text{span}(\mathbf{V}\hat{\mathbf{Q}}_2)$ for all p and $\|\mathbf{w} - \mathbf{v}\| \xrightarrow{P} 0$ as $p \rightarrow \infty$. Thus it suffices to show that $\mathbf{v}^\top \mathbf{u}_j \xrightarrow{P} 0$ as $p \rightarrow \infty$. Let $\mathbf{v} = \mathbf{V}\mathbf{b}$ such that $\mathbf{b} \in \text{span}(\hat{\mathbf{Q}}_2)$. Note that \mathbf{b} is asymptotically orthogonal to $\text{span}(\mathbf{L}) = \text{span}(\mathbf{\Omega})$ where \mathbf{L} and $\mathbf{\Omega}$ are defined in the proof of Theorem 13. Using (33) and (44), we have

$$\mathbf{v}^\top \mathbf{u}_j = \mathbf{b}^\top \mathbf{V}^\top \mathbf{u}_j = \mathbf{b}^\top [\mathbf{\Omega}]^j + o_p(1) \xrightarrow{P} 0 \quad (70)$$

as $p \rightarrow \infty$.

(ii) For any given $\{\mathbf{w}\} \in \bar{\mathcal{A}}$, we assume $\mathbf{w} = \mathbf{V}\mathbf{a}$ where $\mathbf{a} = (a_1, \dots, a_{n-2}, a_{\text{MDP}})^\top$ satisfies $a_{\text{MDP}} \xrightarrow{P} \psi_{\text{MDP}}$ as $p \rightarrow \infty$. Recall that there exists $\{\mathbf{v}\}$ such that $\mathbf{v} \in \text{span}(\mathbf{V}\hat{\mathbf{Q}}_2)$ for all p and $\|\mathbf{w} - \mathbf{v}\| \xrightarrow{P} 0$ as $p \rightarrow \infty$. Write $\mathbf{v} = \mathbf{V}\mathbf{b}$ with $\mathbf{b} = (b_1, \dots, b_{n-2}, b_{\text{MDP}})^\top$. Then $\|\mathbf{w} - \mathbf{v}\| = \|\mathbf{a} - \mathbf{b}\| \xrightarrow{P} 0$ and $b_{\text{MDP}} \xrightarrow{P} \psi_{\text{MDP}}$ as $p \rightarrow \infty$. Note that $p^{-1/2}\mathbf{w}^\top(Y - \bar{X}) = p^{-1/2}\mathbf{v}^\top(Y - \bar{X}) + o_p(1)$ and it suffices to obtain the probability limit of $p^{-1/2}\mathbf{v}^\top(Y - \bar{X})$. For any independent observation Y , which is independent to both of \mathcal{X} and \mathcal{Y} , assume that $\pi(Y) = 1$. Combining (39), (43) and (70) gives

$$\begin{aligned} \frac{1}{\sqrt{p}}\mathbf{v}^\top(Y - \bar{X}) &= \sum_{j=1}^m t_j \mathbf{b}^\top [\mathbf{\Omega}]^j + \frac{\psi_{\text{MDP}}}{\kappa} \left\{ \eta_2(1 - \cos^2 \varphi)\delta^2 - \frac{\tau_1^2 - \tau_2^2}{n} \right\} + o_p(1) \\ &\xrightarrow{P} \frac{\psi_{\text{MDP}}}{\kappa} \left\{ \eta_2(1 - \cos^2 \varphi)\delta^2 - \frac{\tau_1^2 - \tau_2^2}{n} \right\} \end{aligned}$$

as $p \rightarrow \infty$ where t_j is defined in the proof of Theorem 3. Similarly, we can show that

$$\frac{1}{\sqrt{p}}\mathbf{w}^\top(Y - \bar{X}) \xrightarrow{P} \frac{\psi_{\text{MDP}}}{\kappa} \left\{ -\eta_1(1 - \cos^2 \varphi)\delta^2 - \frac{\tau_1^2 - \tau_2^2}{n} \right\}$$

as $p \rightarrow \infty$ for any independent observation Y , which is independent to both of \mathcal{X} and \mathcal{Y} , with $\pi(Y) = 2$. \blacksquare

E.16 Proof of Theorem 15

Proof Theorem 14 tells that, for $\{\mathbf{w}\} \in \bar{\mathcal{A}}$ with $\mathbf{w} = \mathbf{V}\mathbf{a}$ and $a_{\text{MDP}} \xrightarrow{P} \psi_{\text{MDP}}$ as $p \rightarrow \infty$, an asymptotic distance between the two piles of independent test data is $D(\mathbf{w}) = \kappa^{-1}\psi_{\text{MDP}}(1 - \cos^2 \varphi)\delta^2$. Let $\mathbf{w}_{\text{SMDP}} = \mathbf{V}\mathbf{a}_{\text{SMDP}} = \|\hat{\mathbf{Q}}_2 \hat{\mathbf{Q}}_2^\top \mathbf{e}_{\text{MDP}}\|^{-1} \mathbf{V} \hat{\mathbf{Q}}_2 \hat{\mathbf{Q}}_2^\top \mathbf{e}_{\text{MDP}}$ where $\mathbf{e}_{\text{MDP}} = (\mathbf{0}_{n-2}^\top, 1)^\top$. Note that

$$\|\hat{\mathbf{Q}}_2 \hat{\mathbf{Q}}_2^\top \mathbf{e}_{\text{MDP}}\|^{-1} \mathbf{e}_{\text{MDP}}^\top \hat{\mathbf{Q}}_2 \hat{\mathbf{Q}}_2^\top \mathbf{e}_{\text{MDP}} = \|\hat{\mathbf{Q}}_2^\top \mathbf{e}_{\text{MDP}}\|. \quad (71)$$

Using similar arguments in the proof of Theorem 11, we can show that the probability limit of (71) is κv_0 , where v_0 is defined in (62). Hence, we have $D(\mathbf{w}_{\text{SMDP}}) = v_0(1 - \cos^2 \varphi)\delta^2 > 0$ with probability 1.

For each p , let $\{\mathbf{w}_{\text{SMDP}}\} \cup \{\bar{\mathbf{f}}_i\}_{i=1}^{n-m-2}$ be an orthonormal basis of $\text{span}(\mathbf{V}\hat{\mathbf{Q}}_2)$. Also, choose $\{\bar{\mathbf{g}}_i\}_{i=1}^m$ so that $\{\mathbf{w}_{\text{SMDP}}\} \cup \{\bar{\mathbf{f}}_i\}_{i=1}^{n-m-2} \cup \{\bar{\mathbf{g}}_i\}_{i=1}^m$ forms an orthonormal basis of $\mathcal{S}_{\mathcal{X}}$. For $1 \leq i \leq n-m-2$, write $\bar{\mathbf{f}}_i = \|\hat{\mathbf{Q}}_2 \hat{\mathbf{Q}}_2^\top \mathbf{a}_i\|^{-1} \mathbf{V} \hat{\mathbf{Q}}_2 \hat{\mathbf{Q}}_2^\top \mathbf{a}_i$ for some $\mathbf{a}_i \in \mathbb{R}^{n-1}$. To obtain $D(\bar{\mathbf{f}}_i)$, we need to derive the probability limit of

$$\|\hat{\mathbf{Q}}_2 \hat{\mathbf{Q}}_2^\top \mathbf{a}_i\|^{-1} \mathbf{e}_{\text{MDP}}^\top \hat{\mathbf{Q}}_2 \hat{\mathbf{Q}}_2^\top \mathbf{a}_i = \|\hat{\mathbf{Q}}_2^\top \mathbf{a}_i\|^{-1} \mathbf{e}_{\text{MDP}}^\top \hat{\mathbf{Q}}_2 \hat{\mathbf{Q}}_2^\top \mathbf{a}_i. \quad (72)$$

Since \mathbf{w}_{SMDP} is orthogonal to $\bar{\mathbf{f}}_i$, we have

$$\mathbf{w}_{\text{SMDP}}^\top \bar{\mathbf{f}}_i = \frac{\mathbf{e}_{\text{MDP}}^\top \hat{\mathbf{Q}}_2 \hat{\mathbf{Q}}_2^\top \mathbf{a}_i}{\|\hat{\mathbf{Q}}_2^\top \mathbf{e}_{\text{MDP}}\| \|\hat{\mathbf{Q}}_2^\top \mathbf{a}_i\|} = 0$$

for all p . Note that $\|\hat{\mathbf{Q}}_2^\top \mathbf{e}_{\text{MDP}}\|$ converges to $\kappa \nu_0 > 0$ and thus the probability limit of (72) is zero. Hence, $D(\bar{\mathbf{f}}_i) = 0$ for $1 \leq i \leq n-m-2$.

We are now ready to show that \mathbf{w}_{SMDP} is a second maximal data piling direction. For any given $\{\mathbf{w}\} \in \bar{\mathcal{A}}$, write $\mathbf{w} = a_0 \mathbf{w}_{\text{SMDP}} + \sum_{i=1}^{n-m-2} a_i \bar{\mathbf{f}}_i + \sum_{i=1}^m c_i \bar{\mathbf{g}}_i$. Recall that for $\{\mathbf{w}\} \in \bar{\mathcal{A}}$, there exists $\{\mathbf{v}\}$ such that $\mathbf{v} \in \text{span}(\mathbf{V}\hat{\mathbf{Q}}_2)$ for all p and $\|\mathbf{w} - \mathbf{v}\| \xrightarrow{P} 0$ as $p \rightarrow \infty$. Hence, $c_i = o_p(1)$ for $1 \leq i \leq m$. Moreover, since $D(\bar{\mathbf{f}}_i) = 0$ for all $1 \leq i \leq n-m-2$, using similar arguments in the proof of Theorem 12 (ii), we can show that $D(\mathbf{w}) \leq D(\mathbf{w}_{\text{SMDP}})$ for any $\{\mathbf{w}\} \in \bar{\mathcal{A}}$ and the equality holds when $\|\mathbf{w} - \mathbf{w}_{\text{SMDP}}\| \xrightarrow{P} 0$ as $p \rightarrow \infty$. \blacksquare

References

- J. Ahn and J. S. Marron. The maximal data piling direction for discrimination. *Biometrika*, 97(1):254–259, 2010.
- J. Ahn, J. S. Marron, K. M. Muller, and Y.-Y. Chi. The high-dimension, low-sample-size geometric representation holds under mild conditions. *Biometrika*, 94(3):760–766, 2007.
- M. Aoshima and K. Yata. A distance-based, misclassification rate adjusted classifier for multiclass, high-dimensional data. *Annals of the Institute of Statistical Mathematics*, 66(5):983–1010, 2013.
- M. Aoshima and K. Yata. Distance-based classifier by data transformation for high-dimension, strongly spiked eigenvalue models. *Annals of the Institute of Statistical Mathematics*, 71(3):473–503, 2019.
- P. L. Bartlett, P. M. Long, G. Lugosi, and A. Tsigler. Benign overfitting in linear regression. *Proceedings of the National Academy of Sciences*, 117(48):30063–30070, 2020.
- M. Belkin, D. Hsu, S. Ma, and S. Mandal. Reconciling modern machine-learning practice and the classical bias–variance trade-off. *Proceedings of the National Academy of Sciences*, 116(32):15849–15854, 2019.
- R. C. Bradley. Basic properties of strong mixing conditions. A survey and some open questions. *Probability Surveys*, 2:107–144, 2005.

- W. Chang, J. Ahn, and S. Jung. Double data piling leads to perfect classification. *Electronic Journal of Statistics*, 15(2):6382–6428, 2021.
- N. S. Chatterji and P. M. Long. Finite-sample analysis of interpolating linear classifiers in the overparameterized regime. *Journal of Machine Learning Research*, 22(129):1–30, 2021.
- P. Hall, J. S. Marron, and A. Neeman. Geometric representation of high dimension, low sample size data. *Journal of the Royal Statistical Society: Series B (Statistical Methodology)*, 67(3):427–444, 2005.
- T. Hastie, A. Montanari, S. Rosset, and R. J. Tibshirani. Surprises in high-dimensional ridgeless least squares interpolation. *The Annals of Statistics*, 50(2):949–986, 2022.
- D. Holzmüller. On the universality of the double descent peak in ridgeless regression. *arXiv preprint arXiv:2010.01851*, 2020.
- H. Huang. Asymptotic behavior of support vector machine for spiked population model. *Journal of Machine Learning Research*, 18(45):1–21, 2017.
- A. Ishii. A classifier under the strongly spiked eigenvalue model in high-dimension, low-sample-size context. *Communications in Statistics - Theory and Methods*, 49(7):1561–1577, 2020.
- A. Ishii, K. Yata, and M. Aoshima. Geometric classifiers for high-dimensional noisy data. *Journal of Multivariate Analysis*, 188:104850, 2022.
- I. M. Johnstone. On the distribution of the largest eigenvalue in principal components analysis. *The Annals of Statistics*, 29(2):295–327, 2001.
- S. Jung. Continuum directions for supervised dimension reduction. *Computational Statistics & Data Analysis*, 125:27–43, 2018.
- S. Jung and J. S. Marron. PCA consistency in high dimension, low sample size context. *The Annals of Statistics*, 37(6B):4104–4130, 2009.
- S. Jung, A. Sen, and J. Marron. Boundary behavior in high dimension, low sample size asymptotics of PCA. *Journal of Multivariate Analysis*, 109:190–203, 2012.
- S. Jung, M. H. Lee, and J. Ahn. On the number of principal components in high dimensions. *Biometrika*, 105(2):389–402, 2018.
- D. Kobak, J. Lomond, and B. Sanchez. The optimal ridge penalty for real-world high-dimensional data can be zero or negative due to the implicit ridge regularization. *Journal of Machine Learning Research*, 21(169):1–16, 2020.
- A. N. Kolmogorov and Y. A. Rozanov. On strong mixing conditions for stationary gaussian processes. *Theory of Probability & Its Applications*, 5(2):204–208, 1960.

- S. Kritchman and B. Nadler. Determining the number of components in a factor model from limited noisy data. *Chemometrics and Intelligent Laboratory Systems*, 94(1):19–32, 2008.
- M. H. Lee, J. Ahn, and Y. Jeon. HDLSS discrimination with adaptive data piling. *Journal of Computational and Graphical Statistics*, 22(2):433–451, 2013.
- J. T. Leek. Asymptotic conditional singular value decomposition for high-dimensional genomic data. *Biometrics*, 67(2):344–352, 2010.
- J. S. Marron, M. J. Todd, and J. Ahn. Distance-weighted discrimination. *Journal of the American Statistical Association*, 102(480):1267–1271, 2007.
- A. Montanari, F. Ruan, Y. Sohn, and J. Yan. The generalization error of max-margin linear classifiers: High-dimensional asymptotics in the overparametrized regime. *arXiv preprint arXiv:1911.01544*, 2019.
- D. Passemier and J. Yao. Estimation of the number of spikes, possibly equal, in the high-dimensional case. *Journal of Multivariate Analysis*, 127:173–183, 2014.
- X. Qiao, H. H. Zhang, Y. Liu, M. J. Todd, and J. S. Marron. Weighted distance weighted discrimination and its asymptotic properties. *Journal of the American Statistical Association*, 105(489):401–414, 2010.
- D. Shen, H. Shen, and J. S. Marron. A general framework for consistency of principal component analysis. *Journal of Machine Learning Research*, 17(150):1–34, 2016.
- A. Tsigler and P. L. Bartlett. Benign overfitting in ridge regression. *arXiv preprint arXiv:2009.14286*, 2020.
- V. N. Vapnik. *The Nature of Statistical Learning Theory*. Springer, 1995.
- D. Wu and J. Xu. On the optimal weighted l_2 regularization in overparameterized linear regression. In *Advances in Neural Information Processing Systems*, volume 33, pages 10112–10123. Curran Associates, Inc., 2020.
- C. Zhang, S. Bengio, M. Hardt, B. Recht, and O. Vinyals. Understanding deep learning requires rethinking generalization. In *International Conference on Learning Representations*, 2017.